

**THE MEMBRANE AS A BARRIER OR TARGET IN
CANCER CHEMOTHERAPY.**

By

SHUNA M. BURROW BSc. (HONS)

**A thesis submitted in partial fulfilment of the requirements for the degree of
Doctor of Philosophy**

UNIVERSITY OF CENTRAL LANCASHIRE

FEBRUARY 1997

Abstract

The overall aim of the project was to investigate the role of the cell membrane as a barrier and/or target for drug action and relate this to the development of strategies for overcoming multiple drug resistance (MDR).

The effects of doxorubicin on various bacterial strains expressing different levels of anionic phospholipid were compared. Growth of wild-type *Echerichia coli* (*E. coli*) strain MRE600 was severely affected up to 9 hours following doxorubicin treatment (15 μ M), but resistance occurred after 9 hours. *E. coli* strain HDL11 was resistant to doxorubicin (100 μ M) over 9 hours, however, increasing the anionic lipid content showed little difference in sensitivity.

The mouse mammary tumour cell line (EMT6-S) and MDR sub-line (EMT6-R) were characterised with regard to growth kinetics, susceptibility to doxorubicin and membrane lipid composition. The log phase doubling times (h) were found to be 21.8 (EMT6-S) and 25.0 (EMT6-R) and the IC₅₀ values for doxorubicin to be 2.2 x 10⁻⁸ M and 1.8 x 10⁻⁶ M for EMT6-S and EMT6-R cells, respectively. No difference was observed between the phospholipid profiles of the two cell lines and total fatty acid composition was similar, however, the level of linoleic acid appeared to be higher in the resistant cells.

The photocytotoxicity of the cationic dyes methylene blue (MB), toluidine blue (TBO) and Victoria blue BO (VBBO) against the EMT6 cell lines was compared to the cytotoxic effect of doxorubicin and *cis*-platinum. The cytotoxic effect of VBBO was enhanced 10-fold by illumination (7.2 J cm⁻²) in both EMT6-S and EMT6-R cells. In order to overcome resistance, however, the EMT6-R cells required a 10-fold greater level of the dye than the parental cells to reach an IC₅₀ value. By contrast, doxorubicin required almost a 100-fold increase in concentration to overcome this resistance.

Pre-treatment of EMT6-S and EMT6-R cells with low concentrations of VBBO resulted in a 2-fold increase in doxorubicin toxicity in both cell lines. Pre-treatment with MB and TBO resulted in a 1.4-fold and 2-fold increase in doxorubicin toxicity, respectively, in the sensitive cells, increasing to 2-fold and 3-fold, respectively in the resistant cells.

Glutathione (GSH) depletion of EMT6-S and EMT6-R cells did not enhance the photocytotoxicity of VBBO, suggesting that the primary site of action of VBBO is at an intracellular site not protected by GSH or that the mechanism of action is not *via* the *in situ* generation of singlet oxygen. Addition of the chemosensitizer, verapamil (7 μ M), increased the efficacy of doxorubicin by 2-fold in EMT6-S cells and by 18-fold in EMT6-R cells. By contrast, the presence of verapamil did not increase the cytotoxicity of VBBO in either cell line.

A series of compounds, PVB, MVB and MOVV, based on the skeleton of VBBO was examined. VBBO was found to be the most effective photosensitizer. The rate of uptake for VBBO, MVB and PVB appeared to be very similar, whereas that of MOVV was slower. The uptake/dose trend was also similar for all four drugs tested and correlated to the levels of lipophilicity of the agents.

Confocal microscopy studies showed all the photosensitizers to be distributed widely throughout the cytoplasm, with considerable accumulation of VBBO and PVB in the perinuclear region. Time course studies showed the intracellular distribution of VBBO in both cell lines to be similar, although uptake of the drug appeared slower in the resistant cell line. VBBO was clearly localised throughout the cytoplasm, in a punctate pattern, which may be consistent with the widespread distribution of mitochondria. No interaction with the plasma membrane was evident. By contrast, doxorubicin was found to localise mainly in the nucleus of the sensitive cell line, whereas no nuclear involvement was seen in the resistant cells. The drug was also effluxed more rapidly from EMT6-R cells than EMT6-S cells. Time course studies with EMT6-S cells showed that the drug clearly interacts with both the plasma membrane and the nucleus. These results indicate

that the main modes of action for the two drugs differ markedly, suggesting interaction with both the membrane and the nucleus in the case of doxorubicin, but possibly mitochondrial involvement for VBBO.

ACKNOWLEDGEMENTS

I would like to express my grateful thanks to my supervisors, Dr. David Phoenix and Dr. Jack Waring, for their continuing interest, guidance and support throughout my research project. I would also like to thank Dr. Mark Wainwright for all his help and encouragement.

In addition I would like to thank my colleagues at the University of Central Lancashire, all the technical staff and, in particular, Miss Karin Gonzalez for her assistance. Grateful thanks are also extended to Dr. Mark Tobin at Daresbury Laboratory for all his help with the confocal microscopy studies.

Financial assistance from the Biotechnology and Biological Sciences Research Council, the Preston and Chorley Hospital Research Fund and gifts of doxorubicin from Farmacia Carlo Erba Ltd. and the Ridascreen® mycoplasma screening kit from Digen Ltd. are gratefully acknowledged.

Finally, I would especially like to thank my husband, Jim, for his patience and his unfailing encouragement and support throughout my studies.

CONTENTS

	PAGE
CHAPTER ONE : GENERAL INTRODUCTION	1
1.1 Cancer and Carcinogenesis	2
1.1.1 Non-genotoxic Carcinogenesis	9
1.2 Genetics of Cancer	9
1.2.1 The Cell Cycle	10
1.2.2 Oncogenes	13
1.2.3 Tumour Suppressor Genes	17
1.3 Cancer Therapy	19
1.3.1 Multiple Drug Resistance	19
1.3.2 P-glycoprotein	21
1.3.3 Other Mechanisms of MDR	24
1.3.4 Multidrug resistance-associated Protein	24
1.3.5 Lung Resistance-associated Protein	26
1.3.6 Glutathione and Glutathione-S-transferases	29
1.3.7 Circumvention of MDR	31
1.4 Photodynamic Therapy	32
1.4.1 Brief History of Photodynamic Therapy	32
1.4.2 Mechanism of Action of PDT	33
1.4.3 Cancer Treatment Using PDT	36
1.4.4 Cationic Photosensitizers	41
1.5 Aim of Study	43

	PAGE
CHAPTER TWO : DEVELOPMENT OF A PROKARYOTIC MODEL FOR STUDYING ANTHRACYCLINE-MEMBRANE INTERACTIONS.	44
2.1 Abstract	45
2.2 Introduction	46
2.3 Materials and Methods	48
2.3.1 Chemicals	48
2.3.2 Bacterial Strains and Growth Conditions	48
2.3.3 Effect of Doxorubicin on Growth of Bacteria	48
2.3.4 Analysis of Membrane	49
2.4 Results	49
2.4.1 Effect of doxorubicin on <i>E. coli</i> strain MRE600	49
2.4.2 Total Fatty Acid Composition of MRE600 cells in the absence and presence of doxorubicin	52
2.4.3 Effect of doxorubicin on <i>E. coli</i> strain HDL11 in the absence and presence of IPTG	53
2.4.4 Effect of doxorubicin on <i>S. aureus</i> cells	55
2.5 Discussion	56
 CHAPTER THREE : CHARACTERISATION OF THE MOUSE MAMMARY TUMOUR CELL LINE EMT6 WITH REGARD TO GROWTH KINETICS, TOXICITY OF DOXORUBICIN AND MEMBRANE LIPID COMPOSITION	 59
3.1 Abstract	60
3.2 Introduction	61
3.2.1 EMT6 cells	61

	PAGE	
3.2.2	Screening for mycoplasma contamination	61
3.2.3	Lipid composition of membranes from mammalian cells	62
3.2.4	Lipid composition of MDR cells	65
3.3	Methods and Materials	67
3.3.1	Chemicals	67
3.3.2	Maintenance of cell cultures	67
3.3.3	Mycoplasma screening	68
3.3.4	Growth Kinetics	69
3.3.5	Effect of doxorubicin	70
3.3.6	Membrane lipid composition	70
3.3.6.1	Preparation of samples for phospholipid and fatty acid analysis	70
3.3.6.2	Preparation of fatty acid methyl esters and analysis by gas chromatography	71
3.3.6.3	Analysis of phospholipids by thin layer chromatography	71
3.4	Results	72
3.4.1	Mycoplasma screening	72
3.4.2	Growth kinetics	74
3.4.3	Effects of doxorubicin	75
3.4.4	Membrane lipid analysis	76
3.4.4.1	Fatty acid composition	76
3.4.4.2	Phospholipid composition	76
3.5	Discussion	78

	PAGE
CHAPTER FOUR : CELL KILLING BY CATIONIC PHOTSENSITIZERS IN A MULTIDRUG RESISTANT CELL LINE	80
4.1 Abstract	81
4.2 Introduction	83
4.3 Materials and Methods	88
4.3.1 Chemicals	88
4.3.2 Cell culture	88
4.3.3 Phototoxicity : dark toxicity experiments	88
4.3.4 Pre-treatment of EMT6-s and EMT6-R cells with VBBO, MB or TBO, prior to doxorubicin	89
4.3.5 Localisation studies using confocal scanning laser fluorescence microscopy	90
4.4 Results	91
4.4.1 Phototoxicity : dark toxicity	91
4.4.2 Localisation studies using confocal scanning laser fluorescence microscopy	96
4.4.3 Effect of pre-treatment of EMT6-S and EMT6-R cells with VBBO, MB or TBO on the cytotoxicity of doxorubicin.	104
4.5 Discussion	108
CHAPTER FIVE : THE EFFECT OF VERAPAMIL AND BUTHIONINE SULFOXIMINE ON THE CYTOTOXICITY OF VBBO IN EMT6 CELLS	113
5.1 Abstract	114
5.2 Introduction	116
5.3 Materials and Methods	118

	PAGE	
5.3.1	Chemicals	118
5.3.2	Cell culture	118
5.3.3	Effect of BSO on glutathione levels in EMT6-S and EMT6-R cells	119
5.3.4	Effect of glutathione depletion on the cytotoxicity exerted by VBBO against EMT6-S and EMT6-R cells	120
5.3.5	Effect of verapamil on the cytotoxicity exerted by doxorubicin or VBBO against EMT6-S and EMT6-R cells	120
5.4	Results	121
5.4.1	Effect of BSO on glutathione levels in EMT6-S and EMT6-R cells	121
5.4.2	Effect of glutathione depletion on the cytotoxicity exerted by VBBO against EMT6-s and EMT6-R cells	122
5.4.3	Effect of verapamil on the cytotoxicity exerted by doxorubicin or VBBO against EMT6-S and EMT6-R cells	123
5.5	Discussion	124
 CHAPTER SIX : UPTAKE AND CELL-KILLING ACTIVITIES OF A SERIES OF VICTORIA BLUE DERIVATIVES IN A MOUSE MAMMARY TUMOUR CELL LINE		 128
6.1	Abstract	129
6.2	Introduction	130
6.3	Materials and Methods	134
6.3.1	Chemicals	134
6.3.2	Cell culture	134

	PAGE	
6.3.3	Characterisation of drug uptake	135
6.3.3.1	Absorbance Spectra	135
6.3.3.2	Drug Uptake	135
6.3.4	Phototoxicity : dark toxicity experiment	136
6.3.5	Effect of variable illumination	136
6.3.6	Localisation studies using confocal scanning laser fluorescence microscopy	136
6.4	Results	137
6.4.1	Absorbance spectra	137
6.4.2	Drug uptake	137
6.4.3	Mean cytotoxicity following 3 hours' incubation	139
6.4.4	Effect of variable illumination	140
6.4.5	Localisation studies using confocal scanning laser fluorescence microscopy	141
6.5	Discussion	143
 CHAPTER SEVEN : INTRACELLULAR LOCALISATION STUDIES OF DOXORUBICIN AND VICTORIA BLUE BO IN EMT6-S AND EMT6-R CELLS USING CONFOCAL MICROSCOPY		 147
7.1	Abstract	148
7.2	Introduction	149
7.3	Materials and Methods	151
7.3.1	Localisation studies using confocal scanning laser fluorescence microscopy	151
7.3.1.1	Time course studies	151

	PAGE
7.3.1.2 Intracellular localisation of doxorubicin in treated EMT6-S and EMT6-R cells, following recovery in drug-free medium	152
7.4 Results	152
7.4.1 Time course studies	152
7.4.2 Intracellular localisation of doxorubicin in treated EMT6-S and EMT6-R cells, following recovery in drug-free medium	157
7.5 Discussion	160
CHAPTER EIGHT : CLOSING DISCUSSION	162
8.1 Closing dicussion and future studies	163

LIST OF FIGURES AND TABLES

		PAGE
CHAPTER ONE		
Figure 1	Differentiation of cells in normal tissues	3
Figure 2	Schematic diagram showing onset of carcinogenesis	8
Table 1	Cellular role of some proto-oncogenes	10
Figure 3	Diagrammatic representation of the four stages of the cell cycle	11
Table 2	Chemotherapeutic agents specific for the cell cycle	12
Table 3	Viruses commonly associated with human cancers	15
Table 4	Representative oncogenes associated with human cancers	16
Table 5	Representative tumour suppressor genes implicated in human cancers	18
Figure 4	Proposed topological models for P-glycoprotein	23
Figure 5	Proposed topological models for the Multidrug Resistance-associated Protein	26
Figure 6	Proposed model of a vault structure	29
Table 6	Reversing agents of classical MDR	31
Figure 7	Mechanism of action of PDT	35
Figure 8	Typical absorption spectra for porphyrins such as Photofrin and protoporphyrin IX	37
Figure 9	Schematic diagram showing the wavelength dependence of effective penetration depth (δ_{eff}) in soft tissues	38
Figure 10	Schematic diagram of the haeme biosynthetic pathway	40

CHAPTER TWO

Figure 11	Typical growth curve for <i>E. coli</i> (strain MRE600) in the absence or presence of doxorubicin (5-100 μ M)	50
Figure 12	Typical growth curve for <i>E. coli</i> (strain MRE600) in the absence or presence of doxorubicin (5-15 μ M) previously grown for 24 hours in the presence of doxorubicin	50
Figure 13 (a-c)	Typical growth curves for <i>E. coli</i> (strain MRE600) in the absence or presence of doxorubicin (5-15 μ M) and showing the effects of IPTG (30 & 60 μ M)	51
Table 7	Total fatty acid composition of MRE600 cells in the absence and presence of doxorubicin.	52
Figure 14	Typical growth curve for <i>E. coli</i> (strain HDL11) in the absence or presence of doxorubicin (5-100 μ M)	53
Figure 15 (a-c)	Typical growth curves for <i>E. coli</i> (strain HDL11) in the absence or presence of doxorubicin (5-15 μ M) and showing the effects of IPTG (30 & 60 μ M)	54
Figure 16	Typical growth curve for <i>E. coli</i> (strain HDL11) in the absence or presence of doxorubicin (5-100 μ M) and in the absence and presence of 60 μ M IPTG.	55
Figure 17	Typical growth curve for <i>S. aureus</i> (strain 67J1) in the absence or presence of doxorubicin (5-100 μ M)	55

CHAPTER THREE

Figure 18	General structure of a glycerophospholipid	62
Table 8	Fatty acids most commonly found in phospholipids of mammalian cells	63

	PAGE	
Figure 19	Spatial representation of the chemical formulae of the major lipids found in biological membranes	64
Table 9	Lipid composition of membranes from mammalian cells	65
Figure 20	Screening of EMT6-S and EMT6-R cells for mycoplasma infection	73
Figure 21	Growth kinetics of the mouse mammary tumour cell lines EMT6-S and EMT6-R	74
Figure 22	Dose survival curves for EMT6-S and EMT6-R cell lines challenged with doxorubicin.	75
Table 10	Comparison of the percentage of total fatty acid composition of EMT6-S and EMT6-R cells	76
Figure 23	Schematic representation of the separation of phospholipids in EMT6-S and EMT6-R cells by thin-layer chromatography	77
 CHAPTER FOUR		
Figure 24	Victoria blue, toluidine blue O and methylene blue structures and physicochemical properties	85
Figure 25	Structure of doxorubicin	86
Figure 26	Structure of <i>cis</i> -platinum	87
Figure 27	Effect of light on EMT6-S and EMT6-R cells	91
Figure 28	Comparison of % cytotoxicity elicited by VBBO, MB, TBO, doxorubicin & <i>cis</i> -platinum against EMT6-S cells.	93

	PAGE	
Figure 29	Comparison of % cytotoxicity elicited by VBBO, MB, TBO, doxorubicin & <i>cis</i> -platinum against EMT6-R cells.	94
Table 11	IC ₅₀ values for photosensitizers, doxorubicin and <i>cis</i> -platinum.	95
Figure 30	Intracellular distribution of VBBO (5 μM) in EMT6-S cells	98
Figure 31	Intracellular distribution of VBBO (5 μM) in EMT6-R cells	99
Figure 32	Intracellular distribution of MB (25 μM) in EMT6-S cells	100
Figure 33	Intracellular distribution of MB (35 μM) in EMT6-R cells	101
Figure 34	Intracellular distribution of TBO (10 μM) in EMT6-S cells	102
Figure 35	Intracellular distribution of TBO (15 μM) in EMT6-R cells	103
Figure 36	Effect of pre-treatment with VBBO on IC ₅₀ values for doxorubicin, with respect to EMT6-S and EMT6-R cells.	105
Figure 37	Effect of pre-treatment with MB on IC ₅₀ values for doxorubicin, with respect to EMT6-S and EMT6-R cells.	106
Figure 38	Effect of pre-treatment with TBO on IC ₅₀ values for doxorubicin, with respect to EMT6-S and EMT6-R cells.	107

CHAPTER FIVE

Figure 39	Effect of Buthionine Sulfoximine (BSO) on glutathione levels in EMT6-S and EMT6-R cells	121
-----------	---	-----

	PAGE	
Figure 40	Effect of glutathione depletion in EMT6-S and EMT6-R cells on the photocytotoxicity of VBBO.	122
Figure 41	Effect of verapamil on cytotoxicity exerted by VBBO or doxorubicin against EMT6-S and EMT6-R cells.	123
CHAPTER SIX		
Figure 42	Structures and physicochemical data for VBBO derivatives	132
Figure 43	Hyperchem representations of the naphthyl residues in the Victoria blue derivatives	133
Figure 44	Rate of uptake of Victoria blue derivatives by EMT6-S cells	138
Figure 45	Uptake/dose curves for Victoria blue derivatives in EMT6-S cells	138
Figure 46	% cytotoxicity on EMT6-S cells elicited by Victoria blue derivatives following illumination	139
Table 12	IC ₅₀ values / Light Enhancement Factor for Victoria Blue derivatives.	140
Figure 47	Effects of variable light dose on the % cytotoxicity elicited by Victoria blue derivatives against EMT6-S cells.	141
Figure 48	Intracellular distribution of VBBO derivatives in EMT6-S cells	142
Figure 49	Interaction of VBBO with water	143

CHAPTER SEVEN

Figure 50	Schematic diagram showing proposed mechanism of doxorubicin cytotoxicity.	150
Figure 51	Intracellular distribution of doxorubicin (10 μ M) in EMT6-S cells	153
Figure 52	Time course study showing intracellular distribution of VBBO (5 μ M) in EMT6-S cells	155
Figure 53	Time course study showing intracellular distribution of VBBO (5 μ M) in EMT6-R cells	156
Figure 54	Intracellular distribution of doxorubicin in EMT6-S cells following exposure to 10 μ M doxorubicin for 2 hours, prior to rinsing with RPMI 1640 medium.	158
Figure 55	Intracellular distribution of doxorubicin in EMT6-R cells following exposure to 10 μ M doxorubicin for 2 hours, prior to rinsing with RPMI 1640 medium.	159

ABBREVIATIONS

- ABC - ATP binding cassette
- ALA - 5-aminolevulinic acid
- ANS - 8-anilino-1-naphthalenesulfonic acid
- ATP - adenosine triphosphate
- BSO - buthionine sulfoximine
- CL - cardiolipin
- CSFR1 - colony stimulating factor 1
- COPRO - coproporphyrinogen
- CFTR - cystic fibrosis transmembrane conductance regulator protein
- DHFR - dihydrofolate reductase
- DMSO - dimethyl sulfoximine
- DNA - deoxyribonucleic acid
- DTNB - 5,5'-dithiobis-(2-nitrobenzoic acid)
- EGFR - epidermal growth factor
- E. coli* - *Escherichia coli*
- EDTA - ethylenediaminetetraacetic acid
- FADH₂ - reduced flavin nicotinamide dinucleotide
- FAME - fatty acid methyl esters
- GC - gas chromatography
- GSH - glutathione
- GSSG - glutathione disulphide
- GST - glutathione-S-transferases
- gsv - greyscale value range
- HpD , - haematoporphyrin derivatives
- HPLC - high performance liquid chromatography
- HIV - human immunodeficiency virus
- HPV - human papilloma virus
- HTLV - human T-cell virus

IC₅₀ - the concentration which inhibits cell growth by 50%

IPTG - isopropyl β-thiogalactopyranoside

LMB - leuco-methylene blue

LTC(4) - leukotriene C4

LEF - light enhancement factor

LDL - low density lipoprotein

LRP - lung resistance-related protein

MeOH - methanol

MB - methylene blue

mRNA - messenger RNA

MTT - (3-[4,5-dimethylthiazol-2-yl]-2,5-diphenyl-2*H*-tetrazolium bromide)

MRP - multidrug resistance-associated protein

MDRP - multidrug resistant pump

MDR - multiple drug resistanc

NADH - reduced nicotinamide adenine dinucleotide

NADPH - reduced nicotinamide adenine dinucleotide phosphate

NPC - nuclear pore complex

Pgp - P-glycoprotein

PBS - phosphate buffered saline

PC - phosphatidylcholine

PE - phosphatidylethanolamine

PG - phosphatidylglycerol

PI - phosphatidylinositol

PS - phosphatidylserine

PDT - photodynamic therapy

PKC - protein kinase C

PGDF - platelet-derived growth factor

PBG - porphobilinogen

PGBD - porphobilinogen deaminase

PROTO - protoporphyrin IX

RNA	- ribonucleic acid
5-SA	- 5-sulfosalicylic acid
<i>S. aureus</i>	- <i>Staphylococcus aureus</i>
TIMP	- tissue inhibitors of metalloproteins
TLC	- thin layer chromatography
TMA-DPH	- 1-(4-trimethylammonium phenyl)-6-phenyl-1,3,5-hexatriene
TNB	- 2-nitro-5-thiobenzoic acid
TBO	- toluidine blue
TGF- β	- transforming growth factor beta
TAF	- tumour angiogenesis factor
UPG	- uroporphyrinogen
UV	- ultra violet
VEGF	- vascular endothelial growth factor
VBBO	- Victoria blue BO

CHAPTER ONE.

GENERAL INTRODUCTION.

1.1 Cancer and carcinogenesis.

Cancer is a widespread, insidious disease which will affect one in three of the population during their lifetime. Consequently, research into the onset and mechanisms of this complex disease is intense, however, despite increased knowledge, many cancers remain refractory to treatment. One definition of cancer is of a population of cells which has begun the pathway to maturity, but in which the processes of differentiation and proliferation have become uncoupled resulting in transformed cancer cells which divide rapidly but are not fully differentiated [1].

In normal cells, very precise mechanisms control growth and development of tissues and organs. The precursors of these cells undergo repeated cell division and become specialised by differentiation into a variety of cell types, for example, muscle, brain, liver *etc.* (Figure 1). In some tissues, such as the neurons in the central nervous system, there is little or no replacement of the differentiated cells, just a gradual decline with age. However, many tissues of the body are constantly renewed, with the loss of mature cells countered by the proliferation of less mature precursor (stem) cells. Although cells in the embryo are capable of proliferating, most adult cells are not and 'hold in reserve' the stem cells which respond to various stimuli for growth, such as tissue injury. Stem cells divide to produce two daughter cells, one remaining as a stem cell whilst the other has the potential to be differentiated into a specific cell type. During the process of differentiation the cells reach a stage where they are said to be "committed " and can no longer revert to any other cell type in the body [1]. It is at this stage where a specific genetic sequence within the cell's DNA becomes activated in response to a wide variety of signals from the cellular environment, such as circulating hormones and growth factors. When a gene is 'switched on', the encoded protein is synthesised by the cell, however, mutations in the gene can alter the amount of protein produced and/or the function of the protein within the cell. Stem cells express genes whose protein products drive cells through repeated divisions, that is, the genes of cellular proliferation [1]. During this progression from stem cells to mature, differentiated cells, genes of

proliferation become generally less active, whilst genes of differentiation generally increase their activity. Cancerous cells, however, divide rapidly and are no longer capable of completing their differentiation programme. This population of transformed cells is usually derived from the divisions of a single cell whose genes have mutated in some way.

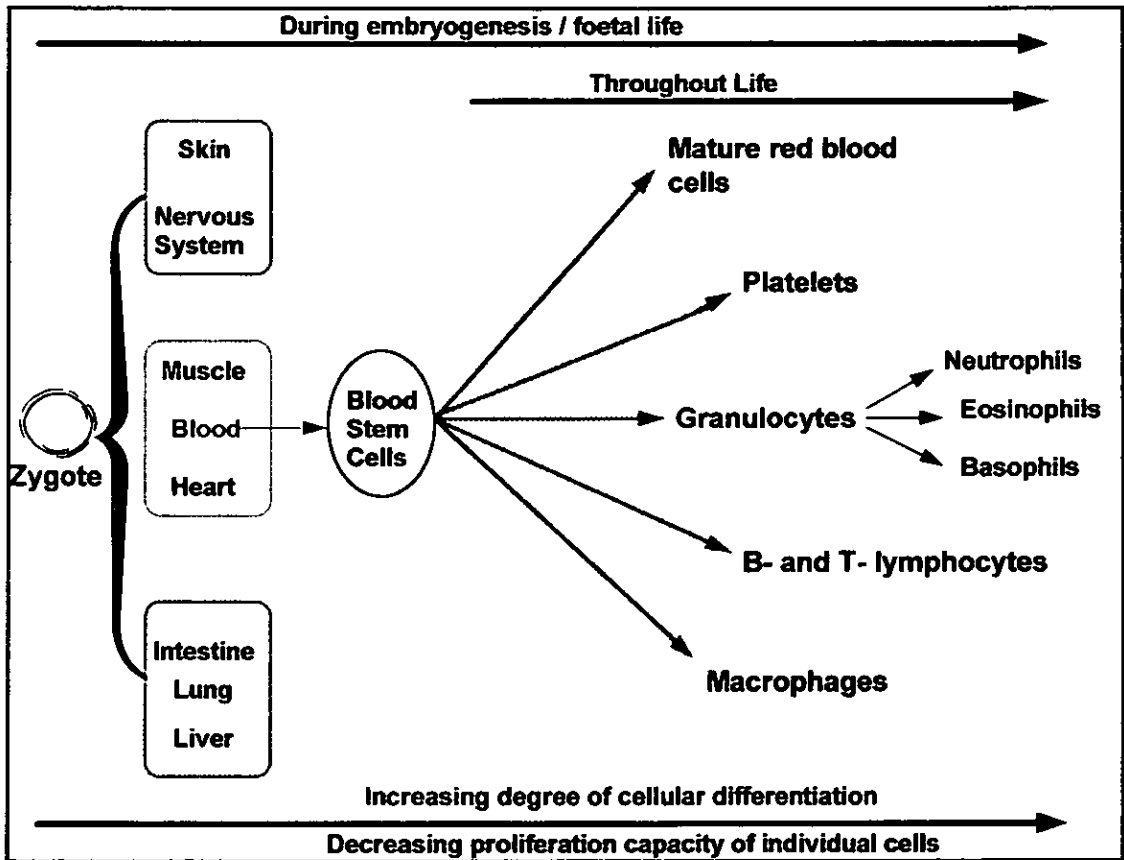


Figure 1: Each adult cell is derived from the zygote by a series of repeated cell divisions. The cells become specialised into specific cell types, such as muscle, liver and brain, by differentiation. Stem cells divide producing two daughter cells, one of which remains as a stem cell, while the other has the capacity to differentiate into a specific cell type. For each specific tissue type cells become specialised for various functions, e.g. red blood cells represent a specific lineage within the blood responsible for carrying oxygen and T- and B-lymphocytes are white blood cells involved in immune defence. (Figure adapted from Vile, 1990 [1]).

Virtually all malignant cells are now thought to be monoclonal in origin, that is, a single precursor cell is transformed and proliferates to form a clone [2]. However, although all the cells in the tumour share features of the original mutated cell, as the tumour develops, cells modify their properties leading to a heterogeneous population. Tumours may be classified into three main groups : benign, *in-situ* and fully developed or malignant tumours [3]. Benign or non-malignant tumours usually develop a fibrous membrane of connective tissue around the tumour which prevents it from spreading [4]. These tumours increase in size and may cause damage by obstruction or local pressure, but in their benign state do not invade surrounding tissues. They have the potential to become malignant, however, a large proportion do not progress to this state. *In situ* tumours usually develop in the epithelium, and their constituent cells are morphologically similar to cancer cells, but, as their name suggests, these tumours do not encroach on surrounding tissues. Malignant tumours, however, invade and destroy local tissue eventually metastasising to other parts of the body. In contrast to benign tumours, they do not have a fibrous barrier and the edges are not well-defined [3,4,5]. Cancer eventually kills through damage caused by the expanding number of malignant cells which progressively occupy vital parts of the body.

Metastasis occurs when cancer cells spread from the site of origin (the primary tumour) to other parts of the body (secondary tumours) [4]. During local invasion of tissue, tumour cells can enter the lymphatics and be carried to the regional lymph nodes. Some malignant cells are destroyed, but others continue to grow and may enter the bloodstream where they are carried around the body. Various proteases, including serine proteases, such as plasmin, thiol proteases, such as the cathepsins and metalloproteases, such as type IV collagenase, which normally function in tissue repair mechanisms, have been implicated in the invasion process [6]. In normal tissue, the activity of these proteases is kept under tight control by various protease inhibitors. Tumour cells also stimulate the production of new blood vessels (angiogenesis) by secreting tumour angiogenesis factor (TAF) in order to increase the supply of nutrients to the growing

tumour [3,6]. A feature of these new blood vessels is that they are weak and allow the passage of malignant cells, thus promoting metastasis.

In order for metastasis to take place, several criteria must be fulfilled [6]:

- [1] invasion of surrounding normal tissue, followed by infiltration into blood vessels and lymphatic channels;
- [2] release of malignant cells into the circulation;
- [3] survival of the malignant cells within the circulation;
- [4] arrest of the cells in capillary beds;
- [5] penetration of the lymphatic or blood vessel walls by the cells, culminating in the growth of secondary tumours at distant sites from the primary neoplasm.

The malignant cells adhere to the endothelium of the normal surrounding tissues inducing retraction and exposure of the underlying extracellular matrix. Part of this matrix comprises the basement membrane, which encloses the blood vessels, muscle cells and nervous system. The lymph vessels and other tissue cells are enclosed by the interstitial stroma, another part of the extracellular matrix, situated adjacent to the basement membrane. The mechanism of invasion by malignant cells has been elucidated by the work of Liotta [4] who maintain that it is an active process involving three main steps :

- [1] adhesion of the tumour cells to the basement membrane - mediated by specific receptors on the surface of the tumour cell;
- [2] activation of lytic enzymes which function to cleave or unravel molecules in the basement membrane;
- [3] the protrusion of pseudopodia from the tumour cells into the damaged tissue, followed by migration of the entire tumour cell.

These studies also showed that a group of enzymes termed metalloproteases, which cleave protein molecules, were intimately involved in the invasion process. Various metalloproteases exist, each with highly specific protein targets. They are produced in an inactive form where a terminal cysteine residue is folded and interacts with the metal ion within the active site of the enzyme. When activated, however, the conformation of the enzyme changes, and the cysteine residue is cleaved, allowing the enzymes to act upon their targets. Inhibitory enzymes are also produced, termed tissue inhibitors of metalloproteins (TIMPs). Various TIMPs are produced in normal tissues, such as cartilage and bone, but are also produced by tumour tissue. Thus cell invasion can be inhibited by TIMPs, sometimes referred to as metastasis suppressor proteins, and only proceeds if the balance is in favour of promoting factors. Another protein associated with suppression of metastasis is nm23 (nonmetastatic 23) [4]. Studies in primary breast cancers found that low levels of this protein were strongly associated with aggressive metastasis and poor survival, whereas high levels of the protein produced the opposite effect. Similar effects have also been seen in other cancers.

A pioneering treatment which specifically targets blood vessels supplying tumours will begin clinical trials shortly [7]. Tumours in mice and guinea pigs have been successfully treated with drugs which cause clots to occur in the small blood vessels supplying tumours. These drugs are specific for the tumour cells since they are linked to an antibody which binds to a specific antigen on the surface of the neoplastic blood vessels, not expressed by normal blood vessels. Vascular endothelial growth factor (VEGF) is secreted by tumour cells to aid in angiogenesis, and forms a complex on the surface of the blood vessel cells which may be targeted by this class of drugs. This factor is normally only expressed in embryos for the formation of new blood vessels, and is also found in wound healing. The drugs also contain a component which induces clot formation in the blood vessels thus blocking nourishment to the tumour.

Tumours are graded according to their state of differentiation, and there appears to be some correlation between the tumour grade and rate of growth [3]. Low grade tumours

(Grade 1) are the most differentiated and slow growing, whereas the higher grade tumours (Grades III and IV) are much more aggressive. Many tumours, however, are difficult to classify since the cell population is heterogeneous and there may be areas of more than one tumour grade present. The type of tumour affects prognosis, for example, approximately 80% of patients with Grade I breast tumours will be alive and well five years or more post-treatment, compared with only about 20% presenting with Grade IV tumours [3].

Carcinogenesis can be described as a multi-stage process, whereby cancer develops in discrete stages resulting from changes in regulatory genes [3,8&9] (Figure 2). Genotoxic agents, such as U.V. light and certain chemicals are thought to be the main causes of these changes, although recent evidence suggests that there are also instances of non-genotoxic carcinogenesis [10]. These will be discussed later. Genotoxic carcinogens are mutagens, but all mutagens are not necessarily carcinogens [10]. Thus, in the former case, a chemical may be Ames' Test positive (a test for mutagens and carcinogens) [11] but may not cause cancer. The effects of many genotoxic carcinogens appear to be overcome by the body's defence mechanisms at low doses, but above a certain threshold permanent genetic change (initiation) takes place.

The first stage, or initiation stage, in carcinogenesis occurs when a brief and irreversible reaction takes place between the carcinogen and the genetic material of the target tissue [3,9]. The cell now has the potential to develop and progress to tumourigenesis, but initiated cells remain latent until acted upon by promoters. Carcinogens can be classified into two groups, complete and incomplete [3]. Complete carcinogens, for example, polycyclic aromatic hydrocarbons and nitrosamines, can act as both promoters and initiators, whereas incomplete carcinogens require subsequent exposure of initiated cells to promoting agents which are not, themselves, carcinogenic [3]. These promoting agents, such as phorbol esters, hormones, high fat diets and the recently identified teleocidin and aplysiatoxin classes, induce the transformed cells to divide and form tumours. It has been found that most promoting agents act in a similar manner, in that

they bind to a specific receptor molecule, protein kinase C, thereby activating intracellular signalling mechanisms [3]. Promoting effects can be prevented in some instances by anti-promoters such as antioxidants and growth inhibiting factors [3,12]. A variety of different mechanisms may contribute to each of these sequential changes, such as the mutation of a gene which normally controls cellular growth and proliferation.

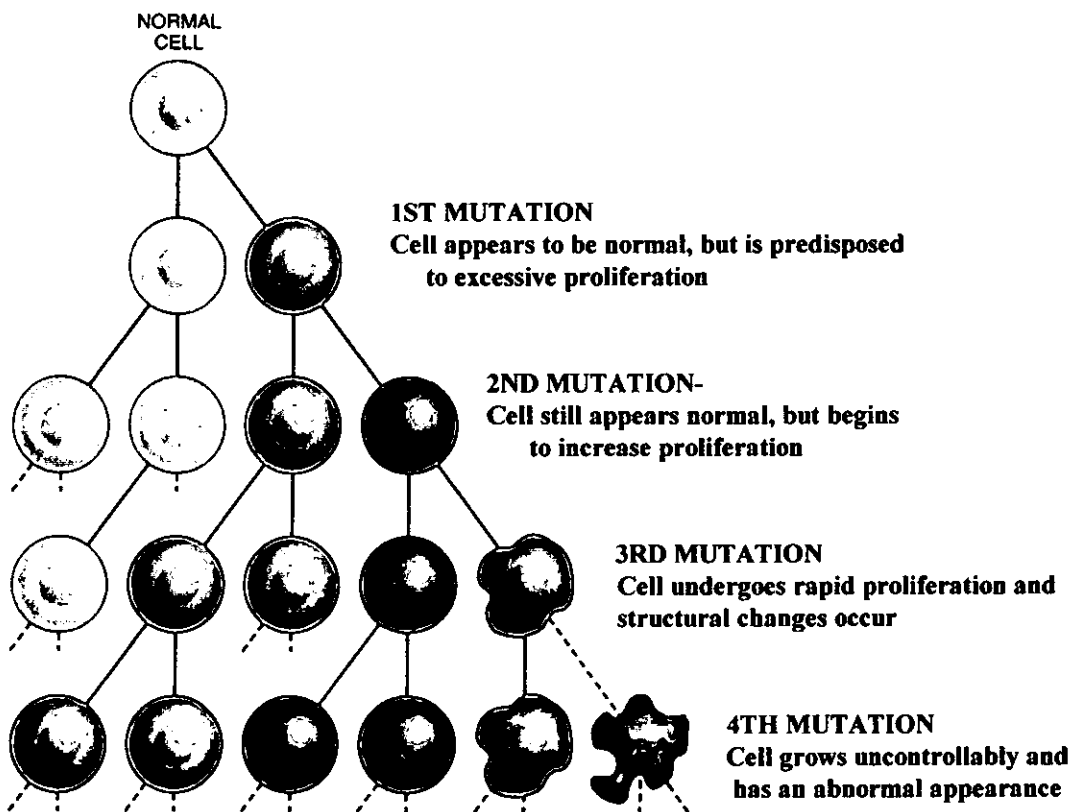


Figure 2 : Schematic diagram showing the onset of carcinogenesis from a normal cell (light brown). In the first stage daughter cell (pink) undergoes a cancer promoting mutation which is irreversible and heritable. At a future point one of the descendent cells (red) acquires a second mutation and a later descendent (green) acquires a third, and so on. These further mutations eventually result in malignant cell formation (purple). (Figure adapted from Cavanee & White, 1995 [13]).

1.1.1 Non-Genotoxic Carcinogenesis.

As discussed earlier, the most popular theory of carcinogenesis involves the two steps of initiation and promotion, however, it has also been shown that several drugs and environmental toxins which are carcinogenic in animal model systems are not mutagenic when tested *in vitro* [10]. This may pose serious implications for the screening of new chemicals and drugs. These agents are termed non-genotoxic carcinogens since they do not *directly* affect cellular DNA [14,15]. As mentioned previously, the balance of growth factors, hormones and cell cycle control factors is essential to normal cell development, therefore the effect of these non-genotoxic agents on the secretion of regulatory substances may subsequently lead to carcinogenesis. Many hormones and chemicals, such as growth hormones, sulfonamides and phenobarbitone [10], are used to some extent in animal husbandry which may subsequently enter the food chain, with potentially serious consequences for the consumer.

1.2 Genetics of Cancer.

Three main types of cellular gene have now been identified as being involved in the various stages of carcinogenesis, oncogenes, which are positive growth regulators, tumour suppressor genes (sometimes referred to as anti-oncogenes), which normally control cellular proliferation and a group of genes which are active in DNA repair mechanisms [8,9]. Some tumours may express a combination of mutated genes from all three classes. In normal circumstances the life-cycle of the cell is tightly controlled with a balance between the proto-oncogenes, which promote growth, and the tumour suppressor genes which have an inhibitory effect. Proto-oncogenes code for growth factors, hormone and growth factor receptors, signal transducing proteins, regulatory kinases, proteins that control these kinases and transcription factors which are intimately involved in controlling levels of gene expression (Table 1). This is a very complex area of research, since many different growth factors have now been identified which are

widely distributed in the body and perform many different functions. Many of these factors act in conjunction with others, and their functions can differ depending on the specific conditions.

Table 1 : Cellular role of some proto-oncogenes [8].

ROLE	ONCOGENE	HOMOLOGY
Proto-oncogene coding for :		
Growth Factors	<i>SIS</i>	Sub-unit of Platelet-Derived Growth Factor (PDGF)
Growth Factor Receptors (or functional homologues)	<i>ERBB</i>	Epidermal Growth Factor (EGFR)
	<i>FMS</i>	Colony Stimulating Factor 1 (CSF1R)
Signal Transducers	<i>ABL</i>	
	<i>MOS</i>	
	<i>RAF</i>	
	<i>RAS</i>	
	<i>SRC</i>	
Nuclear oncogenes	<i>JUN</i>	
	<i>MYB</i>	
	<i>MYC</i>	

1.2.1 The Cell Cycle

The cell cycle is composed of four stages, G₁, S, G₂ and M [2] taking, on average for a somatic cell, 12 to 24 hours to complete (Figure 3). The first stage, G₁ (gap 1), allows the cell to increase in size, accumulate nutrients and synthesise enzymes and proteins in preparation for DNA replication. The DNA is replicated in the next phase of the cycle,

the S (synthesis) stage. At this point the chromosomes are duplicated within the cell. The cell then goes through another gap phase (G_2) in order to prepare for cell division. This division takes place in the final phase of the cell cycle, the M (mitosis) stage. The enlarged parent cell now divides in half, yielding two daughter cells, each containing a full complement of chromosomes. The cells can enter a resting phase following M phase, called G_0 , where they may remain quiescent for hours, days or years [2,16]. Cell surface receptors interact with a variety of signals from growth factors, hormones *etc.* to determine whether the cell persists in cycling mode or enters the resting phase. There are various checkpoints within the cell cycle which determine whether or not the cell will continue through to cell division [3]; in particular there is a restriction point near the end of G_1 before the cell enters the S phase, and another checkpoint at G_2/M . The cell cycle may also be blocked at specific phases by certain chemotherapeutic agents [3] (Table 2).

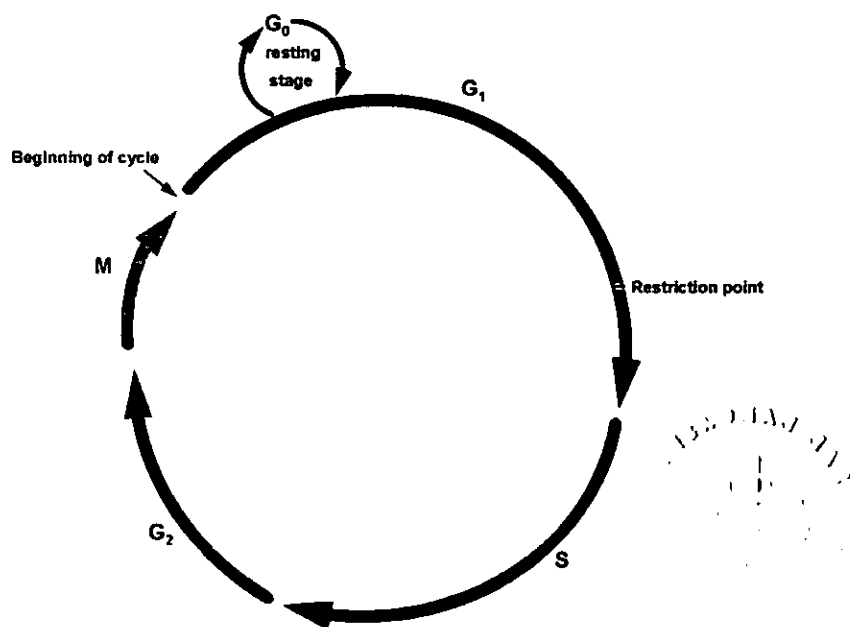


Figure 3 : Diagrammatic representation of the four stages of the cell cycle.

In the 1st stage (G_1) the cell increases in size and prepares to replicate its DNA. The replication occurs in the 2nd stage (S) where the chromosomes are duplicated. In the 3rd stage (G_2), the cell prepares to divide. Mitosis then occurs in the 4th stage (M). Two identical daughter cells are produced which may enter G_1 and go through the cycle again, or may enter the G_0 stage. An important control point, the restriction point occurs near the end of G_1 , where the cell decides whether to commit itself to completing the cycle.

Table 2 : Chemotherapeutic agents specific for the cell cycle. (Adapted from Franks & Teich [3]).

DRUG	SITE OF ACTION	PHASE SPECIFICITY
METHOTREXATE		
CYTOSINE ARABINOSIDE	DNA SYNTHESIS	S PHASE
HYDROXYUREA		
5-FLUOROURACIL	DNA, RNA & PROTEIN	RELATIVELY S PHASE
6-MERCAPTOPURINE	SYNTHESIS	SPECIFIC
NITROGEN MUSTARD	DNA AT ALL PHASES	
NITROSUREA	OF CELL CYCLE	WHOLE CYCLE
CYCLOPHOSPHAMIDE		
VINCRIStINE	MICROTUBULES	M PHASE, $G_1 \leftrightarrow G_0$

The cell cycle clock integrates messages from stimulatory and inhibitory pathways within the cell. Proteins termed cyclins and cyclin-dependent kinases play an essential role in regulation of the cell cycle [2,16]. The protein kinases are enzymes which transfer phosphate groups from adenosine triphosphate (ATP) to specific protein molecules, thereby altering the function of these proteins. At the restriction point in the late stages of the G_1 phase, the cell decides whether or not it will complete the cycle. In order for the cell to progress to the S phase, a molecular switch must be activated. This occurs when levels of cyclin D and then cyclin E are increased and in turn activate cyclin-dependent kinases [16]. These kinases form complexes which transfer phosphate groups from ATP to a protein called pRB. This protein has a major braking effect on the cell cycle which is effected by accumulating a variety of transcription factors. When pRB is phosphorylated, however, these proteins are released, allowing the cell cycle to progress.

Further factors are then produced, such as cyclins A and B and their relevant cyclin-dependent kinases, which serve to drive the cell cycle through to cell division. Various tumour suppressor gene products, such as p53, p15, p16, p21 and p27 act at a variety of points in the cell cycle to control inappropriate cell division [16]. The cell cycle clock is a highly complex system, maintaining a fine balance between stimulatory and inhibitory signals. Clearly, mutations in the genes encoding these proteins can have a potentially devastating effect on cell proliferation by disrupting the cell cycle

1.2.2 Oncogenes.

It has been known for many years that DNA and RNA viruses are capable of infecting cells and subsequently causing their transformation [9]. Although a few of these are human viruses, the majority are associated with animals and are not transmissible to humans. Much research into carcinogenesis has been based on the study of viruses, in particular the retroviruses [8,9]. These are RNA viruses which encode three genes, *gag*, *pol* and *env* which produce, respectively, a core protein, a reverse transcriptase and envelope glycoproteins. However, certain viral genes can also cause malignant transformation, and these encode a fourth type of gene, termed oncogenes. Further work has shown that some human tumours also contain activated oncogenes, which are homologous to the viral oncogenes. Research into the mechanisms employed by viral oncogenes has helped elucidate the mechanisms of carcinogenesis, but it must be emphasised that, so far, relatively few human viruses have been identified as being associated with cancer (Table 3).

Various genetic changes can activate the latent tumourigenicity of oncogenes [8]. The main mechanisms of mutation for non-viral oncogenes have been identified as point mutation, amplification and chromosomal translocation, all of which have been found in human tumours. Point mutations in the coding sequences of oncogenes can affect the resultant protein products. This in turn may affect the interaction between these protein products and regulatory molecules. Translocation of an oncogene to another

chromosome may result in enhanced expression of the oncogene. Some tumours, such as chronic myeloid leukaemia and Burkitt's lymphoma, are known to carry a consistent chromosome translocation [8]. Oncogene amplification, as the name suggests, leads to increased copy numbers of the cellular gene, resulting in increased amounts of protein products. Amplification of oncogenes has been shown to correlate with advanced tumour progression in some cases [9], for example, amplification of the *erb-B2* oncogene in advanced breast cancer.

Retroviral mechanisms for the activation of viral oncogenes have been identified as transduction (the most efficient), promoter/enhancer insertion (the most common) and transactivation. Retroviral transduction of an oncogene affects the expression of the gene, since it is subject to control by viral promoter and enhancer sequences [8]. Subsequent mutations in the oncogene result in altered protein products. Similarly, retroviruses can insert their dominant promoter and enhancer sequences near to cellular oncogenes, leading to increased gene expression. Some retroviruses, such as the human immunodeficiency virus (HIV) and the human T-cell virus (HTLV), are thought to produce a transcription factor which can increase gene expression on interaction with specific gene regulatory sequences [8].

It should be noted that the original cellular genes, with the potential to progress to tumour development, are termed proto-oncogenes. When the proto-oncogenes are mutated, they may become carcinogenic oncogenes which in turn encode for excessive amounts of growth factors or other gene products such as growth factor receptors involved in cell signalling.

Table 3 : Viruses commonly associated with human cancers [8].

VIRUS	ASSOCIATED TUMOURS
DNA viruses :	
Epstein-Barr	Burkitt's Lymphoma
	Nasopharyngeal cancer
Hepatitis B	Liver cancer
Papilloma virus	Benign warts
	Cervical cancer
RNA viruses :	
Human Immunodeficiency Virus (HIV-1)	Kaposi's sarcoma
Human T-cell Leukaemia Virus (Type 1) (HTLV-1)	Adult T-cell leukaemia
HTLV-2	Hairy cell leukaemia
HTLV-5	Cutaneous T-cell leukaemia

Various growth factors may be over-produced as a result of oncogenic activity, such as increased platelet-derived growth factor (PDGF) found in sarcomas and gliomas [16]. Receptor genes may also become oncogenic, resulting in the release of inappropriate signals within the cytoplasm; *erb-B2* receptor molecules seen in breast cancer cells are examples of this. Other oncogenes disrupt intracellular signalling pathways in the cell cytoplasm. Proteins which are encoded by normal *ras* genes function by transmitting stimulatory signals from growth factor receptors to other protein receptors in the signal cascade. When these genes are mutated, however, they transmit stimulatory signals even in the absence of growth factors.

The *myc* family of oncogenes are normally involved in transcription events in the nucleus [8]. These transcription factors are produced as a result of signals from growth factors in normal cells, however, in many types of cancer, abnormally high levels of Myc proteins are detected. Table 4 highlights a number of oncogenes which are now known to be implicated in human cancers.

Table 4 : Representative oncogenes associated with human tumours. (Adapted from Weinberg [16]).

GENE	GENE PRODUCT	ASSOCIATED CANCER(S)
<i>PDGF</i>	Platelet-derived growth factor	Glioma
<i>erb-B</i>	Receptor for epidermal growth factor	Glioblastoma, breast
<i>erb-B2 (HER-2, neu)</i>	Growth factor receptor	Breast, salivary gland, ovary, stomach.
<i>RET</i>	Growth factor receptor	Thyroid
<i>Ki-ras</i>	Signal transducer (stimulatory)	Lung, ovary, pancreas, colon
<i>N-ras</i>	Signal transducer (stimulatory)	Leukaemias
<i>c-myc</i>	Transcription factor	Leukaemias, breast, stomach, lung
<i>N-myc</i>	Transcription factor	Neuroblastoma, glioblastoma
<i>L-myc</i>	Transcription factor	Lung
<i>Bcl-2</i>	Protein blocks apoptosis	Follicular B lymphoma
<i>Bcl-1 (PRAD1)</i>	Cyclin D1 - stimulates cell cycle clock	Breast, head, neck
<i>MDM2</i>	Protein acts as an antagonist of <i>p53</i> tumour suppressor gene	Sarcomas and other cancers

1.2.3 Tumour Suppressor Genes.

Recent research has identified tumour suppressor genes in human tumours (Table 5). A major breakthrough came from the investigation of retinoblastoma, a hereditary cancer which affects the retina, and which is associated with the loss of material from chromosome 13 [13]. Studies suggested that the cause was due to either the loss, or inhibition of expression, of a normal gene rather than the presence or enhanced expression of a mutated form. The presence of the gene therefore appeared necessary for the suppression of tumour growth and was identified as *Rb-1* by Friend *et al.* [17]. Recent work has identified other tumour suppressor genes, in particular the *p53* gene, whose inactivation by mutation has been implicated in an increasing number of human cancers [18]. Interestingly, *p53* has also been shown to act as an oncogene, where many mutations have been shown to occur, causing its activation and subsequent tumourigenesis [9]. The gene product is known to act as a transcription factor which binds to other genes and controls their expression. It has been found to promote expression of the *WAF1/Cip1* gene whose protein product p21 binds to cyclin-dependent kinases and inhibits their action [18,19]. This activity is intimately involved in the cell cycle and is thought to allow DNA repair mechanisms to take place. Other studies have shown that human papilloma virus (HPV), which is associated with over 90% of cervical cancer cases, produces a viral protein EP-AP which interferes with p53 activity [18]. Another gene, *MTS1*, whose normal expression is involved in inhibition of the cell cycle through its protein product p16, has recently been found to be mutated or deleted in a number of tumours [20]. Transforming growth factor beta (TGF- β) functions to stop the growth of various normal cells, however, in certain cancers such as colon cancer, the gene encoding the receptor for TGF- β is inactivated, thus allowing uncontrolled growth [16]. Some tumour suppressor genes also act to counter the effects of growth stimulating products, for example, the protein product of the *NF-1* gene acts directly on a Ras protein to inhibit the release of growth-stimulating products [16].

Table 5 : Representative tumour suppressor genes implicated in human cancers.
(Adapted from Weinberg [16]).

GENE	GENE PRODUCT	ASSOCIATED CANCER(S)
<i>APC</i>	Cytoplasmic protein	Colon, stomach
<i>DPC4</i>	Signal transduction (inhibitory)	Pancreas
<i>NF1</i>	Protein inhibits Ras protein	Neurofibroma, phaeochromocytoma, myeloid leukaemia
<i>NF2</i>	Cytoplasmic protein	Meningioma, ependymoma, schwannoma
<i>MTS1</i>	p16 protein- braking component of cell cycle clock	Wide range of cancers
<i>RB</i>	pRB protein - important regulator of cell cycle	Retinoblastoma, bone, bladder, breast, small cell lung
<i>p53</i>	p53 protein - halts cell division and can induce apoptosis in abnormal cells	Wide range of cancers
<i>WT1</i>	Nuclear protein	Wilms' tumour
<i>BRCA1</i>	Cellular location unclear	Breast, ovary
<i>BRCA2</i>	Cellular location unclear	Breast
<i>VHL</i>	Cellular location unclear	Kidney

1.3 Cancer Therapy

Increased knowledge of cellular immunology and the genetic basis of cancer has widened the scope for treatment of this invidious disease. Genetic therapy and immunotherapy offer exciting new advances and hope for the future, but many of these treatments are still experimental and are often used as adjuncts to more conventional modalities. Primary cancers which have not spread from their site of origin can be successfully treated with surgery and/or radiotherapy, with, hopefully, minimal damage to surrounding tissue. Unfortunately, most cancers are not diagnosed at this early stage and thus, on clinical presentation, metastasis has already taken place. In this situation, treatment must be applied systemically (often in conjunction with surgery and radiotherapy). The utopian aim of chemotherapy is to selectively target the malignant cells, but without damage to normal cells. In practice, this is very difficult to achieve, since there are close similarities between the malignant cells and normal cells. Many anti-cancer drugs therefore produce unpleasant, toxic side-effects at therapeutic doses since they also affect normal cells, in particular rapidly dividing cells such as those in the gut mucosa, hair follicles, bone marrow and thymus. Other commonly encountered problems are cardiotoxicity and nephrotoxicity. Although much progress has been made, the overall prognosis is still very poor.

1.3.1 Multiple Drug Resistance

A number of factors may contribute to the failure of chemotherapy, the main ones being the inability of the drug to reach the cellular target, due to the lack of specificity mentioned above, physiological factors such as the size, distribution and localisation of the tumour, coupled with metabolic considerations [5] and, as a major problem, the development of drug resistance at a cellular level. In many cases the initial response to treatment is encouraging, with tumour shrinkage due to the elimination of drug sensitive cells, however, when relapse occurs, it is often associated with the development of drug resistance. Drug resistance may have many forms; it may sometimes be specific to a

particular drug, for example, increased production of the target enzyme dihydrofolate reductase (DHFR) in methotrexate resistance [21]. Methotrexate acts by inhibiting DHFR, an essential enzyme involved in DNA synthesis, however, the drug must be present continuously in a free form to effect this inhibition [3]. Treatment with a single drug also frequently results in the development of cross-resistance to other, non-related drugs. This phenomenon is referred to as multiple drug resistance (MDR) and further chemotherapy is often ineffective. Although these drugs are chemically unrelated, many of them are positively charged at neutral pH and are relatively hydrophobic [22]. Some progress has been made using combinations of drugs and certain cancers such as Hodgkin's disease, large cell lymphoma, acute lymphocytic leukaemia, testicular cancer and early stage breast cancer [23] are now potentially curable, with others showing good clinical responses, for example, ovarian cancer [23]. However, many cancers still remain refractory to treatment, with MDR being a major barrier to success.

There are two distinct types of cellular resistance : *de novo* or intrinsic resistance and acquired pleiotrophic resistance [24]. Many neoplasms, such as melanoma, colon and non-small cell cancers, are refractory to treatment, since the cells are intrinsically resistant to chemotherapy at the time of transformation. Acquired resistance, as the name implies, occurs after exposure to chemotherapeutic agents. This cellular resistance is often associated with a decreased intracellular concentration of the drug. Two theories were initially proposed for this phenomenon, either active drug efflux from the cell or decreased permeability of the membrane. Since the plasma membrane is the first line of defence of the cell, it was reasoned that this was the probable site of action. However, studies thus far have shown that the main mechanism for this decreased accumulation of drug is due to an energy dependent pump, P-glycoprotein (Pgp) situated in the plasma membrane of the cell [25], although decreased drug uptake has also been identified in many cell lines with a variety of drugs [26]. Recent research has highlighted the existence of two other proteins which are also now thought to play an important role in MDR : the Multidrug Resistance-associated Protein (MRP) [22] and the Lung Resistance-related Protein (LRP) [27] which have been isolated in many multidrug

resistant tumours. Other mechanisms of drug resistance do, however, exist and will be discussed later.

1.3.2 P-glycoprotein.

Tumour cells displaying the 'classic' MDR phenotype are resistant to anthracyclines, *Vinca* alkaloids, epipodophyllotoxins, taxol and actinomycin D [26]. Cells displaying this phenotype have been found to overexpress a 170-180 kDa glycoprotein in their cell membrane, commonly referred to as P-glycoprotein (Pgp). This protein is encoded by an MDR gene in both humans and rodents [26,28]. Two MDR genes, *MDR1* and *MDR3* (sometimes cited as *MDR2*), have been isolated in humans, but only the *MDR1* gene seems to be active in encoding Pgp mRNA of approximately 4.5 kilobases in drug resistant cell lines. Although the *MDR3* gene is closely related, its function has not yet been determined. The human *MDR1* gene has been localised to chromosome 7q 21.1. Increased *MDR1* mRNA has been shown to result from gene amplification in both rodent and human cell lines, however, increases in *MDR1* mRNA have also occurred in the absence of amplification, suggesting that the *MDR1* gene may be regulated by transcription and / or translation [29, 30].

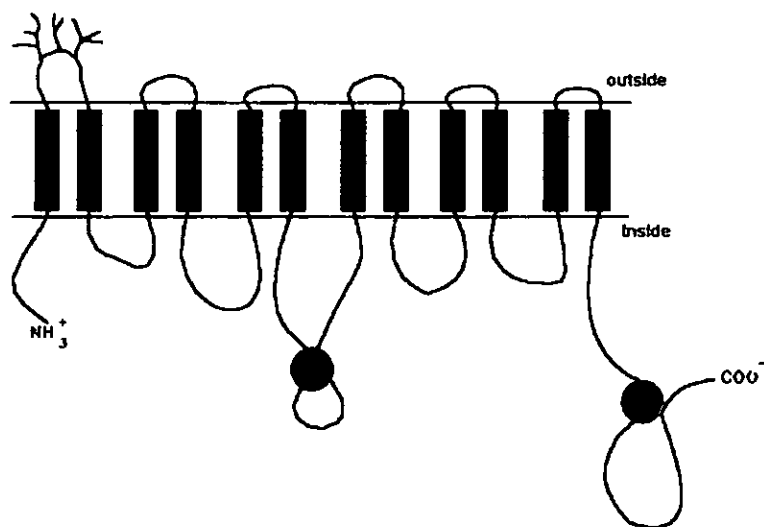
Pgp consists of 1280 amino acids, expressed as a single polypeptide chain containing two homologous portions of equal length [31, 32, 33]. The two hydrophilic domains in the cytoplasm each contain an ATP binding site, are approximately 43% homologous and are located near the carboxy-terminal of Pgp [34]. Initially, it was thought that Pgp consisted of twelve transmembrane domains with six extracellular loops and two cytoplasmic ATP binding domains (Figure 4a) [25] and this has been supported by antibody localisation data [35]. However, an alternative model has now been proposed (Figure 4b) [36]. Another glycosylation site has been identified in the second half of the Pgp, in addition to the sites previously found in the first extracellular loop [37, 38, 39]. This glycosylation site links transmembrane domains 8 and 9 of the original Pgp model thus it is suggested that they are located extracellularly [36].

Pgp has been identified as an energy-dependent drug efflux pump belonging to the adenosine triphosphate binding cassette (ABC) family of transporters [25]. It is homologous to the haemolysin B pump which is present in the cytoplasmic membrane of some bacteria [40]. Recent studies, however, have indicated that it may function as a flippase [41]. Higgins & Gottesman [41] suggested that hydrophobic drugs may be removed from the plasma membrane before they reach the cytoplasm, using the analogy of a 'hydrophobic vacuum cleaner' to describe the function of the transporter. This model helps to explain discrepancies in transport kinetics since it has been shown that drugs initially partition into the lipid bilayer and then interact with Pgp. Thus, the ability of the drug to partition into the bilayer, coupled with the lipid composition of the membrane, will affect the concentration of the drug available to the transporter, but will not necessarily correlate to the concentration of the drug being administered [36].

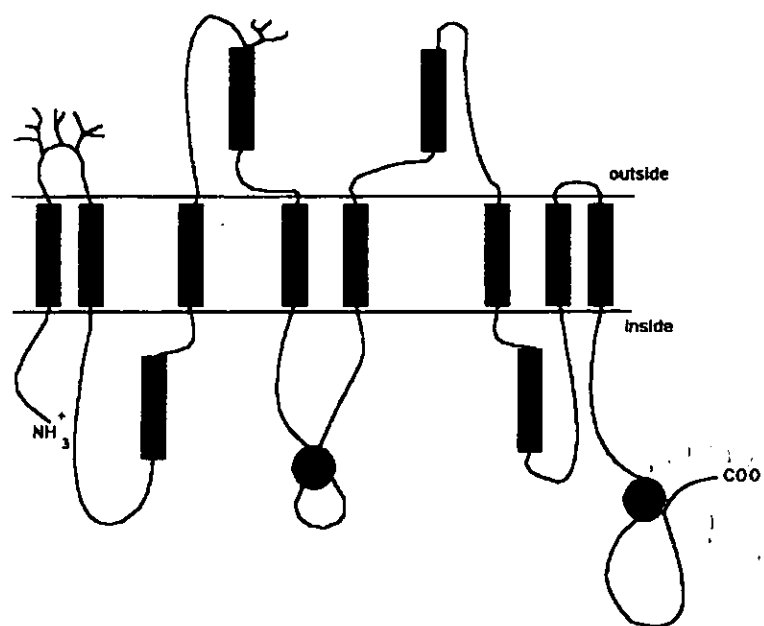
Several normal tissues also express high levels of Pgp : hepatocytes, pancreas, small and large bowel, kidney, adrenal cortex, endothelial cells of the CNS, testis, human placenta and CD34+ bone marrow cells [22, 42]. It has been suggested that Pgp may function in normal cells to excrete xenobiotics and endogenous hydrophobic compounds, such as steroid hormones, in order to protect these tissues from toxic compounds [43]. Many of the tumours which are intrinsically resistant to chemotherapy are derived from tissues which normally express the product of the *MDR1* gene. For example, carcinomas of the colon, kidney and adrenal cortex and hepatomas and pheochromocytomas all express high levels of *MDR1* mRNA [44].

Pgp is highly homologous to the cystic fibrosis transmembrane conductance regulator protein (CFTR), which functions as an ATP-dependent cyclic adenosine monophosphate-regulated chloride channel. It has recently been postulated that P-glycoprotein is associated with volume-regulated chloride channel activity [45], suggesting that it might not be used as a drug transporter in some of the tissues, rather that it may function as a chloride channel, however; this observation is now in doubt [46]. A recent study by Viana *et al.*, [47] compared the characteristics of volume-activated chloride currents,

drug transport function and levels of Pgp expression between a parental human leukaemia cell line (K562) and a resistant sub-line, derived by vinblastine selection (K562 VBL400), but found no association between Pgp expression and volume-sensitive chloride channels.



(a)



(b)

Figure 4 : Proposed topological models for P-glycoprotein (Pgp). The original model, based on the hydropathy profile, is represented by Figure 4a, and the alternative model, postulated by Zhang & Ling [37], is represented by Figure 4b. The red circles represent ATP-binding sites. (Adapted from Bellamy [36]).

1.3.3 Other Mechanisms of MDR.

Classical MDR, or typical MDR, has been traditionally associated with the overexpression of Pgp mRNA, however, it has become clear that certain cell lines also exhibit MDR in the absence of Pgp. Some of these cell lines are cross-resistant to a variety of natural product chemotherapeutic agents, but not to the *Vinca* alkaloids and colchicine. Studies found them to have unaltered drug uptake, accumulation and efflux, but to contain an altered form of the nuclear enzyme, topoisomerase II [48, 49]. The enzyme has been shown either to be present in a mutated form or in decreased intracellular levels. This type of MDR was identified as 'atypical' MDR by Danks *et al.* in 1988 [50]. Topoisomerase II is also involved in classical MDR since it is an important target enzyme for many of the anti-tumour drugs exported by Pgp, and this overlap between classical MDR and atypical MDR adds to the complexity of elucidating cellular resistance mechanisms.

Non-Pgp MDR has also been recognised, for example, cross-resistance to *Vinca* alkaloids, anthracyclines and actinomycin C has been associated with decreased intracellular drug concentration, but in the absence of P-glycoprotein [51, 52]. Many proteins have now been identified as being overexpressed in MDR cell lines [48], but definitive proof of their role in MDR is so far unavailable. However, as previously mentioned, two proteins which have attracted the most recent attention are the Multidrug Resistance-associated Protein (MRP) and the Lung Resistance-related Protein (LRP).

1.3.4 Mutidrug Resistance-associated Protein.

MRP, the product of the *MRP* gene, has now been shown to be very important in MDR and has recently generated a great deal of research [53,54,55]. Cole *et al.* [53] demonstrated the overexpression of MRP mRNA in a doxorubicin-resistant lung cancer cell line which displayed classical cross-resistance to anthracyclines, *Vinca* alkaloids and

epipodophyllotoxins, but did not overexpress Pgp mRNA. MRP is a 1531-amino acid *N*-glycosylated integral membrane protein, encoded by a 6.5 kilobase mRNA and has been localised to chromosome 16p 13.1 [53]. It has been identified as a 190 kDa protein belonging to the large ABC transporter family, in common with Pgp [53] and has been located in the plasma membrane and the endoplasmic reticular membrane [56]. The proposed structure of the MRP protein is shown in Figure 5.

Overexpression of the *MRP* gene in human cancer cells has been associated with increased activity of the glutathione *S*-conjugate carrier in isolated plasma membrane vesicles [57]. The function of this efflux pump is to mediate excretion of bivalent anionic conjugates from mammalian cells and it is also thought to be involved in the excretion of xenobiotic conjugates [57]. Müller *et al.* [57, 58] suggest that MRP is involved with multidrug resistance by promoting the export of drug modification products from cells. Drug resistance attributed to altered glutathione (GSH) and/or GST levels within the cells may therefore be involved with MRP expression. Leier *et al.* [54] have shown that MRP mediates the ATP-dependent transport of the endogenous glutathione conjugate leukotriene C₄ (LTC₄), and further studies have found that MRP also mediates the ATP-dependent transport of anionic conjugates of lipophilic compounds and glutathione disulfide [59].

MRP mRNA has been shown to be expressed at low levels in most, if not all, normal tissues, including peripheral blood, endocrine glands, striated muscle, lymphoreticular system, digestive tract, respiratory tract and urogenital tract [60]. Various human cancers have been studied with regard to MRP mRNA expression, with the highest expression being shown in chronic lymphocytic leukaemia and prolymphocytic leukaemia [60,61]. MRP mRNA has also been found to be overexpressed in other cancers such as acute myelocytic leukaemia, squamous cell carcinoma, oesophageal and non-small cell lung cancers [60,62]. Association with a number of other neoplasms has also been noted, such as soft tissue sarcomas, melanoma, cancers of the prostate, breast, kidney, bladder, testis, ovary, colon and other haematological malignancies. However, MRP

mRNA is usually expressed at low levels in these cases [60]. A further study has shown that expression of the *MRP* gene also correlates with the amplification and overexpression of the *N-myc* oncogene in childhood neuroblastoma [63].

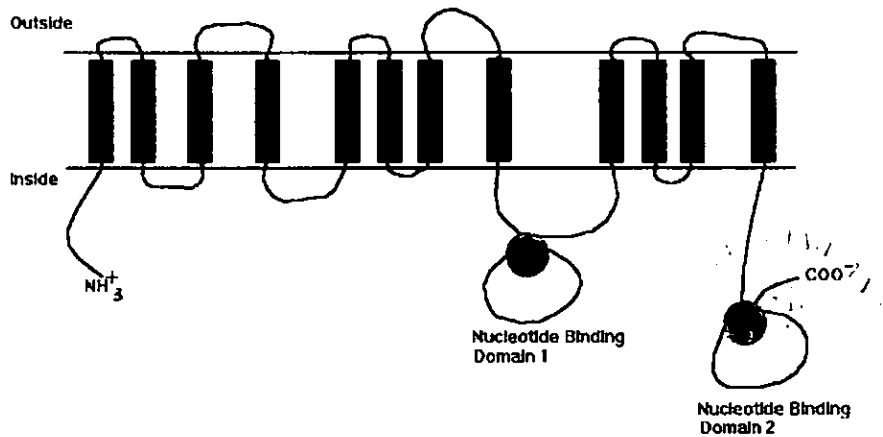


Figure 5: Proposed topological model for the Multidrug Resistance-associated Protein (MRP).

Red circles represent ATP-binding sites. (Adapted from Bellamy [36]).

1.3.5 Lung Resistance-associated Protein.

LRP is a 110 kDa protein which is overexpressed in many non-Pgp expressing cell lines and has been found to be a good predictive marker for resistance to chemotherapy in acute myeloid leukaemia and ovarian cancer [64,65,66]. The *lrp* gene has been localised to the short arm of chromosome 16, within the 16p 13.1-16p 11.2 chromosomal region [67,68]. Interestingly, two other genes which are associated with MDR, the *MRP* gene and the gene encoding protein kinase C- β , have also been mapped to this region [66]. Protein kinase C is known to be implicated in MDR since it increases the activity of Pgp upon phosphorylation. Most of the MDR cell lines which overexpress the *lrp* gene also overexpress *MRP* [69,70], however, although these two genes are often co-upregulated in MDR cell lines, studies have shown that each gene can be regulated independently [66]. By contrast, most MDR cell lines which overexpress the *MDR1* gene, encoding Pgp, do not overexpress *lrp* [69]. There are, however, some exceptions, such as the MCF7/D40 breast cancer cell line and some 8226 myeloma sub-lines, which overexpress

both *MDR1* and *lrp* genes [69,71]. A recent study of melanoma cell lines and melanocytic lesions, comparing Pgp, MRP and LRP overexpression, found little or no MRP and Pgp expression, but high expression of LRP [72].

LRP has been found to be highly conserved across species, suggesting a constitutive role in cellular function. It has been shown to be widely distributed in both normal and neoplastic tissue [69,73], although the distribution is varied. Normal tissues which are exposed to xenobiotics, metabolically active tissue and macrophages typically display high levels of LRP [73], suggesting a protective role for LRP against xenobiotic agents. A similar pattern of distribution has been noted for other proteins associated with MDR, such as MRP and Pgp [74]. Other normal tissue shows a more variable distribution of LRP [73] and neoplastic tissue also shows varied expression of LRP, which appears to correlate with the susceptibility of the tumour to chemotherapy. Tumours which are refractory to chemotherapy, for example, renal, pancreatic and colon cancers, are usually LRP positive, whereas those which are highly chemosensitive, such as leukaemias, germ cell tumours and neuroblastoma, rarely express the protein [73].

A cDNA coding for the *lrp* gene has been isolated from a human fibrosarcoma cell line (HT1080/DR4) [67] and comparative sequence analysis has demonstrated that LRP shares 57% amino acid homology with that of the major vault protein of *Dicytostelium discoideum* [75] and 87.7% amino acid homology with that of *Rattus norvegicus* [76]. LRP has subsequently been identified as the major human vault protein (MVP) and is described as 'the most abundant component of the previously described multisubunit particles termed vaults' [77,78].

Vaults are ribonucleoprotein particles and were first identified in 1986 as contaminant particles of clathrin-coated vesicle preparations derived from rat liver [77,78]. Animal studies have shown vaults to be most widely distributed in epithelial cells and in macrophages, which correspond to LRP distribution in human tissue [79]. Most vaults are present in the cytoplasm and the majority of cells contain thousands of vaults [73],

however, to date, their functions are not fully understood. They are novel cellular organelles widely distributed and highly conserved among various eukaryotic cells, suggesting that they are involved in fundamental cellular processes [57]. Studies using electron microscopy have shown vault proteins to be barrel-like structures (approximately 57 x 32 nm), with a molecular mass of around 13MDa (Figure 6), and as such are the largest ribonucleoprotein particles reported to date [79]. The barrel structure is symmetrical, comprising two identical cup-like halves, each of which opens up into a flower-like arrangement with eight petals arranged around a central ring.

Approximately 5% of the vaults are nuclear-associated and localise to the nuclear pore complexes (NPC) [80] possibly constituting the central plug of the NPC [81]. They are thought to be the transporter units of the NPC and it has been suggested that they may play a role in MDR by mediating the bidirectional transport of various substrates between the cytoplasm and the nucleus thereby regulating cytotoxic drug levels [78]. A different intracellular distribution of certain chemotherapeutic agents, such as daunorubicin, is exhibited by some MDR cell lines in comparison to their parental cell lines [81] and this has been suggested to be linked to the function of vaults. Gervasoni *et al.* [81] have shown MDR cells to distribute daunorubicin into the perinuclear region initially, then subsequently to redistribute the drug away from the nucleus into the cytoplasm. Conversely, the same authors showed that the parental cells localised daunorubicin in a diffuse nuclear and cytoplasmic pattern. Reduced nuclear accumulation of daunorubicin has also been reported in the MDR cell line 2R120 which overexpresses *lrp* [82]. It has not yet been established to which structures daunorubicin localises in the perinuclear and cytoplasmic regions of MDR cells, but it has been postulated that vaults may be such structures [73]. Izquierdo *et al.* [66] hypothesised that vaults may play a role in MDR by regulating both the cytoplasmic redistribution and the nucleocytoplasmic transport of drugs.

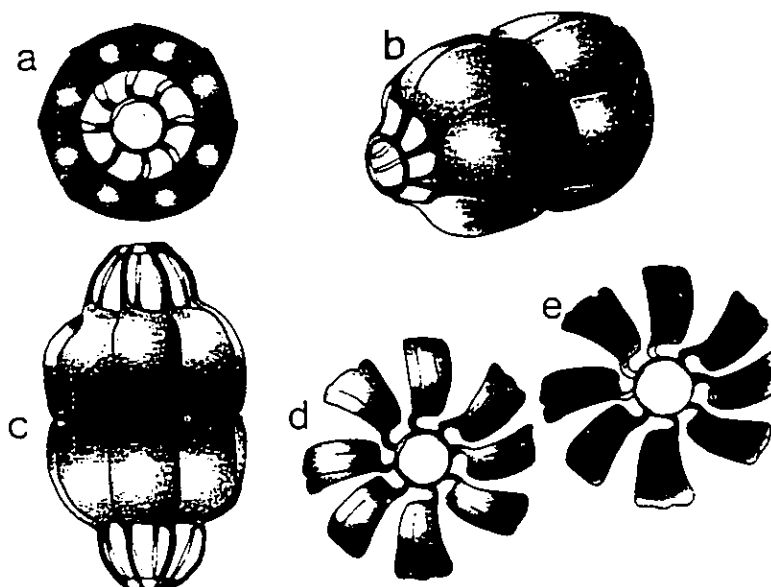


Figure 6 : Proposed model of a vault structure. [66]

The intact vault particle is a barrel-like structure, represented here in end-on, oblique and side views (a), (b) & (c), respectively. The vault has 2-fold symmetry and each half can be opened up into a flower-like structure, containing eight 'petals' surrounding a central ring [79], represented by (d) & (e).

1.3.6 Glutathione and glutathione *S*-transferases.

Studies of mutant cells exhibiting the MDR phenotype have also shown that there may be several other mechanisms involved in MDR. Many biochemical changes have been associated with these cells, such as altered metabolic enzymes and proteins as well as lipids and enzymes involved in membrane fluidity and signal transduction [3,83]. Glutathione-*S*-transferases (GSTs) are important Phase II metabolic enzymes which have been implicated in MDR [84]. This group of enzymes catalyse the conjugation of reduced glutathione (gamma-L-glutamyl-L-cysteinylglycine) to a variety of molecules prior to their excretion. Several GST isozymes have been described and are classified as alpha (α), mu (μ) and pi (π) [60]. Mannervik *et al.* [85] have recently described the subunits of these classes as follows : α class GST subunits as GSTA1-1 and GSTA2-2; μ class GST subunits as GSTM1a-1a, GSTM1b-1b, GSTM2-2 and GSTM 3-3; and π GST

subunits as GSTP1-1. Various studies have correlated increased cellular GST levels with resistance [84,86-89], however, other studies have found conflicting evidence [90,91]. Overexpression of the α class of GSTs has been associated with increased resistance to alkylating agents used in cancer chemotherapy [92]. The π class of GSTs has consistently been found to be elevated in human cancer tissue and MDR cell lines, and is also used as a tumour tissue marker in some cases [92]. Singh *et al.* [93] demonstrated that many chemotherapeutic agents are substrates for GSTs, such as cyclophosphamide, nitrogen mustard, melphalan, chlorambucil, VP-16, 6-thiopurine, mitomycin C and mitoxantrine, however, these are not traditionally associated with MDR. A recent review of the role of glutathione and glutathione-related enzymes in MDR by Moscow and Dixon [91] casts doubt upon the role of GST-conjugation in MDR. They found scant biochemical evidence to support the conjugation of MDR drugs prior to their excretion, and, in particular, that no evidence of GSH conjugates of doxorubicin, vincristine, etoposide or actinomycin D has been documented. The only exception appears to be the effect of microsomal GST, a membrane bound enzyme, which has been shown to be involved in the metabolism of mitoxantrone [94].

Glutathione also binds strongly to hydrophobic compounds, thus playing a protective role in the cells by binding toxic substances, and thereby preventing their interaction with specific cellular targets. It has been suggested that GSTs may exert their effect in MDR by binding anti-tumour agents to glutathione and transporting them to the Pgp pump for export [95], however, Moscow and Dixon again report that there is no evidence to support this with regard to MDR drugs and their metabolites [91]. Similarly, Black *et al.* [96] found no evidence that GSTP1-1 and GSTA1-1 could bind doxorubicin. Organic peroxides are produced as metabolites of certain anti-cancer agents and it has been suggested that the intrinsic peroxidase activity of certain GST classes, in particular the α GSTs, may be protective in these cases. However, the π GSTs, which are most frequently elevated in MDR tissue, have very little intrinsic peroxidase activity [97]. The recently identified involvement of MRP may shed new light upon the role of GSH and GSTs in MDR.

1.3.7 Circumvention of MDR.

A large number of agents have been found to circumvent multi-drug resistance, with varying success (Table 6). The main mechanism by which these agents exert their effect is *via* competitive inhibition of the hydrophobic binding of drugs to Pgp, thereby increasing the intracellular accumulation of the agent [98]. Two drugs frequently used are verapamil [99] and cyclosporin A [100]. There are, however, limitations, and although many of these agents are effective *in vitro*, severe toxic side effects, such as cardiotoxicity, often ensue *in vivo* [23]. A recent interesting finding by Clynes *et al.* [83] shows that salicylate can reverse MDR in a variety of cell lines. Other reversal strategies include the modification of the MDR1 gene or its mRNA [101]. Clearly, identifying and/or synthesising agents which can circumvent MDR at safe therapeutic doses is an important objective for cancer research.

Table 6 : Reversing agents of classical MDR. (Adapted from Lehnert, 1994 [98]).

CLASSIFICATION	DRUG
Calcium channel blockers	Verapamil; bepridil; nifedipine; diltiazem; flunarizine; nitredipine; nimodipine.
Calmodulin inhibitors	Trifluoperazine; thioridazine; chlorpromazine; clomipramine.
Lysomotropic agents	Quinine; quinidine; chloroquine; quinacrine.
Steroids	Progesterone.
Anti-oestrogens	Tamoxifen; toremifene.
Cyclic peptide antibiotics	Cyclosporin A.
Miscellaneous	Dipyridamole; amiodarone; cefoperazone; cefriatraxone; erythromycin; reserpine; tween 80; amphotericin B.

1.4 Photodynamic Therapy.

1.4.1 Brief History of Photodynamic Therapy.

Photodynamic therapy (PDT) exerts its cytotoxic action *via* the combination of a photosensitizer, light of a suitable wavelength and molecular oxygen [102]. PDT is not a new concept, indeed, one of the earliest recorded uses was the treatment of skin disorders with psoralens extracted from weeds growing in the river Nile in ancient Egypt [103]. The first observation of the photodynamic effect was seen by Raab in 1900 [104] who demonstrated the cytotoxic action of light, in the presence of oxygen, in paramoecium which had previously been sensitized by acridine orange. Similarly, von Tappeiner and Jesionek (1903) [105] treated skin cancer with topically applied eosin exposed to sunlight. Although much research was carried out in the intervening years into the mechanisms of action of PDT, little progress was made with clinical treatment due to problems with poor light absorption and ineffective light delivery.

A resurgence of interest in PDT occurred in the 1960s and 1970s due to the development of haematoporphyrin derivatives and more sophisticated laser light delivery systems. Haematoporphyrin, a derivative of the naturally occurring protoporphyrin IX, was found to be a very effective photosensitizer, but it did not accumulate in tumour tissue and was therefore not a good candidate for PDT [106]. In 1960, Lipson and Baldes [cited in 107] developed some haematoporphyrin derivatives (HpDs) which were also very good photosensitizers and had the added advantage of selective tumour localisation. In the early 1970s the first experimental treatments on animal tumours were carried out [108,109]. Further porphyrin analogues such as the chlorins [110] and the phthalocyanines [111], the so-called second generation photosensitizers, were developed and an improved Photofrin has been in clinical use for skin disorders, including neoplasms, for some time [104,112]. The mechanism of action of psoralen, a natural product common in leguminous plants, was also elucidated in the 1970s, when it was found to insert into cellular DNA on exposure to UV light, causing cross-linking, thus

interfering with cell division [112]. Psoralen and its derivatives, in particular 8-methoxypsoralen [106], have been long established in the treatment of psoriasis. There are, however, some drawbacks in the long term use of psoralen, not least its effect on the DNA of healthy cells, which may result in potentially serious side effects, including skin cancer.

1.4.2 Mechanism of Action of PDT.

Cell killing in PDT is known to occur *via* two pathways [113] : redox reactions between the photoexcited sensitizer and biomolecules (Type I) or *in situ* generation of cytotoxic singlet oxygen by the photosensitizer (Type II) (Fig.7). The photosensitizer, in its ground state, absorbs a photon on exposure to light and assumes an excited singlet state which is very unstable and has a very short half-life. At this stage, the photosensitizer may decay back to the original ground state emitting fluorescence and resulting in no photodynamic effect. Alternatively, the excited photosensitizer may cross over to the triplet excited state which confers much more stability to the molecule and increases its half-life by approximately 10 fold. In Type I reactions, the excited triplet photosensitizer may react with a biomolecule by electron or hydrogen transfer, which produces radical forms of the substrate. These radicals react directly with molecular oxygen, producing various free radicals such as hydroxyl ions, hydrogen peroxide and superoxide. Type II reactions are thought to be more common, and in this case the excited triplet state interacts with ground state oxygen, and the transfer of energy which ensues generates singlet oxygen, a highly reactive species. The two reactions may occur simultaneously, and the ratio between the two processes is highly influenced by the photosensitizer and the environment.

Most of the studies into actual sites of action and drug localisation have been carried out on the porphyrin-based drugs, but the initial target site is still not clear since the toxic compounds interact efficiently with many cellular sites. Cellular membranes are known to be damaged by lipid peroxidation, and protein cross-linking, and the photooxidation of

unsaturated fatty acids also occurs [102]. Moan *et al.* [114] showed that porphyrins bind to the plasma membrane, and some light-induced alterations to the membrane, such as K^+ leakage or inhibition of certain membrane transport systems have been reported in cultured cells [115]. Mitochondria are particularly vulnerable targets for PDT damage, since porphyrin and other photosensitizers have been shown to localise there preferentially. Various sites of mitochondrial photodamage, such as membrane disruption, changes in membrane potential and damage to the cristae have been observed [116]. Nuclear damage is not thought to be a primary target in porphyrin-induced PDT damage, although there have been some reports of DNA damage, particularly to the guanine base [117]. HpD has been shown to convert guanine into 8-hydroxyguanine. DNA polymerases and DNA ligases may also be inhibited as a result of photosensitization, although this mechanism has not yet been fully elucidated [116].

In addition to intracellular damage, there is substantial evidence to show that porphyrin PDT induces vascular injury, and it has been suggested that initial sites of action may involve the sub-endothelial collagen matrix and endothelial cells of the microvasculature [102]. Reduced blood supply to the tumour, due to vasoconstriction and cell aggregation results in the eventual destruction of the tumour [116]. Studies have shown that various cyclooxygenase products, such as thromboxanes and prostaglandin E_2 are released following phototherapy, which induce vascular injury [118]. In addition, *in vivo*, tissues treated with PDT appear to be infiltrated by lymphocytes and plasma cells and various cytokines are released, suggesting an immune response. Immunosuppression has also been described by Jolles *et al.* [119].

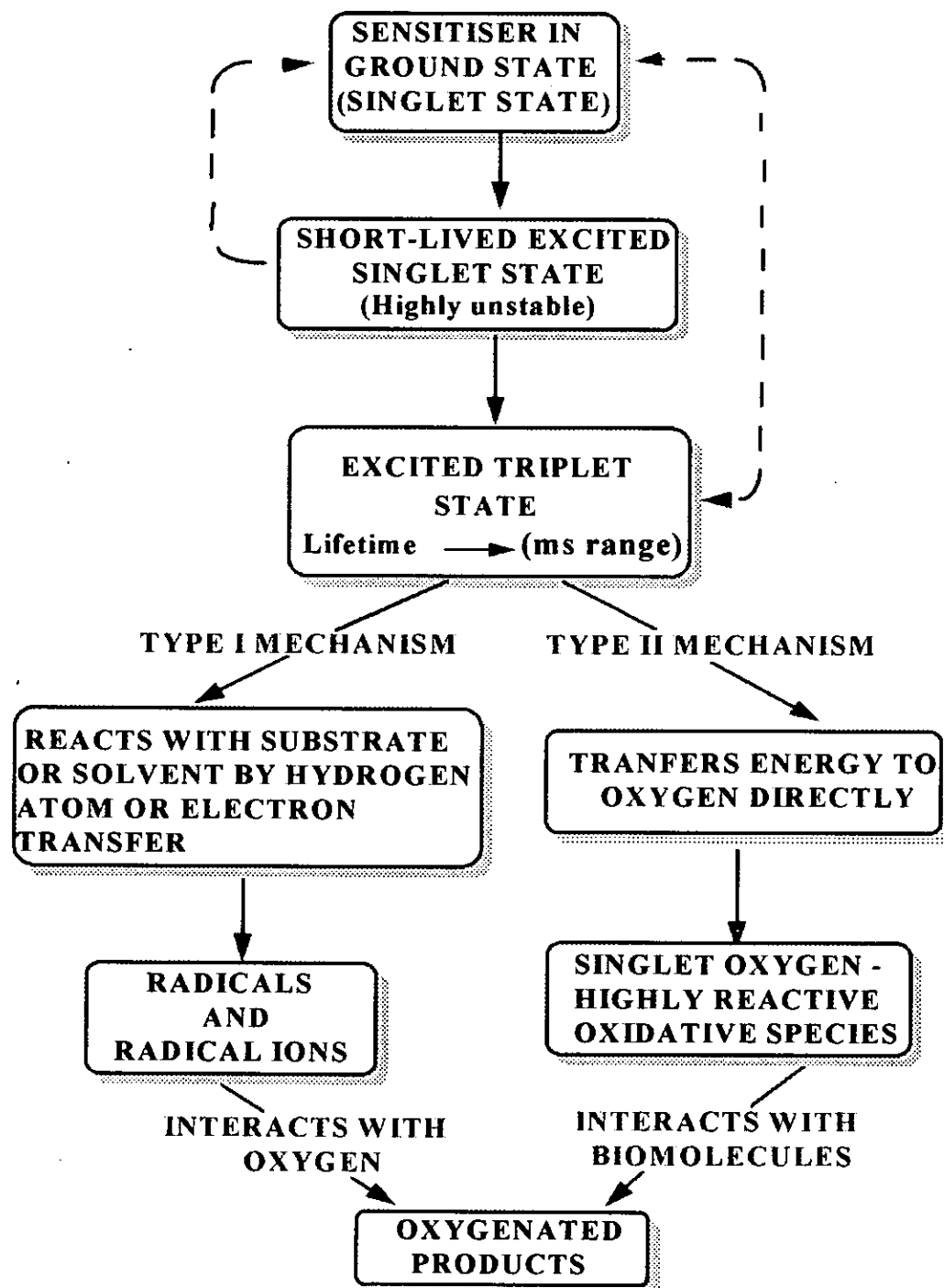


Figure 7 : Mechanism of action of PDT. The photosensitizer, in its ground state, absorbs a photon on exposure to light and assumes an excited singlet state (highly unstable). The photosensitizer may decay back to the original ground state, emitting fluorescence (no photodynamic effect). Alternatively, the excited photosensitizer may cross over to the triplet excited state. In Type 1 reactions, the excited triplet photosensitizer may react with a biomolecule by electron or hydrogen transfer, which produces radical forms of the substrate. These radicals react directly with molecular oxygen, producing various free radicals such as hydroxyl ions, hydrogen peroxide and superoxide. Type II reactions are thought to be more common where the excited triplet state interacts with ground state oxygen, generating singlet oxygen (highly reactive). The two reactions may occur simultaneously, and the ratio between the two processes is influenced by the sensitizer and the environment.

1.4.3 Cancer Treatment Using PDT.

Photodynamic therapy is now well-established and is gaining increasing acceptance in the treatment of cancer [106]. It is a novel form of treatment, with very few side-effects since it has low systemic toxicity when not illuminated. If the photosensitizer is administered systemically (as opposed to topical application), detailed studies of the pharmacokinetics of the drug are necessary, since the drug must be given time to localise at the tumour site before illumination. Many of the photosensitizers are taken up or retained preferentially by tumour tissue, and since the *specific* tumour site can be illuminated (with the use of fibre optics and tuneable lasers), minimal tissue damage may be inflicted on the surrounding tissues. The reason for the preferential accumulation of some photosensitizers in tumours is not clear, although it has been shown that haematoporphyrin derivatives have a high affinity for lipoproteins [120]. HpDs can bind to various lipoprotein fractions in the serum, including low density lipoproteins (LDLs). Interestingly, neoplastic tissues express increased numbers of LDL receptors and they are also highly vascularised, suggesting that these factors could be implicated in the increased accumulation of the drug. Although it is a relatively new treatment, many types of cancer, including that of the bronchus, oesophagus, bladder, head and neck, skin and eye have been treated with PDT [120], and it may be particularly useful in cancers of the mouth and larynx, where surgery can be extremely difficult and sometimes very disfiguring [121]. Much attention has been focussed on the use of PDT as an adjuvant treatment in cancer, particularly following tumour removal by surgery. As mentioned previously, one of the major obstacles to successful cancer treatment is the emergence of a multidrug resistant population of cells. PDT can be used after surgery at the tumour site to try to eliminate microscopic traces of the malignant tumour.

In general, most of the drugs in clinical trial at present are based on the porphyrin derivatives, although, for example, the phenothiazinium dye methylene blue has been used in oral, oesophageal and bladder cancer treatment [121-123]. One of the original drawbacks of using Photofrin was that it only absorbed light maximally at relatively low

wavelengths (around 400 nm), however, there are four additional, weaker absorption bands between 500 and 650nm and, in practice, illumination is usually carried out at around 630 nm (Figure 8). This is a critical factor in tissue penetration, since the light fluence decreases exponentially with distance, that is, the effective penetration depth (ϵ) is inversely proportional to the effective attenuation coefficient (α), ($\alpha = 1/\epsilon$ depth) [102].

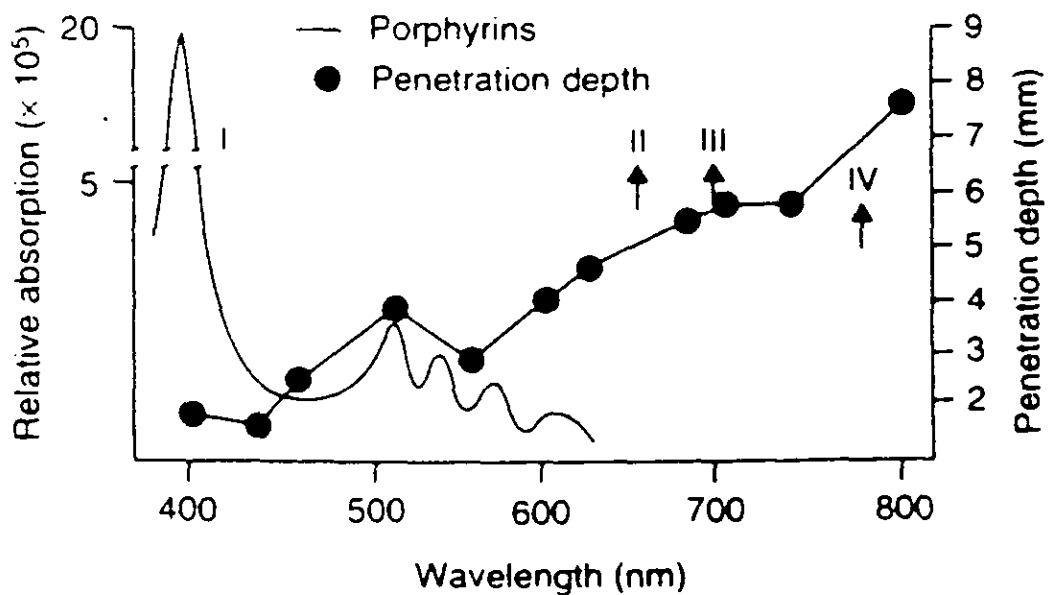


Figure 8 : Typical absorption spectrum for porphyrins such as Photofrin & protoporphyrin IX (I) and relative penetration depth of light in bovine muscle vs. wavelength. The various absorbance peaks of second generation photosensitizers are indicated by the arrows : (II) phthalocyanines & chlorins; (III) phthalocyanines, purpurins, verdins, benzoporphyrin derivative, (IV) bacteriochlorin A. Depth of penetration depends on the tissue involved, ranging from 0.1 to 1 mm in highly pigmented tissue, such as liver, to 1 to 5 mm in lightly pigmented tissue, such as brain. (Diagram taken from van Hillegersberg , Kort & Wilson, 1994 [104]).

Penetration into the tissue is hampered by light scattering and absorption by tissue chromophores (particularly haemoglobin and melanin). These parameters vary with tissue type, for example, liver is prone to poor penetration since it contains a high

proportion of haemoglobin, and the brain tissue is prone to light scattering. If the wavelength maximum is short, the effective depth of tissue penetration is very low (Figure 9). The development of new drugs for PDT has thus focussed on compounds which absorb in the longer wavelength region, since tissue penetration typically doubles at wavelengths between 630 and 750 nm [102,124]. The phthalocyanines have structural similarities to porphyrin, but show strong absorbance between 650 and 700 nm (Figure 8). Similarly, some of the chlorins and the purpurins have absorbance maxima in this region [104]. In addition to its poor photoproperties, HpD causes prolonged skin photosensitization and this also has led to the search for new and improved drugs.

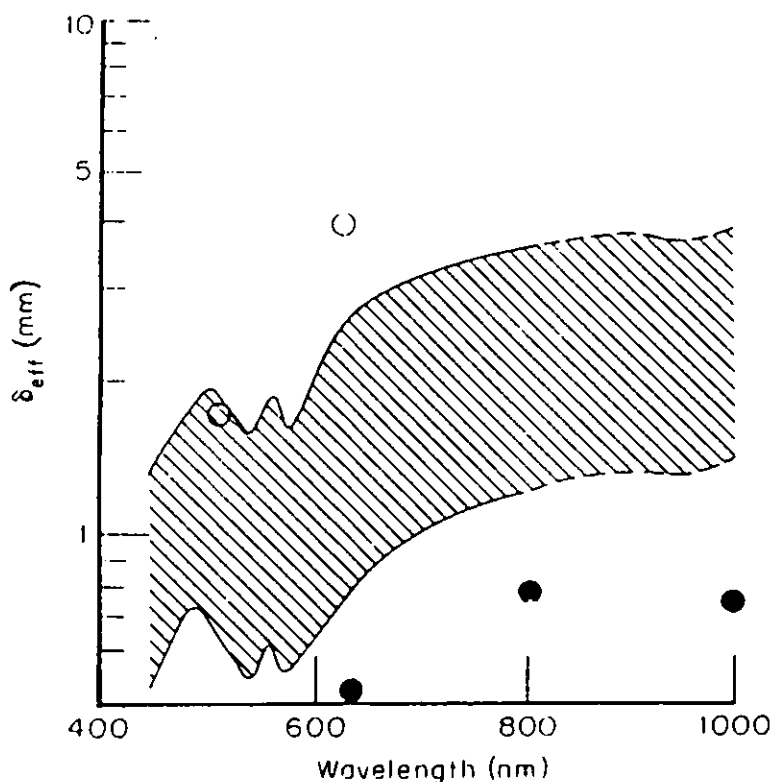


Figure 9 : Schematic diagram showing the wavelength dependence of effective penetration depth (δ_{eff}) in soft tissues. Penetration of lightly pigmented tissue (e.g. brain) is shown by the upper range and of highly pigmented tissue (e.g. liver) by the lower range. The structures at 500-600 nm and 90-1000 nm are oxyhaemoglobin and water absorption peaks, respectively. The individual data represent extremes in published results, ○ neonatal brain *in vitro*; ● rat liver *in vitro*. (Figure and data taken from Wilson, 1989 [124]).

One of the most promising recent advances has been the development of systemic treatment with 5-aminolevulinic acid (ALA) [104]. This treatment is based on the fact that all cells contain porphyrins as precursors of haeme, and ferrochelatase, the enzyme which converts protoporphyrin to haeme, is decreased in various malignant and regenerating tissues [104]. By contrast, another enzyme, porphobilinogen deaminase (PGBD), also involved in the chain of reactions in haeme synthesis, is increased in these cells (Figure 10). Researchers reasoned that the oral administration of ALA would overcome this decreased production of haeme, and would result in the selective localisation of the endogenous porphyrin, protoporphyrin IX, in the malignant cells [104]. Van Hillegersberg *et al.* showed, using a rat liver metastasis model, that protoporphyrin accumulated progressively in colon carcinoma with increased duration of ALA treatment, compared to protoporphyrin levels in normal liver.

Promising results have been achieved with this drug, which has an absorbance maximum of 630 nm. Another advantage of the treatment is the reduced skin photosensitivity, reported to be as low as 24 hours. Excellent results in the treatment of Bowen's disease, using the topical application of 5-ALA have also been reported [125].

The field of photodynamic therapy is expanding, but the requirements for a successful photosensitizer remain : high selectivity for malignant cells, effective photosensitizer activity, low dark toxicity, lack of skin photosensitization, ease of production of pure drugs, biochemical stability and rapid clearance from the tissues. As mentioned previously, most of the photosensitizers in clinical use are based on porphyrin derivatives, and much research into new drug development has been focussed on these compounds and their analogues. However, some commercial dyes are effective photosensitizing agents and are interesting candidates for drug development, since their chemistry and synthetic routes are well-known. Several examples of commercial photosensitizers have been investigated [126-129] but dark toxicity has often been shown to be a problem.

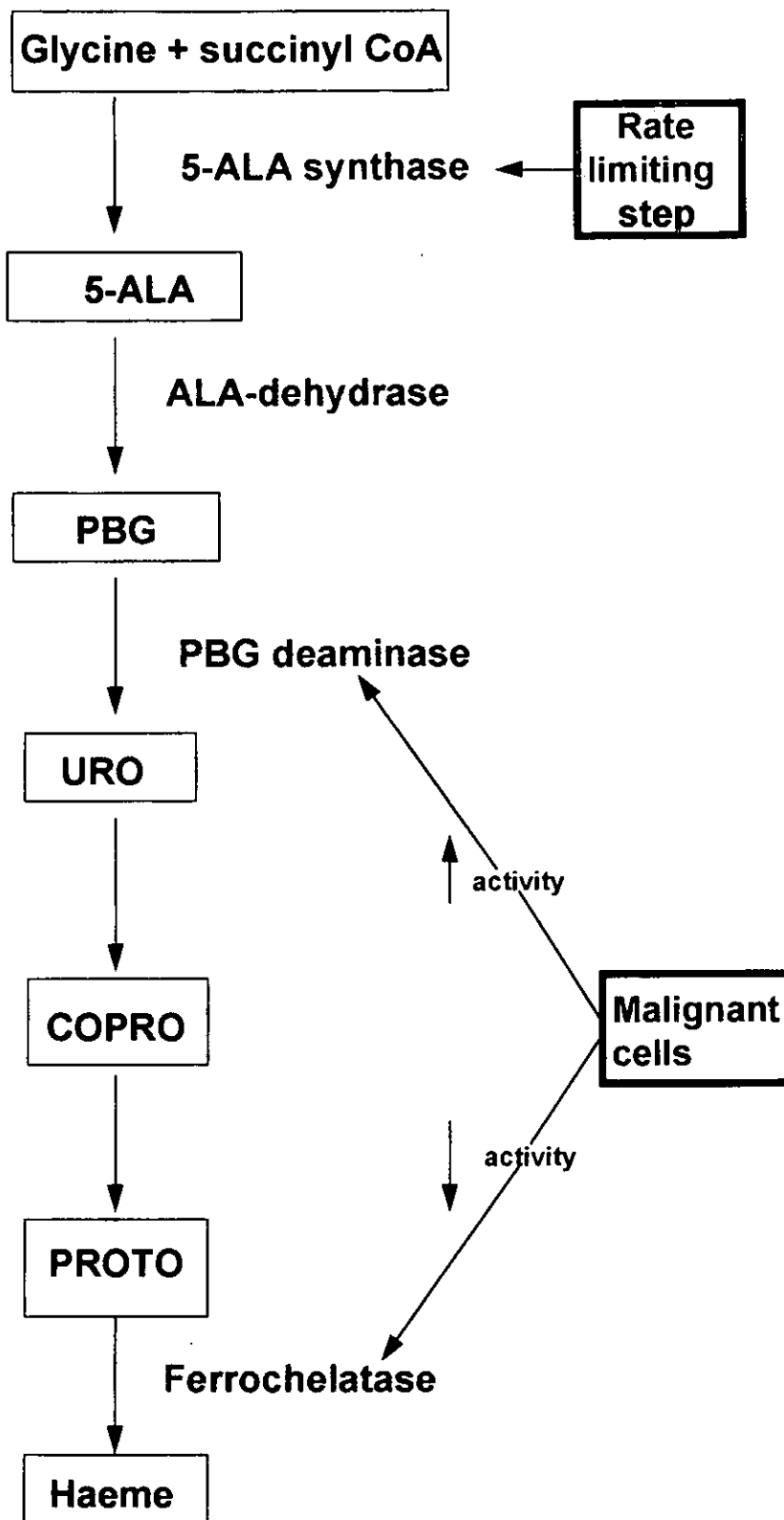


Figure 10: Schematic diagram of the haeme biosynthetic pathway. The first intermediate is 5-aminolevulinic acid (ALA), an aminoketone formed by the condensation of glycine and succinyl coenzyme A (CoA). Two molecules of ALA combine to form porphobilinogen (PBG), a monopyrrole, then four molecules of PBG combine to form uroporphyrinogen (UPG) a tetrapyrrole. URO is converted to coproporphyrinogen (COPRO) and subsequently to protoporphyrin IX (PROTO). Malignant cells may have altered activities of the enzymes PBG deaminase and ferrochelatase compared to normal cells (Figure adapted from van Hillegersberg *et al.* [104]).

1.4.4 Cationic Photosensitizers.

Recent interest has been shown in various cationic photosensitizers. As early as the 1940s, Lewis *et al.* (130) tested many dyes and identified a variety of cationic dyes including oxazine, xanthene, thiazine and acridine derivatives to be efficient biological stains which were selectively retained by tumour tissue. Further research has shown that lipophilic cationic photosensitizers such as rhodamine 123, triarylmethane derivatives, chalcogenapyrylium dyes and cryptocyanines preferentially accumulate in malignant cells *in vitro* and *in vivo* [131, 132, 133]. The high affinity of cationic dyes for tumour cells has been attributed mainly to the negative potential across the plasma and mitochondrial membranes. Tumour cells have been shown to have a high negative mitochondrial membrane potential, suggesting that this may indeed be the reason for selective retention of the dyes by malignant tissue. In general, tumour cells also have a poor oxygen supply and high glycolytic activity, resulting in a low intracellular pH. Certain cationic dyes increase in lipophilicity with decreasing pH levels [134] thus facilitating cellular uptake in this environment. Interestingly, Shea *et al.* have shown that exposure to light appears to increase the intracellular retention of these agents [135].

Another feature of the cationic dyes is that they usually absorb light in the near infra-red region of the spectrum. This is an important consideration for efficient skin penetration. A number of these dyes have been found to have an anti-cancer effect, even in the dark (136), and are also effective photosensitizers. This, coupled with their ease of preparation, thus promotes their potential use in photodynamic therapy.

Commercial photosensitizers have the advantage of well established chemistries, and ready availability, but often the disadvantage of higher inherent toxicity. Cationic examples include the triarylmethane dye Victoria blue BO (VBBO) and the phenothiazinium photosensitizers toluidine blue (TBO) and methylene blue (MB). It has been suggested that the flexibility of the ring structure of triarylmethanes causes a fast relaxation of the singlet excited state, and thus a low degree of photosensitizing activity

[133]. When immobilised, however, the photosensitizing activity of these compounds is greatly increased; immobilisation by binding to biomolecules may endow a greater rigidity and concomitant increase in photosensitizing ability [137]. The Victoria blue series are triarylmethane dyes related to crystal violet, where one of the phenyl groups is replaced by naphthyl. Dyes such as crystal violet have been known for over a century and have indeed been widely used in topical antimicrobial medicine [138]. VBBO has been reported to exhibit photocytotoxic effects in several mammalian cell lines, including human squamous cell carcinoma (FaDu) and human melanoma (NEL), though some dark toxicity was observed [133]. No evidence of singlet oxygen production has been found *in vitro*, however, electron paramagnetic resonance has been used to demonstrate that VBBO can photosensitize superoxide production [139].

The phenothiazinium dyes have a rigid, planar structure and are well established Type II photosensitizers [128]. In solution, MB and TBO are both hydrophilic ($\log P = -0.01$ and -0.21 , respectively) [130], however, in biological systems, TBO is partially converted into a neutral form by deprotonation and both dyes are subject to metabolic reduction to the neutral species which are highly lipophilic ($\log P \geq +3$) [140]. MB is a well-known vital stain and has been used extensively in the diagnosis of many diseases. It has also been used to a lesser extent in the field of PDT, most notably in the treatment of bladder, oesophageal and other cancers [121-123]. The efficacy of MB is somewhat limited, however, since the dye is reduced to leuco-methylene blue (LMB) by the cellular enzymes NADH and FADH₂ [140]. LMB is a colourless compound which therefore will not be activated by the long wavelength employed in PDT. Another problem is low pK_a value of LMB compared to that of MB, which results in a lower level of ionisation [140]. A high level of ionisation is necessary for DNA intercalation to take place, thought to be the major effect of MB photocytotoxicity.

TBO has a similar structure to MB and is thought to exert its photocytotoxicity in a similar manner by DNA intercalation. This agent has been used extensively in the treatment of oral diseases and is also a selective stain for the diagnosis of oral cancer. In

addition, many studies have been carried out recently into the use of TBO as a photodynamic anti-microbial agent, particularly against oral pathogens [141].

1.5 Aim of the study

The overall aim of the project is to investigate resistance mechanisms relevant to cancer chemotherapy and relate this to the development of strategies for overcoming MDR. A significant area of investigation is the role of the cell membrane as a barrier and/or target for drug action. This may include the search for agents which are not susceptible to MDR or adjuvants used in conjunction with cytotoxic drugs to enhance their activity against MDR cells.

CHAPTER TWO.

DEVELOPMENT OF A PROKARYOTIC MODEL FOR STUDYING ANTHRACYCLINE-MEMBRANE INTERACTIONS.

2.1 Abstract.

Growth of wild-type *E.coli* strain MRE600 was severely affected up to 9 hours following treatment with the anthracycline doxorubicin (15 μ M), however, after 9 hours the cells became resistant. The onset of resistance coincided with some changes in the relative proportions of total saturated, monounsaturated and cyclopropane fatty acids, which would be predicted to affect membrane dynamics.

Growth of *S. aureus* strain 6571 was severely affected after 3 hours' incubation with doxorubicin ($\geq 10\mu$ M) and further inhibited between 3 hours and 9 hours. Re-growth occurred between 9 & 24 hours, as had been previously noted with MRE600, however, *S. aureus* was found to be more sensitive to doxorubicin.

The anionic lipid content in *E. coli* strain HDL11 is under *lac* control and synthesis can be induced by incubation with the *lac* inducer IPTG. HDL11, with low levels of anionic phospholipid, was unaffected by doxorubicin (100 μ M) over 9 hours, with only slight inhibition of growth seen over 24 hours. When the anionic lipid content of HDL11 was increased, there was a slight increase in the efficacy of doxorubicin, providing further evidence for a membrane based step in doxorubicin action.

2.2 Introduction.

Anthracycline antibiotics are potent cytotoxic drugs, widely used as anti-cancer agents. One of the most effective and best characterised of these is doxorubicin (adriamycin), however, problems such as multiple drug resistance (MDR) and cardiotoxicity are associated with its use [142]. The mode of action of doxorubicin is very complex and has not been fully elucidated. Several mechanisms have been proposed, the most popular being its effect on cellular DNA *via* interaction with nucleic acids and nuclear components, such as topoisomerase II [143], however, studies have shown that doxorubicin can be strongly cytotoxic without entering the cell [144]. Recent investigations have indicated that this cytotoxicity may be directly related to plasma membrane composition [145] and doxorubicin has been shown to bind strongly to anionic phospholipids in model synthetic membranes, inducing disordering of acyl chains [146]. Although much information has been gained by the use of synthetic model membrane systems, very little is known about the interactions of anthracyclines with biological membranes *in vivo*. Unfortunately, as yet, a mammalian model system does not exist in which the phospholipid content of the plasma membrane can be easily manipulated. Recent genetic advances have, however, produced an excellent model plasma membrane system which is derived from *Escherichia coli* (*E. coli*) [146, 147].

The predominant membrane phospholipid of wild-type *E. coli* is phosphatidylethanolamine (PE) (75% w/w), which is zwitterionic, and the remainder comprises phosphatidylglycerol (PG) (15-20% w/w) and cardiolipin (CL) (5-10% w/w), which are both anionic [148]. Mutant strains of *E. coli* have been developed in which the phospholipid content can be altered. *E. coli* strain HDL11 is such a mutant in which the *pgsA* gene encoding phosphatidylglycerolphosphate synthetase has been placed under the control of a *lac* promoter [147]. If the bacteria are incubated in the presence of varying levels of the *lac* inducer isopropyl β -thiogalactopyranoside (IPTG), it is possible to control the level of *pgsA* expression, which in turn controls the level of PG and CL production. In the absence of IPTG, phosphatidylglycerolphosphate synthetase is still

produced at a low, basal level, maintaining the viability of the strain, given the additional presence of an *lpp2* deletion [149]. The level of anionic phospholipids in the inner membrane of HDL11, under normal growth conditions, is 2% w/w PG and 3% w/w CL, based on total phospholipid, but incubated in the presence of 60 μ M IPTG, the content of PG and CL may be increased to wild-type levels of 28% w/w of the total [146].

The aim of this study was to develop a prokaryotic model system to investigate anthracycline-membrane interactions which could subsequently be related to a eukaryotic model system.

2.3 Materials and Methods.

2.3.1 Chemicals

Doxorubicin was a gift from Farmitalia Carlo Erba Ltd., St. Albans, U.K. and isopropyl- β -thiogalactopyranoside (IPTG) was purchased from Sigma Poole, U.K.

2.3.2 Bacterial strains and growth conditions.

Escherichia coli strain MRE600 and *Escherichia coli* strain HDL11 (*pgsA::kan*, ϕ (*lacOP-pgsA*⁺), *lacZ'*, *lacY::Tn9*, *lpp2*, *zdg::Tn10*) [150] and *Staphylococcus aureus* strain 6571 were grown at 37°C in Nutrient broth (Lab M, Bury, U.K.) in the absence and presence of doxorubicin and IPTG. Prior to the experiment, *E. coli* strain HDL11 was checked for resistance to chloramphenicol and kanamycin.

2.3.3 Effect of doxorubicin on growth of bacteria.

Preliminary growth experiments were carried out using *E. coli* MRE600 and HDL11 in the presence and absence of 5-100 μ M doxorubicin. Overnight cultures were inoculated into nutrient agar (1:200 dilution), protected from light to prevent deterioration of the drug, and incubated at 37°C in an orbital incubator. Growth was monitored by measuring optical density at 660 nm (OD_{660}) at time zero and after 3 hours, 6 hours, 9 hours and 24 hours. Subsequent experiments were performed, as described, on *E. coli* strains MRE600 and HDL11 and *S. aureus* strain 6571, but using doxorubicin in the range 0-15 μ M. Growth kinetics of both HDL11 and MRE600 were also monitored in the absence and presence of 30 μ M and 60 μ M IPTG, in addition to doxorubicin. In this instance, the stock cultures were grown overnight, prior to inoculation, in the presence of IPTG.

2.3.4 Analysis of membrane.

Total lipids were extracted according to the method of Bligh & Dyer [151] and fatty acid methyl esters were prepared and analysed by gas liquid chromatography according to the method of Rolph & Goad [152]. Induction of *pgsA* by IPTG was confirmed by ¹⁴C acetate labelling of phospholipids which were resolved *via* TLC and quantified by scintillation counting (F. Harris, UCLAN, personal communication) .

2.4 Results.

2.4.1 Effect of doxorubicin on *E. coli* strain MRE600 .

Initial experiments showed doxorubicin (5-100 μ M) to inhibit growth of MRE600 in a concentration-dependent manner with almost 100% inhibition achieved by 100 μ M doxorubicin (Figure 11). However, although 15 - 50 μ M doxorubicin severely affected growth between 3 and 9 hours, rapid growth ensued between 9 and 24 hours. Subsequent experiments used a range of 5-15 μ M doxorubicin to allow investigation of this phenomenon. MRE600 cells previously grown over 24 hours in the presence of 15 μ M doxorubicin and then sub-cultured into medium containing varying concentrations (5-15 μ M) of doxorubicin showed complete resistance to the drug (Figure12). This indicated the induction of a resistance mechanism by the bacteria, rather than spontaneous breakdown of the drug over time.

Addition of 30 μ M IPTG or 60 μ M IPTG to MRE600 cells in the presence of 5-15 μ M doxorubicin showed very similar results to the controls (Figures 13a-c), thus it was concluded that the presence of IPTG had not affected the efficacy of doxorubicin.

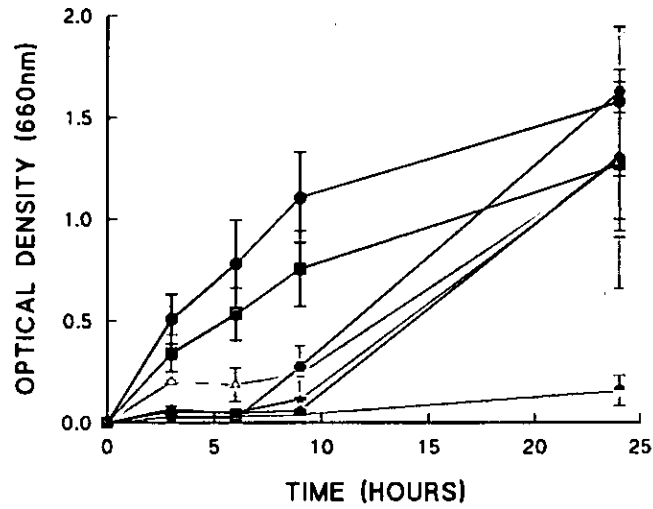


Figure 11: Typical growth curve for *E.coli* (strain MRE600) grown at 37°C over 24 hours, in the absence of doxorubicin (●) or in the presence of 5 μM (■), 10 μM (▲), 15 μM (◆), 25 μM (✱), 50 μM (✳) or 100 μM (✴) doxorubicin. Each point represents mean ± SD (n=2).

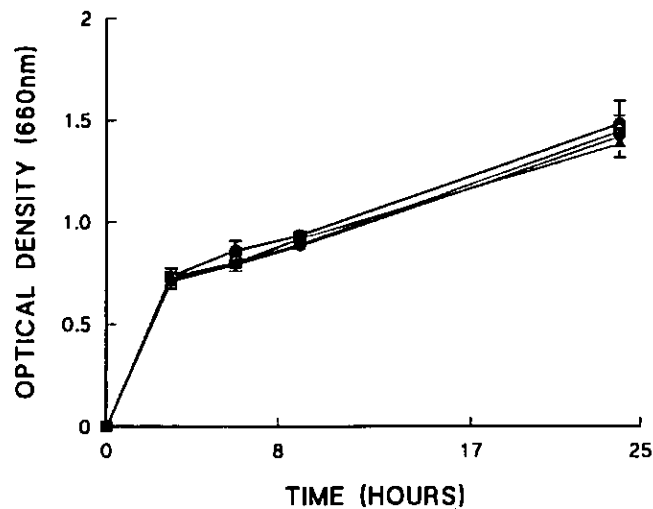


Figure 12: Typical growth curve for *E.coli* (strain MRE600) grown at 37°C over 24 hours, in the absence of doxorubicin (●) or in the presence of 5 μM (■), 10 μM (▲), or 15 μM (◆) previously grown for 24 hours in the presence of 15 μM doxorubicin. Each point represents mean ± SEM (n=4).

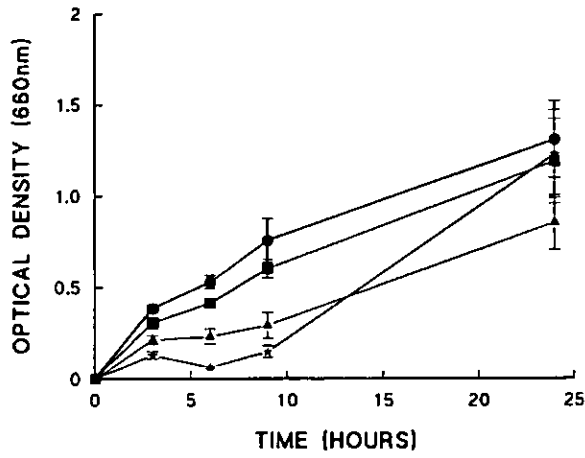


Figure 13a: Typical growth curve for *E.coli* (strain MRE600) grown at 37°C over 24 hours, in the absence of doxorubicin (●) or in the presence of 5 μM doxorubicin (■), 10 μM doxorubicin (▲), or 15 μM doxorubicin (✕). Each point represents mean ± SEM (n=at least 4).

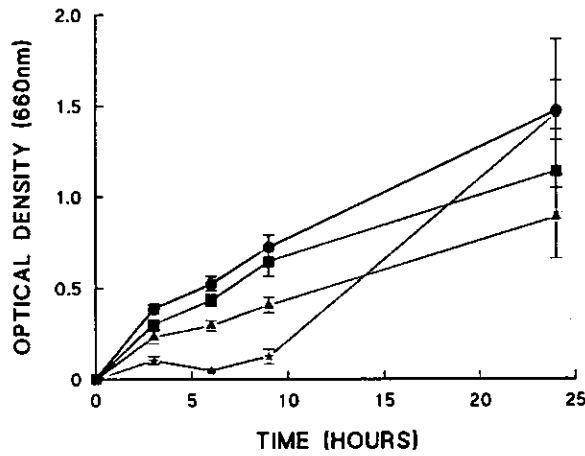


Figure 13b: Typical growth curve for *E.coli*(strain MRE600) grown at 37°C over 24 hours, in the presence of 30μM IPTG and in the absence of doxorubicin (●) or in the presence of 5 μM doxorubicin (■), 10 μM doxorubicin (▲) and 15 μM doxorubicin (✕). Each point represents mean ± SEM (n=at least 4).

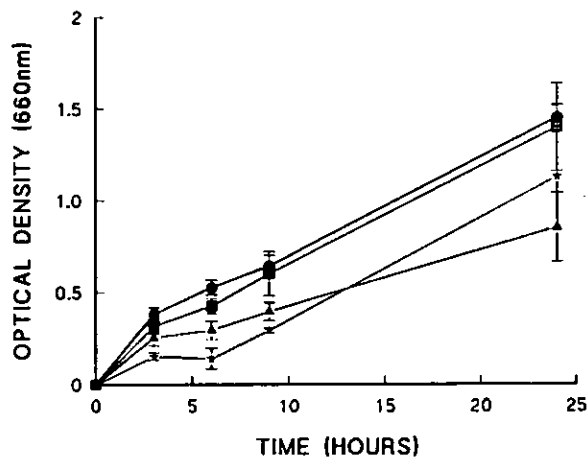


Figure 13c: Typical growth curve for *E.coli*(strain MRE600) grown at 37°C over 24 hours, in the presence of 60μM IPTG and in the absence of doxorubicin (●) or in the presence of 5 μM doxorubicin (■), 10 μM doxorubicin (▲) and 15 μM doxorubicin (✕). Each point represents mean ± SEM (n=4).

2.4.2 Total fatty acid composition of MRE600 cells in the presence and absence doxorubicin.

Following 6 hours' doxorubicin treatment of MRE600 cells, some changes in the relative proportions of total saturated, monounsaturated and cyclopropane fatty acids were noted (Table 7). Whilst small, these changes altered the ratio of monounsaturates : saturates from 1:1 to 1:1.3, which would be expected to have some effect on membrane dynamics. In addition, there was a reduction in cyclopropane content. However, after 24 hours, the relative proportions of the fatty acids in the treated cells again resembled the controls. This effect at 6 hours may possibly be due to the effect of doxorubicin interacting with the membrane lipids, rather than a resistance mechanism *per se*.

Table 7 : Total fatty acid composition of MRE600 cells in the absence and presence of doxorubicin. Each value represents the mean \pm SEM.

SAMPLE	% w/w SATURATES	% w/w MONOUNSATURATES	% w/w CYCLOPROPANES
MRE600			
0 hr (n=3)	26.9 \pm 1.5	52.4 \pm 2.1	16.9 \pm 1.9
6 hr (n=5)	37.8 \pm 0.6	37.8 \pm 1.9	17.5 \pm 1.2
24 hr (n=4)	37.2 \pm 2.6	25.7 \pm 5.3	30.5 \pm 5.9
MRE600 +15 μM dox.			
0 hr (n=3)	26.9 \pm 1.5	52.4 \pm 2.1	16.9 \pm 1.9
6 hr (n=5)	43.7 \pm 2.5	34.0 \pm 1.1	11.1 \pm 3.2
24 hr (n=4)	41.3 \pm 4.5	25.4 \pm 2.4	25.6 \pm 1.7

2.4.3 Effect of doxorubicin on *E. coli* strain HDL11 cells in the absence and presence of IPTG.

All experiments were initially carried out using 5-100 μM doxorubicin, however, since no significant enhancement of effect was seen using concentrations above 15 μM (Figure 14), subsequent experiments were performed using 5-15 μM doxorubicin.

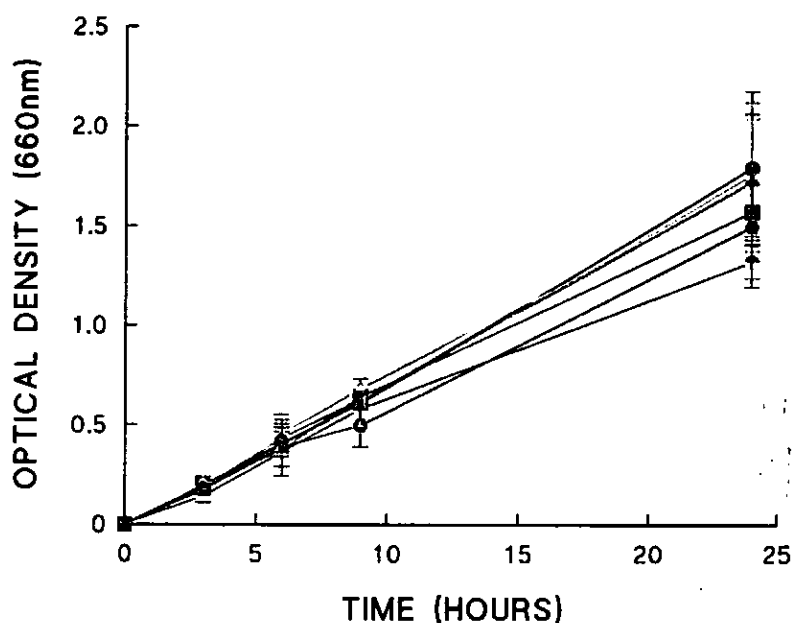


Figure 14: Typical growth curve for *E. coli* (strain HDL11) grown at 37°C over 24 hours, in the absence of doxorubicin (●) and in the presence of 5 μM (■), 10 μM (△), 15 μM (◆), 25 μM (*), 50 μM (◐) or 100 μM (◑) doxorubicin. Each point represents mean \pm SD (n=2).

HDL11 grown in the absence and presence of doxorubicin (5-15 μM) showed a very different growth pattern to that of MRE600 grown under the same conditions, in that the drug exerted very little inhibitory effect (Figure 15a). Addition of 30 μM IPTG to HDL11 cells in the presence of 5-15 μM doxorubicin did not appear to enhance the effect of doxorubicin significantly (Figure 15b). Addition of 60 μM IPTG improved the growth rate of HDL11 cells and growth between 9 and 24 hours was inhibited by 5-15 μM doxorubicin in a concentration dependent manner (Figure 15c). However, the level of inhibition was much lower than that observed with MRE600 and was not greatly increased by addition of 100 μM doxorubicin (Figure 16), implying that this phenotype is inherently less susceptible to the agent.

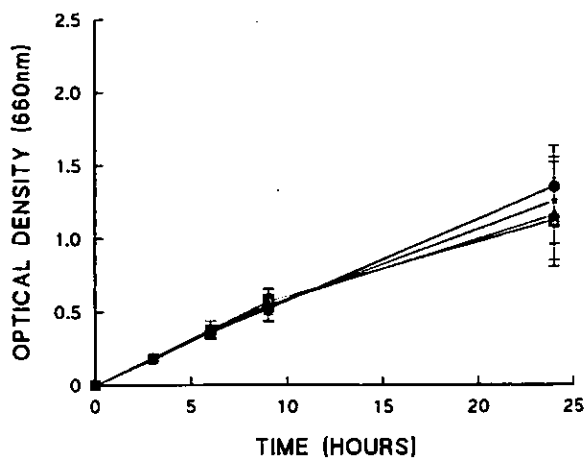


Figure 15a: Typical growth curve for *E.coli* (strain HDL11) grown at 37°C over 24 hours, in the absence of doxorubicin (●) and in the presence of 5 μM doxorubicin (■), 10 μM doxorubicin (▲) and 15 μM doxorubicin (*). Each point represents mean ± SEM (n=4).

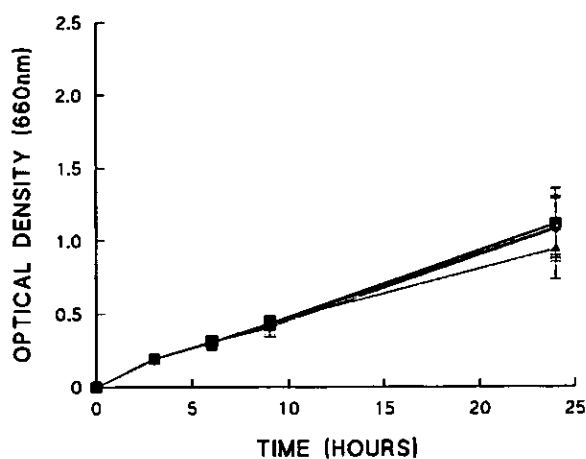


Figure 15b: Typical growth curve for *E.coli* strain HDL11 in the presence of 30 μM IPTG and in the absence of doxorubicin (●), or the presence of 5 μM doxorubicin (■), 10 μM doxorubicin (▲) or 15 μM doxorubicin (*). Each point represents mean ± SEM (n=6).

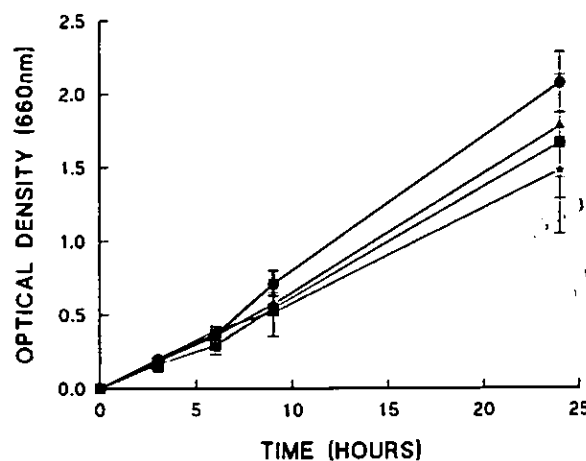


Figure 15c: Typical growth curve for *E.coli* (strain HDL11) in the presence of 60 μM IPTG and in the absence of doxorubicin (●) or the presence of 5 μM (■), 10 μM (▲) or 15 μM (*) doxorubicin. Each point represents mean ± SD (n=2).

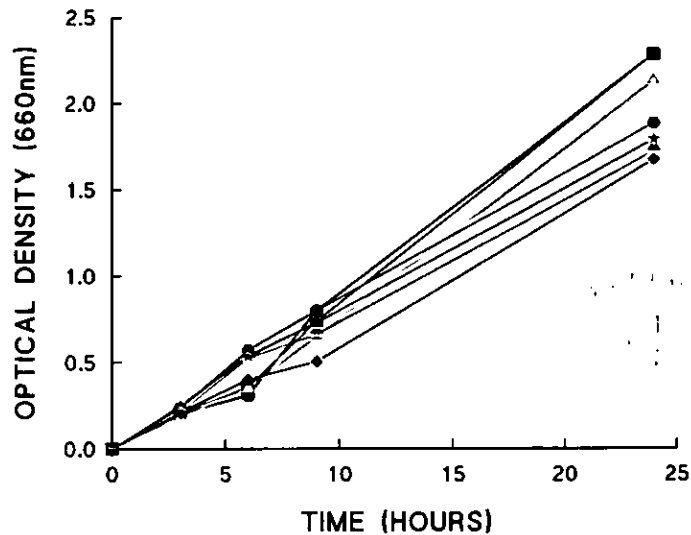


Figure 16: Typical growth curve for *E. coli* (strain HDL11) in the presence of 60 μM IPTG and in the absence of doxorubicin (●) or in the presence of 5 μM (■), 10 μM (▲), 15 μM (◆), 25 μM (★), 50 μM (●) or 100 (-) μM doxorubicin (n=1).

2.4.4 Effect of doxorubicin on *S. aureus* cells.

Growth of *S. aureus* strain 6571 was severely inhibited after 3 hours' incubation with doxorubicin ($\geq 10 \mu\text{M}$) and further inhibited between 3 hours and 9 hours (Figure 17). Re-growth occurred between 9 & 24 hours, as had been previously noted with MRE600, however, *S. aureus* was found to be more sensitive to doxorubicin.

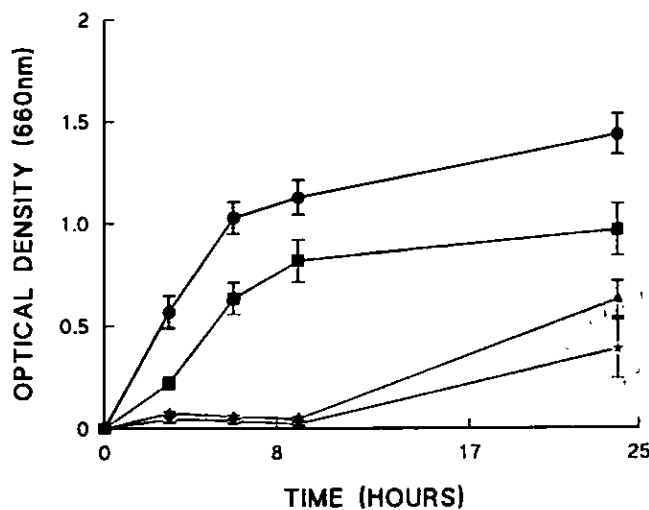


Figure 17: Typical growth curve for *S. aureus* (strain 67J1) grown at 37°C over 24 hours in the absence of doxorubicin (●) and in the presence of 5 μM doxorubicin (■), 10 μM doxorubicin (▲) and 15 μM doxorubicin (◆). Each point represents mean \pm SEM (n=6).

2.5 Discussion.

Many previous studies have indicated that the binding of doxorubicin to plasma membranes is intimately involved with anionic phospholipids [146,153]. By using intact cells from bacterial strains in which levels of anionic phospholipids can be manipulated, it was hoped to develop a prokaryotic model to substantiate these findings. In contrast to previous studies [146] intact *E. coli* MRE600 cells were found to be susceptible to doxorubicin at relatively low concentrations (5-15 μM). The mutant *E. coli* strain HDL11, with very low anionic phospholipid content, was not affected by doxorubicin, even at a concentration of 100 μM . However, induction of phosphatidylglycerol (PG) synthesis by the *lac* inducer IPTG (F. Harris, UCLAN, personal communication), led to a limited increase in susceptibility of HDL11 cells, thus it was not possible to provide strong evidence that doxorubicin acts *via* interaction with anionic phospholipids. *S. aureus*, a Gram positive organism with no outer membrane and expressing a high percentage of anionic phospholipid in the membrane [154], predictably, showed greater sensitivity to doxorubicin.

Previous work by de Wolf *et al.* [146] on various bacterial phospholipid extracts or membranes, including HDL11, showed that doxorubicin binding was dependent upon anionic phospholipids. However, when using plasma membrane vesicles of HDL11 in the absence and presence of IPTG, rather anomolous results were obtained. Not only was there very little difference between the two samples, but the doxorubicin binding was shown to be 15-30 % *higher* than MRE600. They concluded that the effect of anionic phospholipids in plasma membranes of strain HDL11 may be masked due to "the presence of other binding sites as well as unknown membrane structure effects". The present study showed there to be little effect of doxorubicin on intact HDL11 cells in the presence of IPTG, suggesting that the strain may be phenotypically resistant to doxorubicin due, for example, to cell wall structure or expression of a membrane extrusion pump.

MRE600 showed a very interesting response to doxorubicin. Although, initially, growth was severely affected by doxorubicin ($\geq 15 \mu\text{M}$), after 9 hours, growth increased rapidly, suggesting the induction of a resistance mechanism, the selection of a resistant sub-population or that doxorubicin had lost efficacy by this stage. MRE600 cells previously exposed to $15 \mu\text{M}$ doxorubicin for 24 hours and then re-subcultured into various concentrations of doxorubicin showed total resistance to the drug over 24 hours, thus indicating that the resumption of growth after 9 hours is primarily due to the development of resistance rather than reduced concentration of doxorubicin due to photodegradation. Various possibilities for this resistance mechanism exist and they are not necessarily mutually exclusive.

Enzyme induction, promoting the metabolic breakdown of doxorubicin was considered, since this is an extremely common defence mechanism utilised by bacteria [155]. Certainly some enzyme activity was suggested, since HPLC assay of doxorubicin extracted from the cultures showed significant degradation of the drug after 9 hours (D.Phoenix, UCLAN, personal communication).

Doxorubicin is also known to disrupt acyl chains in the plasma membrane [156], thus the total fatty acid composition of the cell membranes was investigated. Treatment of MRE600 cells with doxorubicin over 6 hours led to some changes in the relative proportions of total saturated, monounsaturated and cyclopropane fatty acids which coincided with the onset of doxorubicin resistance. Such changes are likely to affect membrane fluidity and hence limit the passive uptake of doxorubicin. Effects of changes in membrane composition on drug uptake have been investigated by Burns *et al.* [156] who found that increasing the level of polyunsaturated acyl chains in tumour cells stimulated drug uptake. However, it is possible that this effect at 6 hours may be due to doxorubicin interacting with the membrane and affecting lipid biosynthesis, but that after 24 hours resistance mechanisms have been induced which may remove doxorubicin and overcome the initial effect.

Another resistance mechanism considered was the overexpression of a membrane translocase protein in the plasma membrane, acting as a multidrug resistant pump (MDRP). MDRPs are now known to be widespread in bacteria. There appear to be seven distinct MDRPs in *E. coli* and most common bacterial MDRPs belong to the major facilitator family of membrane translocases [157]. Lewis [157] suggests that MDRPs have evolved from specific translocases which have broadened their substrate spectra, thus increasing the defence mechanisms of the cell against ever increasing environmental toxins. Doxorubicin, a natural antibiotic produced by *Streptomyces peucetius*, is normally exported by an ABC (ATP binding cassette) type pump [157]. If, as has been suggested, MDRPs have evolved due to a loss of specificity for their substrate, this translocase also has the potential to be overexpressed and become a MDRP. In the eukaryotic system, multiple drug resistance (MDR) is a major problem in cancer chemotherapy, and in many cases is strongly associated with the overexpression of a 170 - 180 KDa protein in the plasma membrane, known as P-glycoprotein [25]. P-glycoprotein is also a member of a large family of ABC translocases and is homologous to the bacterial haemolysin B pump [25]. The role of ABC translocases in bacteria is currently being investigated, since the genes which encode members of this superfamily have been isolated from drug-resistant micro-organisms [158]. Studies on microbial ABC transporters which may be involved in MDR thus offer considerable scope for exploring mechanisms of resistance in the eukaryotic system.

In summary, it appears that some strains of *E. coli* are susceptible to doxorubicin, but that resistance can develop rapidly. There may be a role for membrane-induced changes in the induction of this resistance mechanism, thus implying that the membrane could play a part either in the uptake or activity of the anthracycline.

CHAPTER THREE.

CHARACTERISATION OF THE MOUSE MAMMARY TUMOUR CELL LINE EMT6 WITH REGARD TO GROWTH KINETICS, TOXICITY OF DOXORUBICIN AND MEMBRANE LIPID COMPOSITION.

3.1 Abstract.

The drug sensitive mouse mammary tumour cell line (EMT6-S) and a multidrug resistant sub-line (EMT6-R) were characterised with regard to their growth kinetics, susceptibility to doxorubicin and membrane lipid composition. The former two parameters both differed between the two cell lines. The log phase doubling times (hour) were 21.8 and 25.0 for EMT6-S and EMT6-R cells, respectively, and the IC_{50} values for doxorubicin were found to be 2.2×10^{-8} M in EMT6-S cells and 1.8×10^{-6} M in EMT6-R cells. The resistance factor (IC_{50} for EMT6-R cells : IC_{50} for EMT6-S cells) was found to be 82. Comparison of the percentage of the total fatty acid composition of the major phospholipids found in mammalian membranes showed there to be no significant difference between the two cell lines ($p > 0.05$) with the exception of linoleic acid (18:2), where the level appeared to be higher in the resistant cell membranes ($p = 0.05$). Similarly, no difference was observed between the phospholipid profiles of the two cell lines, using TLC.

3.2 Introduction.

3.2.1 EMT6 cells

Tumour cells displaying the MDR phenotype are resistant to a variety of unrelated drugs [28] and typically show decreased intracellular accumulation of the drugs [25]. The mouse mammary tumour cell line EMT6 has previously been shown to be sensitive to treatment with doxorubicin [5]. The resistant sub-line, EMT6-R, was developed from the parental line by successive exposure to increasing concentrations of the anthracycline antibiotic, doxorubicin [5] and is routinely maintained in the presence of 5 μ M doxorubicin. Cox (1994) [5] demonstrated this sub-line to be cross-resistant to the *Vinca* alkaloid, vincristine, and colchicine, both of which are lipophilic agents, but to be susceptible to *cis*-platinum and methotrexate, both of which are hydrophilic. The 170 kDa membrane glycoprotein known as P-glycoprotein was also found to be over-expressed.

3.2.2 Screening for Mycoplasma Contamination.

Contamination of cultured cells due to bacteria, fungi, yeast and mycoplasma can be a major problem in biological research and must be eliminated if detected. Whereas the former three contaminants can be detected microscopically, mycoplasma organisms pose a greater problem as they are smaller than bacteria, do not have a cell wall and may multiply inside contaminated cells [159]. Mycoplasma contamination is difficult to detect since it does not affect the appearance of the nutrient medium and cannot be seen under the light microscope. In addition, if undetected, mycoplasma can cause a variety of changes in cell characteristics, such as changes in metabolism, immunologic or biochemical properties, growth rate and morphology. It is therefore essential to screen continuous cell cultures regularly for mycoplasma. There are a variety of screening kits now available, the most recent products being based on immunofluorescence techniques.

Ridascreen[®] is such an assay and was used routinely to screen for mycoplasma contamination in these studies.

3.2.3 Lipid composition of membranes from mammalian cells.

All membrane phospholipids are amphiphilic, that is, one end of the molecule is charged or polar and hydrophilic whereas the other is non-polar and hydrophobic. This is an integral feature of the phospholipid bilayer which constitutes biological membranes, where the polar head groups associate with water on the outside of the bilayer and the non-polar fatty acid chains are oriented to the interior of the bilayer [160]. Phospholipids are the most abundant class of lipid found in biological membranes and are based on either glycerol or sphingosine, where glycerophospholipids are the most important. The structure of a glycerophospholipid comprises two fatty acid chains, a glycerol backbone and a phosphorylated alcohol (the head group) (Figure 18).

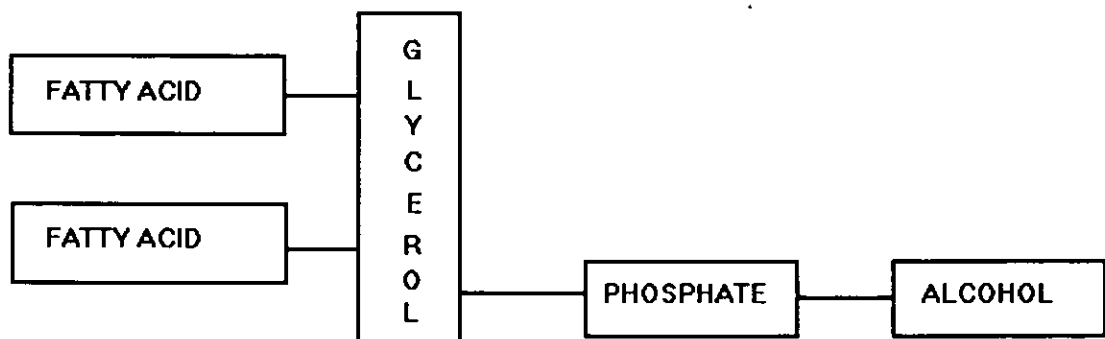


Figure 18 : General structure of a glycerophospholipid.

The fatty acids in mammalian cells possess an even number of carbon atoms, usually between 14 and 24 and are unbranched. Most phospholipids contain one saturated and one unsaturated fatty acid chain. Table 8 shows the fatty acids most commonly found in the phospholipids of mammalian cells.

TABLE 8 : Fatty acids most commonly found in phospholipids of mammalian cells
(Lockwood & Lee [160]).

NAME	STRUCTURE	NOTATION
PALMITIC ACID	$\text{CH}_3 (\text{CH}_2)_{14} \text{COOH}$	16:0
STEARIC ACID	$\text{CH}_3 (\text{CH}_2)_{16} \text{COOH}$	18:0
OLEIC ACID	$\text{CH}_3 (\text{CH}_2)_7 \text{CH}=\text{CH} (\text{CH}_2)_7 \text{COOH}$	18:1
LINOLEIC ACID	$\text{CH}_3 (\text{CH}_2)_4 (\text{CH}=\text{CHCH}_2)_2 (\text{CH}_2)_6 \text{COOH}$	18:2
ARACHIDONIC ACID	$\text{CH}_3 (\text{CH}_2)_4 (\text{CH}=\text{CHCH}_2)_4 (\text{CH}_2)_2 \text{COOH}$	20:4

The most common phospholipids found in mammalian membranes are phosphatidylcholine (lecithin) (PC), phosphatidylethanolamine (PE) and phosphatidylserine (PS) [160] (Figure 19). The net charge carried by each class of phospholipid at a physiological pH varies according to the structure. Each phospholipid carries a phosphate group which confers a negative charge at a physiological pH, however, choline and ethanolamine contain amino groups which are positively charged at pH 7. Thus phosphatidylcholines and phosphatidylethanolamines carry no net charge and are zwitterions at pH 7. By contrast, serine has one positive and one negative charge at pH 7, therefore phosphatidylserines carry a net negative charge and are anions at pH 7 [160].

Sphingolipids and glycerophospholipids are structurally very similar (Figure 19), however, sphingolipids have an aminoalcohol for the backbone rather than glycerol. The head group is the same as in PC and a sugar group may be attached giving cerebrosides. Complex glycolipids may contain branched chains of up to seven sugar groups.

The third main type of lipid found in mammalian membranes is cholesterol (Figure 19) and is usually found in high concentrations in the outer membrane of the cells, whereas the organelle membranes contain very little cholesterol [160].

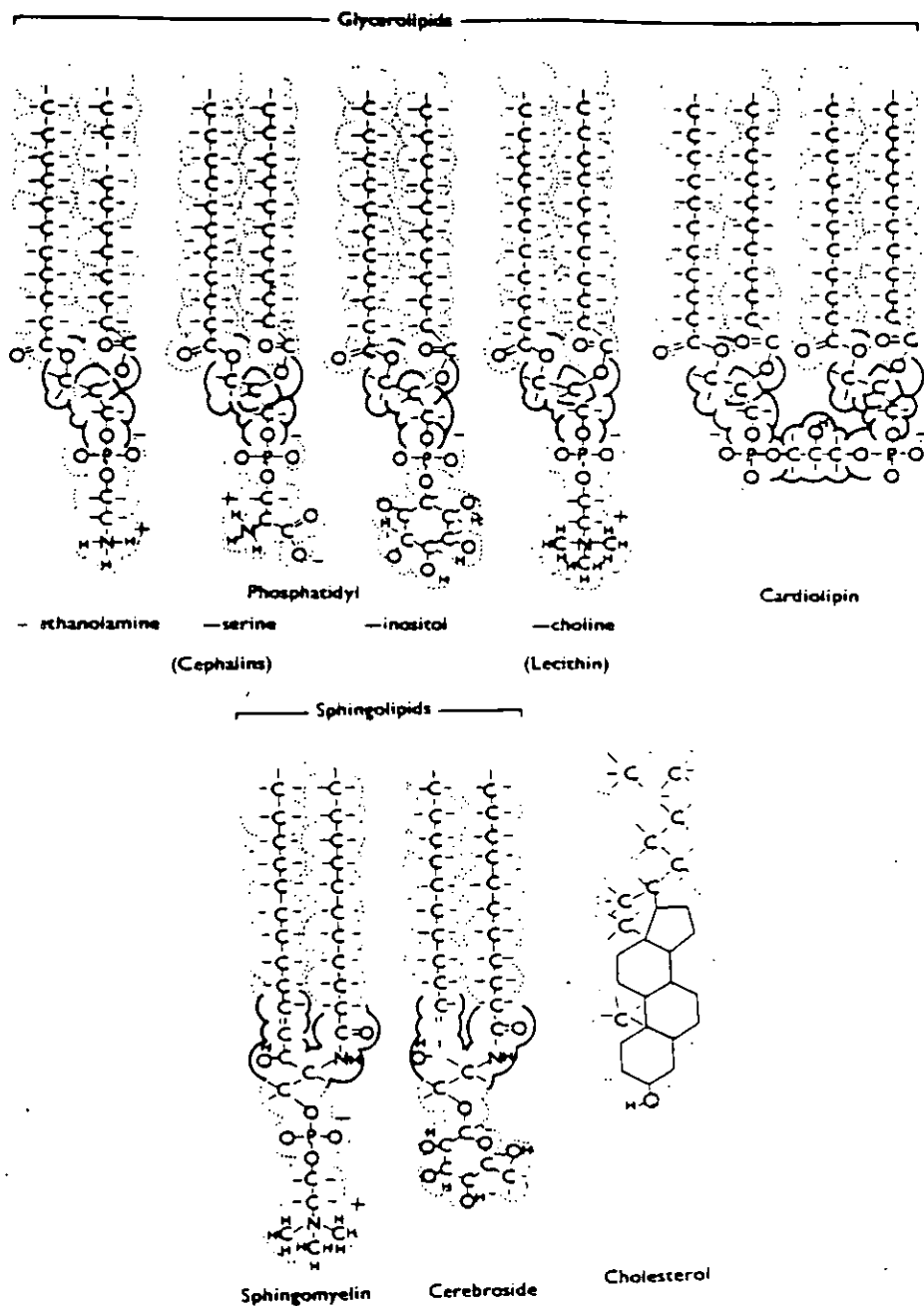


Figure 19 : Spatial representation of the chemical formulae of the major lipids found in biological membranes [160].

The relative proportions of the lipid classes vary between cell types and also between different membranes within the cell (Table 9). In general, zwitterionic lipids account for about 80% (w/w) of the total phospholipid and anionic lipids constitute about 20% (w/w) of the total [160].

Table 9 : Lipid composition of membranes from mammalian cells (expressed as weight percentages of total lipids) (Robinson, G.B., cited in Lockwood & Lee [160]).

LIPID CLASS ¹	PLASMA MEMBRANES	NUCLEAR MEMBRANES	MITOCHONDRIAL MEMBRANES
PHOSPHATIDYLCHOLINE	18.5	44.0	37.5
PHOSPHATIDYLETHANOLAMINE	11.5	16.5	28.5
PHOSPHATIDYLSERINE	7.0	3.5	0
SPHINGOMYELIN	12.0	3.0	0
CHOLESTEROL	19.5	10.0	2.5

¹ Membranes also contain other lipids such as cardiolipin (CL) and phosphatidylinositol (PI), not listed in this table.

3.2.4 Lipid Composition of MDR Cells.

MDR is associated with decreased cellular accumulation of cytotoxic drugs in resistant cell lines compared to that of sensitive parental cell lines [25]. The main mechanism for this phenomenon has been attributed to the overexpression of the *MDR1* gene encoding the energy-dependent drug efflux pump [25; sections 1.3 & 1.3.1]. This protein is situated in the plasma membrane and serves to efflux cytotoxic agents. Changes in the permeability of the membrane may also be implicated in the decreased intracellular drug accumulation. The anthracycline-resistant sub-line of P388 murine leukaemia cells (P388/Adr) shows cross-resistance to other chemotherapeutic agents [161] and studies have shown there to be differences in the structural lipid order of sensitive and resistant P388 cells [161]. A further study also found differences in the triglyceride levels and phosphatidylcholine / sphingomyelin ratio of this cell line and it was suggested that these alterations may be intimately involved in the resistance mechanism of P388/Adr cells [162]. The main differences observed were in the phospholipid profile of the two cell lines and the amount of triglycerides present. This study has examined the phospholipid

profile and percentage of the total fatty acid composition of EMT6-S and EMT6-R cells in order to establish any differences which may be associated with the resistance mechanism of EMT6-R cells.

The aim of this study was to characterise the two cell lines with regard to their growth kinetics, susceptibility to doxorubicin and membrane lipid composition. The screening of cell lines for mycoplasma infection was also described.

3.3 Methods and Materials.

3.3.1 Chemicals.

Analar chloroform, methanol and petroleum ether were obtained from Merck, Lutterworth, U.K. Glacial acetic acid, ANS (8-anilino-1-naphthalenesulfonic acid) (0.25% in MeOH), Dragendorff's spray reagent (0.1 M potassium iodide and 0.6 mM bismuth subnitrate in 3.5 M acetic acid) and ninhydrin spray reagent (0.2% ninhydrin in ethanol) were obtained from Sigma, Poole, U.K.

The Ridascreen® immunofluorescence assay was a gift from Digen Ltd., Oxford, U.K.

3.3.2 Maintenance of cell cultures.

The drug sensitive parental cell line used in this study was the murine mammary tumour cell line, EMT6 [163] and was designated EMT6-S. A multidrug resistant sub-line (EMT6-R), previously established by successive exposure to increasing concentrations of doxorubicin [5], was routinely maintained in RPMI 1640 growth medium (Life Technologies, Paisley, U.K.) supplemented with 5 µM doxorubicin (Farmitalia Carlo Erba Ltd., St. Albans, U.K.). Both cell lines were cultured in RPMI 1640 medium (Life Technologies) supplemented with 10% (v/v) foetal calf serum (M.B.Meldrum Ltd., Bourne End, U.K.), penicillin/streptomycin solution (Sigma, Poole, U.K.) at 1×10^4 units ml^{-1} and 10 mg ml^{-1} , respectively, in 0.9% NaCl and 2 mM L-glutamine (Sigma) at 37°C, 5% CO₂ : 95% air in a humidified Gallenkamp CO₂ incubator. The confluent cell monolayers were dissociated using 0.25% (w/v) trypsin (activity 1200 BAEE units/mg solid) (Sigma) in 0.5% (w/v) ethylenediaminetetraacetic acid (EDTA) (Sigma) in phosphate buffered saline (PBS) and resuspended at 5×10^4 and 1×10^5 cells per 10 ml medium in 25 cm² tissue culture flasks (Falcon, Fahrenheit Laboratories, Rotherham, U.K.) for EMT6-S and EMT6-R cells, respectively.

Stock cultures were preserved in liquid nitrogen at a density of 5×10^6 cells ml^{-1} in RPMI 1640 medium containing 20% (v/v) foetal calf serum and 10% (v/v) DMSO (Sigma). Cells were frozen at a rate of approximately 1°C min^{-1} . Frozen stocks were rapidly thawed by immersion of the freezing vials (Sigma) in a 37°C water bath. The cells were then washed with RPMI 1640 medium, centrifuged at 160 g for 5 minutes, the medium aspirated and replaced with fresh medium, in order to remove the DMSO. Cell lines were passaged at least twice prior to experimental use. All manipulations were carried out aseptically in a laminar air flow cabinet (Flow Gelaire BSB 4A).

3.3.3 Mycoplasma Screening.

Cells were routinely examined for mycoplasma infection using a commercial mycoplasma screening kit (Ridascreen[®]) based on an immunofluorescence assay. This assay contains a monoclonal antibody with specificity for a broad range of Mycoplasma species [164,165] and by combining this reaction with a fluorochrome-labelled secondary antibody, it provides a very sensitive method for mycoplasma detection.

EMT6-S and EMT6-R cells were grown in antibiotic-free RPMI 1640 medium supplemented with 10% (v/v) foetal calf serum and 200 mM L-glutamine, under growth conditions previously described, and were not sub-cultured for at least two days prior to screening. The cell monolayer was removed by trypsinisation and the cells counted, as previously described. The cells were then centrifuged at 160 g for five minutes, the supernatant removed, and washed twice with PBS. Finally, the cells were re-suspended in PBS to give a cell density of approximately 1×10^6 cells ml^{-1} . 20 μl of this sample (that is, approximately 20 000 cells) were placed into a 6-10 mm well area on a coated glass microscope slide and allowed to dry at 50°C for 45 minutes. When dry, the sample was fixed for 60 seconds in cold, 70% (v/v) ethanol (-20°C) and allowed to dry at room temperature. One drop of Fluorescein-labelled monoclonal antibody (designated Reagent 1) was added to the fixed cell preparation, ensuring that the reagent covered the entire well, and the sample was incubated for twenty minutes at room temperature. In all

staining procedures, the stain was not allowed to dry out, or non-specific staining would have occurred. The slide was washed with PBS and this was repeated twice more for two minutes. One drop of Goat Anti-Mouse-Fluorescein conjugate (designated Reagent 2) was added to the fixed cell preparation, again ensuring that the entire well area was covered, and was incubated for twenty minutes at room temperature. The slide was then washed twice in PBS for a total of two minutes and allowed to dry at room temperature. One drop of mounting fluid (designated Reagent 3) was placed in the centre of each well and a cover slip placed over the well area. Fixed specimen slides for positive and negative controls, provided in the kit, were stained using the same procedure as described above. The well areas of the sample slides were then scanned using a Leitz Diaplan fluorescence microscope with a filter system for Fluorescein (maximum excitation wavelength 490 nm, mean emission wavelength 520 nm) at $\times 400$ magnification and compared to the positive and negative control slides. Positive samples show yellow-green fluorescence on the shape of infected cells or between cells which appear bright red. In many cases, mycoplasmas are concentrated on a spot on the cell's surface. Various mycoplasma species may be present and these may vary in shape from small, coccoid bodies with bright fluorescence to short filaments which may be stained more diffusely.

3.3.4 Growth Kinetics.

Cells in exponential growth phase were trypsinised and resuspended at a cell density of 7.5×10^3 cells ml⁻¹. 2 ml aliquots of this suspension were seeded into 35 mm tissue culture plates and incubated in a humidified atmosphere at 37°C, 5% CO₂ : 95% air. At 24 hour intervals, plates were removed and the cell number determined by counting with an improved Neubauer haemocytometer. The medium was replaced on the remaining plates after 72 hours' incubation. The growth of each cell line was calculated as cell number per plate, and growth curves comparing the two cell lines were plotted.

3.3.5 Effect of doxorubicin.

Cells in exponential growth phase were trypsinised and resuspended at a density of 7.5×10^3 cells ml^{-1} . 2 ml aliquots of this suspension were seeded into 35 mm tissue culture plates and incubated at 37°C , 5% CO_2 : 95% air for 24 hours to allow cellular attachment. The medium was then aspirated and replaced with medium containing varying amounts of doxorubicin (0-10 μM). The plates were then incubated, as previously described, for a further 72 hours. Cell numbers were determined by counting with an improved Neubauer haemocytometer and were expressed as a percentage of the control cell number. The concentration of doxorubicin which inhibited cell growth by 50%, the IC_{50} value, was determined for each cell line.

3.3.6 Membrane lipid composition.

3.3.6.1 Preparation of samples for phospholipid and fatty acid analysis.

20 ml aliquots of EMT6-S or EMT6-R cells in RPMI medium were seeded at a cell density of 5×10^3 and 1×10^4 cells ml^{-1} , respectively, into 75 cm^2 tissue culture flasks and grown to confluence at 37°C , 5% CO_2 :95% air. A representative flask from each cell line was trypsinised, as described previously, and the cell number ml^{-1} was determined using an improved Neubauer haemocytometer. Care was taken to ensure equal sample size (determined by cell numbers) in order to give a valid comparison of results. The sample flasks were treated as follows : the RPMI medium was aspirated and the cell monolayer washed three times with 4 ml PBS. The cells were then scraped carefully from the flask, mixed with 2 ml distilled water and mixed well. Three samples were then pooled into a pre-cleaned methylating tube. The pooled samples were centrifuged at 160 g for 5 minutes, the supernatant aspirated and replaced with 2 ml distilled water. The cells were then vortex mixed and sonicated. The suspension was added to 2.5 ml methanol (pre-heated to 60°C) in a pre-cleaned methylating tube, heated for 30 minutes at 70°C , cooled and centrifuged at 160 g for ten minutes. The upper

aqueous layer was removed and discarded and the lower phase washed three times with a mixture of chloroform, methanol and water in the proportions 3 : 48 : 47 (by volume), respectively. The washed layer was then split into two samples, one for fatty acid analysis and the other for phospholipid analysis. Each of these samples was dried under a stream of nitrogen to prevent oxidation.

3.3.6.2 Preparation of Fatty Acid Methyl Esters and Analysis by Gas Chromatography .

Fatty acid methyl esters (FAMES) were prepared by transmethylation with 2.5% (v/v) sulfuric acid in anhydrous methanol at 70°C for 2 hours. FAMES were extracted with 3 x 3 ml petroleum ether and separated by gas chromatography (GC) using a Unicam 610 gas chromatograph equipped with a megawax fused silica capillary column (30 m x 0.25 mm (internal diameter); film thickness 0.25 µM) operating in cooled on-column injection mode. The following temperature programme was used : injection at 55°C, held for 1 minute, increasing to 205°C at a rate of 15°C min⁻¹. A mixture of known FAME standards was separated at the commencement of each run, and 20 µg of the FAME standard 15:0 was incorporated into each sample prior to transmethylation. The percentage fatty acid composition was determined from the GC traces by comparing each peak area to the peak area of the internal standard .

3.3.6.3 Analysis of Phospholipids by Thin Layer Chromatography.

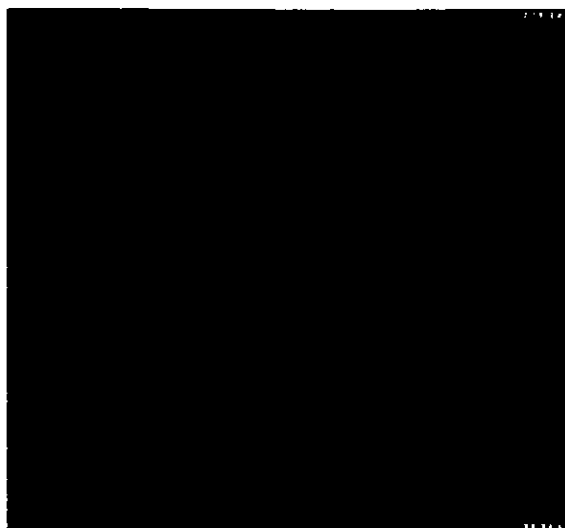
Cell samples previously prepared (see 3.3.4.1) were each re-suspended in chloroform, mixed well and applied to a silica gel chromatography plate (Silica Gel 60, Merck Ltd., Lutterworth, U.K.) Each plate was treated with one sample extracted from EMT6-S cells and one sample extracted from EMT6-R cells, both applied as thin streaks 5-10 mm long. Single spots of commercial phospholipid standards (Lipid Products, Redhill, U.K.) were also applied. TLC was then performed using a running solvent of chloroform, methanol, glacial acetic acid and water in the following proportions : 170 : 30 : 20 : 7 (by

volume), respectively. Phospholipid components were visualised by spraying the plate with ANS (8-anilino-1-naphthalenesulfonic acid) (0.25% (w/v) in MeOH) and examining under UV light. Individual phospholipids were identified by comparison to the commercial standards and confirmed by the use of specific stains : Dragendorff's reagent (0.1 M potassium iodide and 0.6 mM bismuth subnitrate in 3.5 M acetic acid) specific for PC, lyso-PC and sphingomyelin; ninhydrin (0.2% in ethanol) specific for PE, PS and their lyso-derivatives [166].

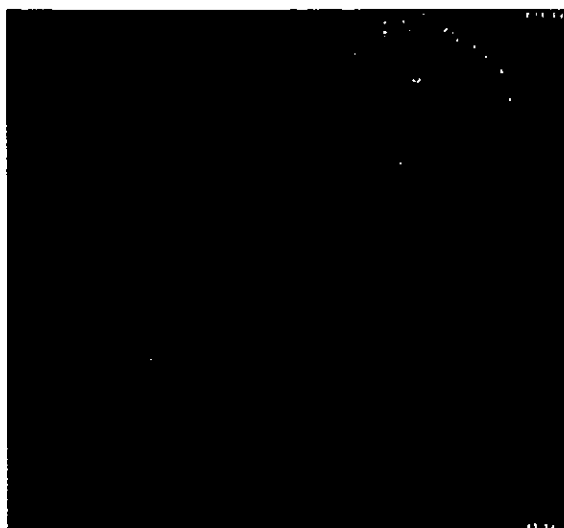
3.4 Results.

3.4.1 Mycoplasma Screening.

The EMT6-S and EMT6-R cell lines were found to be free from mycoplasma contamination when tested on a routine basis. Figure 20 (a & b) shows a representative selection of EMT6-R and EMT6-S cells, respectively, which have been exposed to the fluorescence-labelled Mycoplasma-specific monoclonal antibodies using the Ridascreen[®] mycoplasma screening kit. Figure 20 (c & d) shows the positive and negative control cells, respectively. The yellow-green fluorescence around the positive control cells clearly shows the presence of mycoplasma infection. No fluorescence was detected in the negative control cells or either cell line.



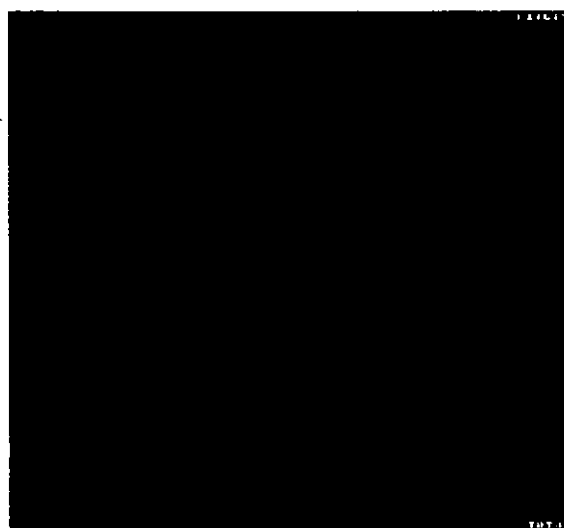
(a)



(b)



(c)



(d)

Figure 20 : Screening of EMT6-S and EMT6-R cells for mycoplasma infection using the Ridascreen[®] immunofluorescence assay.

Immunofluorescence, indicating mycoplasma infection, was clearly evident around the positive control cells (c), however, no fluorescence was detected in the negative control cells (d), the EMT6-R cells or the EMT6-S cells (a & b, respectively).

3.4.2 Growth kinetics.

The log phase doubling time (h) was found to be markedly longer for the drug resistant cell line EMT6-R than for that of the drug sensitive parent cell line EMT6-S, that is 25.0 and 21.8, respectively (Figure 21).

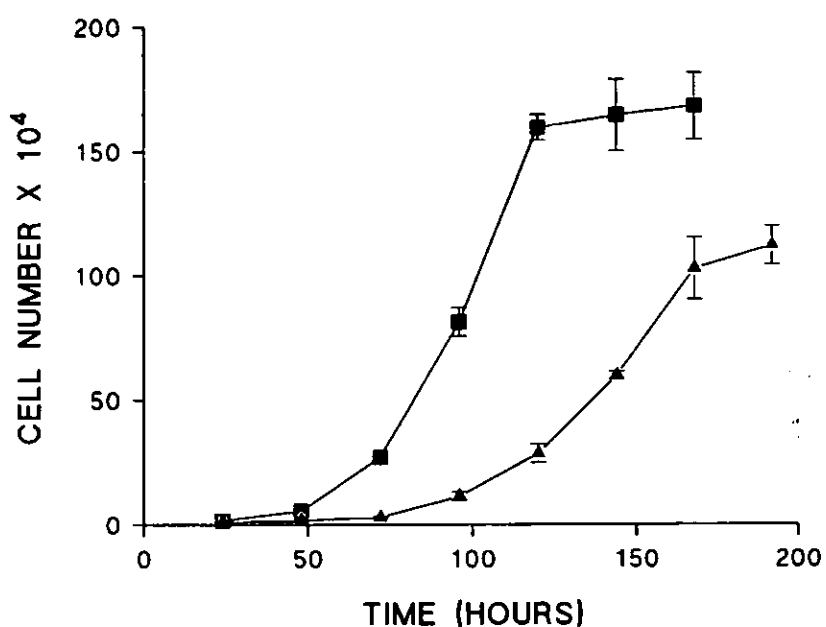


Figure 21 : Growth kinetics of the mouse mammary tumour cell lines EMT6-S (■) and EMT6-R (▲), incubated at 37°C in the presence of 95% air, 5% CO₂. Each point represents mean \pm SEM (n=3).

3.4.3 Effect of doxorubicin.

The IC_{50} values (defined as the concentration of drug which causes a 50% reduction in growth compared to the control) for doxorubicin were found to be 2.2×10^{-8} M and 1.8×10^{-6} M, for EMT6-S and EMT6-R cells, respectively (Figure 22). The resistance factor was found to be 82.

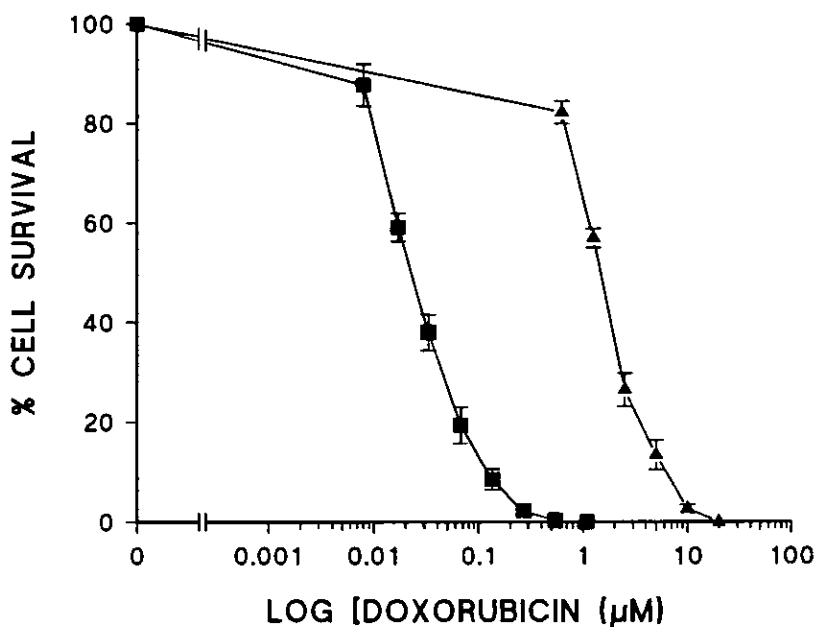


Figure 22 : Dose survival curve for EMT6-S (■) and EMT6-R (▲) cell lines challenged with doxorubicin. Each point represents mean \pm SEM (n=10).

3.4.4 Membrane lipid analysis.

3.4.4.1 Fatty Acid Composition.

The percentage fatty acid composition was determined for the most common fatty acids found in the phospholipids of biological membranes. This was compared between EMT-S and EMT6-R cells (Table 10). No significant difference was found between the overall fatty acid composition of the membranes, although the level of linoleic acid in the resistant cells appeared to be increased ($p = 0.05$).

Table 10 : Comparison of the percentage of total fatty acid composition of EMT6-S and EMT6-R cells (commonly occurring fatty acids).

Results are given as mean \pm SEM ($n=5$ for EMT6-S, $n=4$ for EMT6-R). Statistical analysis by the Student's t-test (ns = not significant , s = significant at the 5% level)).

% (w/w)				
TOTAL FATTY ACID COMPOSITION				
FATTY ACID	NOTATION	EMT6-S CELLS	EMT6-R CELLS	p VALUE
PALMITIC ACID	16:0	27.7 \pm 2.4	29.3 \pm 2.5	0.66 (ns)
STEARIC ACID	18:0	20.2 \pm 1.1	21.1 \pm 4.0	0.82 (ns)
OLEIC ACID	18:1	43.4 \pm 1.2	52.0 \pm 5.7	0.13 (ns)
LINOLEIC ACID	18:2	2.7 \pm 0.1	4.3 \pm 0.7	0.05 (s)
ARACHIDONIC ACID	20:4	6.3 \pm 0.3	5.1 \pm 1.5	0.40 (ns)

3.4.4.2 Phospholipid Composition.

No difference was observed between the phospholipid profile of the membranes of EMT6-S cells and EMT6-R cells as determined by one-way TLC. Very reproducible results were achieved ($n=4$). Figure 22 is a graphical representation of a typical separation of the phospholipids in EMT6-S and EMT6-R cells.

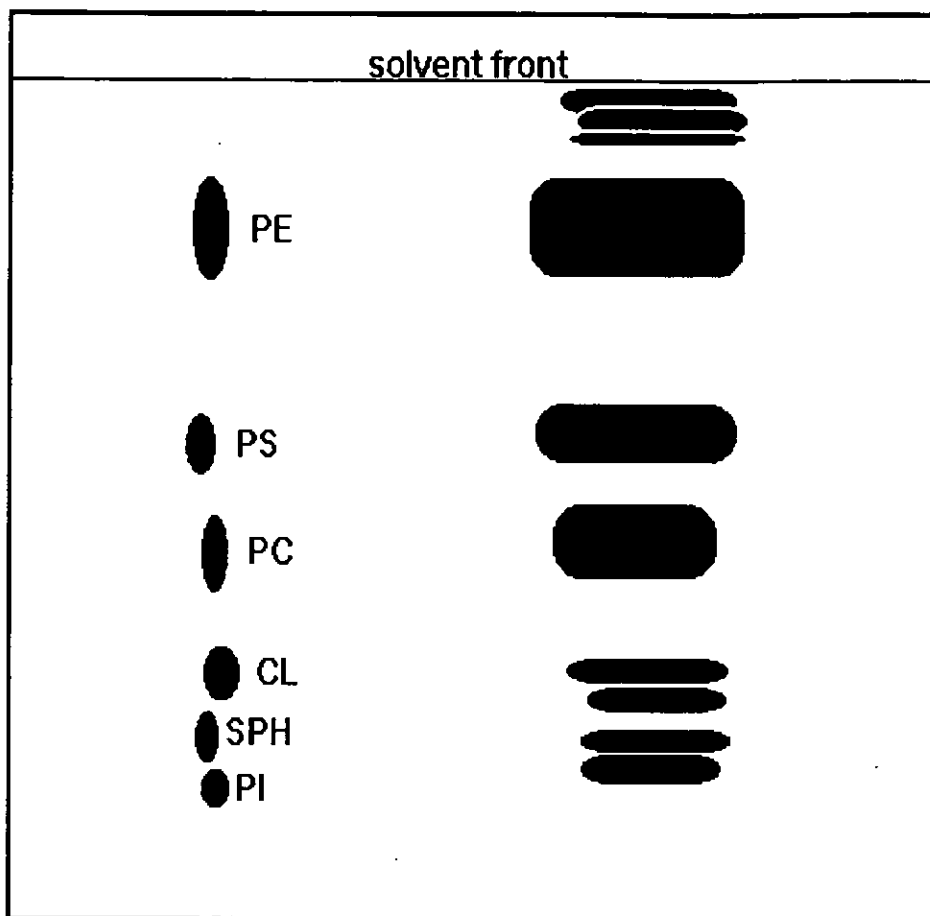


Figure 23 : Schematic representation of the separation of phospholipids in EMT6-S and EMT6-R cells by thin-layer chromatography.

Phospholipids were separated using thin layer chromatography on silica gel plates using a running solvent of chloroform, methanol, glacial acetic acid and water in the following proportions : 170 : 30 : 20 : 7 (by volume), respectively. Phospholipid components were visualised by spraying the plate with ANS (8-anilino-1-naphthalenesulfonic acid) (0.25% (w/v) in MeOH) and examining under UV light. Individual phospholipids were identified by comparison to the commercial standards and confirmed by the use of specific stains. Phosphatidylethanolamine (PE); phosphatidylcholine (PC); phosphatidylserine (PS); sphingomyelin (SPH); cardiolipin (CL) & phosphatidylinositol (PI). The three bands immediately below the solvent front appeared to be neutral lipids, and the band below CL was identified as lyso-phosphatidylcholine.

3.5 Discussion.

As discussed previously, a number of phenotypic changes have been demonstrated by MDR cells [5]. The basic growth characteristics of these cell lines, compared to the parental cell lines, must be established prior to any studies undertaken, so that these parameters may be taken into account in the design of experiments. The log phase doubling time and IC₅₀ values with respect to EMT6-S and EMT6-R cell lines were indeed found to be different, in good agreement with values previously established by Cox [5]. In addition, since insidious infections of continuous cell cultures, such as mycoplasma, can also affect cellular characteristics and functions, routine monitoring of cell cultures must be undertaken to prevent contamination and consequential erroneous results. The immunofluorescence assay, Ridascreen®, proved to be a convenient, reliable screening tool. Both cell lines were found to be free from contamination.

Decreased drug accumulation in MDR cells has been linked to alterations in lipid profiles in some studies, however, no difference was observed in the phospholipid profiles of EMT6-S and EMT6-R cells. Comparison of the percentage of the total fatty acid composition showed there to be no significant difference between the two cell lines ($p > 0.05$) with the exception of linoleic acid (18:2), where the level appeared to be higher in the resistant cell membranes ($p = 0.05$). Ramu *et al.* [161] identified differences in the structural lipid order in P388 and P388/Adr cells. No significant differences in the free cholesterol or total phospholipid content were found although alterations were shown in the composition of the phospholipids [162]. The content of PE and CL was unchanged, however, the PC / sphingomyelin ratio of P388/Adr cells was significantly lower than that of the sensitive, parental line. They suggest that this altered ratio is associated with higher plasma membrane structural order which affects membrane permeability and may lead to lower intracellular drug accumulation. It may be argued that the alteration in linoleic acid content in EMT6-R cells would be predicted to increase membrane fluidity, however, Cox [5] found there to be no significant difference in fluidity of the membranes of EMT6-S and EMT6-R cells at any temperatures tested, using the fluorescent probe

1-(4-trimethylammonium phenyl)-6-phenyl-1,3,5-hexatriene (TMA-DPH) to determine the fluorescence anisotropy.

CHAPTER FOUR

CELL KILLING BY CATIONIC PHOTSENSITIZERS IN A MULTIDRUG RESISTANT CELL LINE.

4.1 Abstract

Methylene blue (MB) and toluidine blue (TBO) are known bioactive photosensitizers. Victoria blue BO (VBBO) may also fall into this category, but chemical tests have failed to detect the generation of singlet oxygen in this study. The ability of these three dyes to induce a photocytotoxic response in a murine mammary tumour cell line (EMT6-S) and a multidrug resistant sub-line (EMT6-R) was investigated and their ability to overcome multidrug resistance was compared to that of the conventional chemotherapeutic agents doxorubicin and *cis*-platinum. The cytotoxic effect of VBBO was found to be enhanced 10-fold by illumination (7.2 J cm^{-2}) in both the sensitive and resistant cell lines. In order to overcome resistance, however, the EMT6-R cells required a 10-fold greater level of the dye than the parental cells to reach an IC_{50} value. VBBO was thus susceptible to MDR, but to a considerably lesser extent than the conventional agent doxorubicin which required almost a 100-fold increase in concentration to overcome resistance. VBBO also has the ability to act as a photosensitizer whereas illumination (7.2 J cm^{-2}) had no apparent effect on the activity of doxorubicin and *cis*-platin. Both TBO and MB showed limited light activation (2-fold) in both the sensitive and resistant cell lines and it appeared that the main cytotoxic response was due to the dark toxicity of the agents. This dark toxicity seemed to overcome MDR, possibly implying that these agents were able to avoid exclusion by P-glycoprotein (Pgp).

Pre-treatment of EMT6-S and EMT6-R cells with low concentrations of VBBO, MB or TBO, (equivalent to 1/8th IC_{50} value for each photosensitizer), prior to exposure to doxorubicin, enhanced the cytotoxicity of doxorubicin in all cases. Pre-treatment with VBBO resulted in a two-fold increase in doxorubicin toxicity in both cell lines, suggesting that the action of VBBO is independent of the Pgp drug efflux pump which is overexpressed in the resistant cell line. Pre-treatment with MB, however, increased doxorubicin toxicity in EMT6-R cells two-fold, but had less effect on the sensitive cell line (increase x 1.4). This suggests a different mechanism of action to that of VBBO, which may involve interaction with Pgp. Pre-treatment with TBO resulted in an increase

in toxicity of almost two-fold in EMT6-S cells, but this was increased to three-fold in the resistant cell line, again suggesting possible interaction with Pgp.

4.2 Introduction

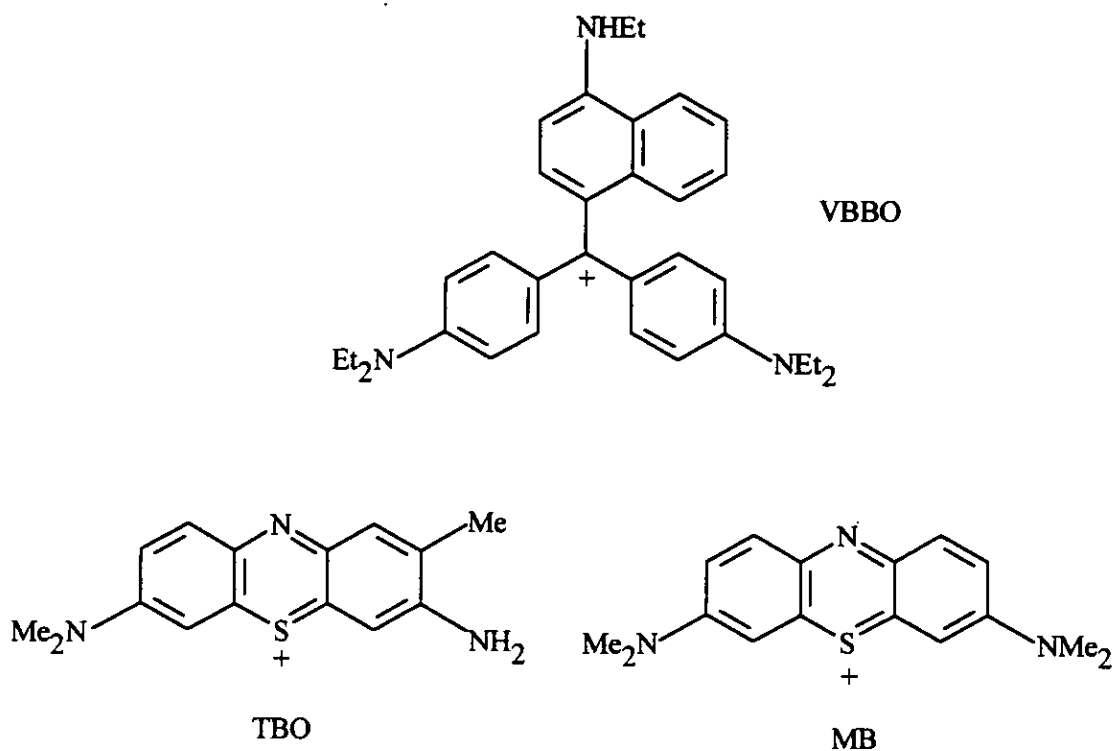
Multidrug resistance is a major obstacle to the successful treatment of cancer. Pleiotropic MDR occurs when treatment with a single cytotoxic agent results in the development of cross-resistance to other structurally non-related drugs and is associated with a decreased intracellular accumulation of the drug [26]. Photodynamic therapy (PDT) has been used increasingly in neoplastic disease and offers considerable scope for the circumvention of MDR. PDT requires the combination of a photosensitizing drug, light of the correct wavelength and molecular oxygen to exert its effect [102]. The generally accepted routes by which cell death is initiated in PDT are free radical formation by biomolecules (Type I) and chemical reactions involving the cytotoxin singlet oxygen (Type II) [113 ; section 1.4.2].

A wide range of photosensitizing drugs is available including porphyrin-based drugs and their analogues, such as chlorins, and larger aromatic systems such as the phthalocyanines [110,111]. Clinical application of commercial photosensitizers has also been investigated, since these compounds have the advantage of well established chemistries and ready availability, however higher inherent toxicity has often proved problematic. Cationic examples of this commercial class are the triarylmethane dye Victoria Blue BO (VBBO) and the phenothiazinium photosensitizers toluidine blue (TBO) and methylene blue (MB) (Figure 24).

The Victoria blue series consists of triarylmethane dyes related to crystal violet, where one of the phenyl groups is replaced by 1-naphthyl. It has been suggested that the flexibility of the ring structure of triarylmethanes causes a fast relaxation of the singlet excited state, resulting in a low degree of photosensitizing activity [133]. When immobilised, however, the photosensitizing activity of these compounds is greatly increased. This is thought to occur when binding of the structure to biomolecules endows greater structural rigidity [137]. The phenothiazinium dyes have a rigid, planar structure and are well established Type II photosensitizers [128]. Conversely Victoria

blue BO shows no evidence for the formation of singlet oxygen in solution, but has previously been shown to have some photosensitizing activity in several mammalian cell lines, including human squamous cell carcinoma (FaDu) and human melanoma (NEL) [133, 167]. MB has been used as a vital stain for over a century and is used as a diagnostic agent in many diseases, and as a tumour marker. It has been used to a lesser extent in the field of PDT, most notably in the treatment of bladder, oesophageal and other cancers [121-123], however, its efficacy is limited by reduction to leuco-methylene blue (140) in biological systems (see section 1.4.4). MB is thought to exert its photocytotoxic effects by DNA intercalation. TBO is similar in structure to MB (Figure 24) and is used as a selective stain for oral cancer and is also used in oral disease as an antibacterial agent [141].

The cellular localisation of the photosensitizers used in this study, VBBO, MB and TBO has been investigated previously [132,168,169]. The phenothiazine derivatives MB and TBO are highly hydrophilic in nature and as such are membrane interactive [170]. In solution, both cations are hydrophilic ($\log P = -0.1$ (MB), -0.21 (TBO)) (Figure 24), however, both dyes are subject to metabolic reduction in biological systems producing neutral species, and TBO is partially converted to a neutral form by deprotonation [140]. By contrast, VBBO is highly lipophilic ($\log P = +3.5$) (Figure 24). The much higher lipophilicity of VBBO, compared to MB and TBO, suggests that it is able to diffuse through the plasma membrane and to reach the cell interior. VBBO is known to be specific for mitochondria [132,167] and on photoirradiation is reported to act by selective inhibition of mitochondrial Respiratory Complex I, whereas the dark toxicity is accounted for by uncoupling of oxidative phosphorylation [132]. TBO has been found to localise in the cytoplasm of HeLa cells [128] and also in the mitochondria of an epidermoid cancer cell line [168]. By contrast, MB has been shown to localise in lysosomes [169], however, Yu *et al.* [171] reported that photoinactivation by MB is a multistage process with synchronous involvement of the cell membrane, cytoplasm and nucleus.



Drug		λ_{\max} (nm) ^a	$\log \epsilon_{\max}$ ^b	$\log P$ ^c
Victoria Blue BO	VBBO	612	4.58	+3.5
Toluidine blue	TBO	626	4.76	-0.21
Methylene blue	MB	656	4.98	-0.10

^aWavelength of maximum absorption and ^blogarithm of the extinction coefficient measured in aqueous buffer, pH 7.3 and ^clogarithm of the partition coefficient between water and 1-octanol.

Figure 24 : Victoria blue, toluidine blue O and methylene blue: structures and physicochemical properties.

As mentioned above, PDT is being used increasingly in the treatment of many neoplasms and offers the potential for overcoming drug resistance. Multiple drug resistance to anthracyclines and other chemotherapeutic agents is commonly attributed to increased expression of the 170 - 180 kDa membrane protein, P-glycoprotein, which is thought to act either as a drug efflux pump [25] or as a flippase [40] to reduce the intracellular concentration of the drug. Studies have shown, however, that P-glycoprotein is not always involved, but rather that MDR is multifactorial and may involve many other biochemical changes and protein alterations [83,172].

Doxorubicin is an anthracycline antibiotic widely used in cancer chemotherapy (Figure 25). It has a complex mechanism of action and many theories regarding this have been postulated. Recent work [143] seems to indicate that doxorubicin acts initially at the membrane, increasing phosphatidylinositol turnover, which in turn disrupts cellular signalling mechanisms [173]. Following membrane perturbation, doxorubicin binds to the DNA by intercalation and affects DNA / RNA synthesis *via* altered topoisomerase II activity [174]. Studies have also shown that the anthraquinone nucleus of anthracyclines is reversibly converted to a free radical semiquinone forming superoxide and hydroxyl radicals [175], which may lead to damage by methods such as lipid peroxidation.

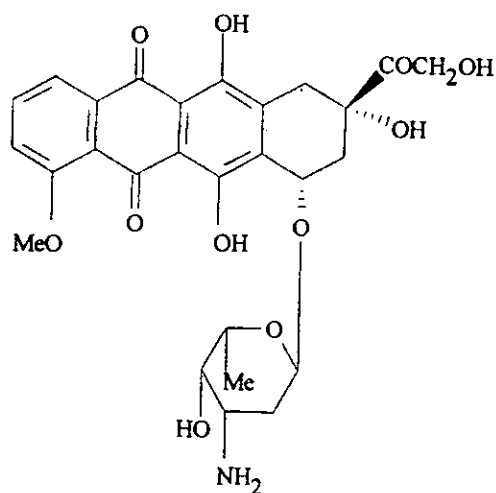


Figure 25 : Structure of doxorubicin.

cis-Diamminedichloroplatinum (II) (*cis*-platinum) [Figure 26] has broad anti-neoplastic activity and is used in the treatment of various cancers, such as epithelial, testicular, head and neck, bladder, small-cell lung and ovarian cancers [176]. It is an inorganic water-soluble, platinum-containing complex which appears to enter cells by diffusion. The platinum complexes can react with DNA to form both intrastrand and interstrand cross-links [176].

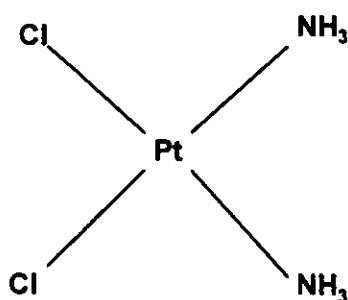


Figure 26 : Structure of (*cis*-Platinum).

The aim of this study was to compare the activity of the cationic photosensitizers VBBO, MB and TBO to that of the more conventional chemotherapeutic agents doxorubicin and *cis*-platinum against a mouse mammary tumour cell line, EMT6. The parental cell line (EMT6-S) is sensitive to treatment with doxorubicin, but the sub-line (EMT6-R) is resistant to doxorubicin, over-expresses Pgp in the cell membrane, and shows cross-resistance to other non-related chemotherapeutic agents [5]. Confocal microscopy was also employed to compare the localisation of VBBO, MB and TBO in both EMT6-S and EMT6-R cell lines.

4.3 Materials and Methods

4.3.1 Chemicals

Methylene blue, toluidine blue, Victoria blue BO, and 1-octanol were purchased from Aldrich Chemicals (Gillingham, UK) and were used without further purification. *cis*-Platinum (*cis*-diamminedichloroplatinum (II)), MTT (3-[4,5-dimethylthiazol-2-yl]-2,5-diphenyl-2*H*-tetrazolium bromide), DMSO (dimethyl sulfoxide) and verapamil were obtained from Sigma, Poole, U.K. and doxorubicin was a gift from Farmitalia Carlo Erba Ltd., St. Albans, U.K.

4.3.2 Cell Culture

The murine mammary tumour cell line (EMT6) was originally obtained from Zeneca Pharmaceuticals, Macclesfield, Cheshire, U.K. Cultures were routinely maintained at 37°C, 5% CO₂ : 95% air in RPMI 1640 culture medium (Life Technologies, Paisley, U.K.), supplemented with 10% (v/v) foetal calf serum (M.B.Meldrum Ltd., Bourne End, U.K.), 200 mM glutamine (Sigma, Poole, U.K.) and penicillin/streptomycin solution at 1x10⁴ units ml⁻¹ and 10 mg ml⁻¹, respectively, in 0.9% NaCl (Sigma). Trypsin (activity 1200 BAEE units/mg solid) was obtained from Sigma.

4.3.3 Phototoxicity : Dark Toxicity Experiments

Light from a source of variable wavelength, with maximum emission in the 600-700 nm region and a fluence of 4 mW cm⁻², was used to illuminate the cells which had been exposed to the various dyes. The light dose was measured with a Skye SKP 200 light meter (Skye Instruments Ltd.). The temperature of the system was monitored constantly during irradiation but no heating effect was observed.

4.3.5 Localisation Studies Using Scanning Laser Confocal Microscopy

2 ml aliquots of EMT6-S or EMT6-R cells were seeded at a cell density of 1×10^4 cells ml^{-1} into 35 mm petri dishes (Falcon, Fahrenheit Laboratories, Rotherham, U.K.) in RPMI 1640 medium, supplemented with 10% (v/v) foetal calf serum, 200 mM L-glutamine and penicillin/streptomycin solution at 1×10^4 units ml^{-1} and 10 mg ml^{-1} , respectively, as previously described. A sterile quartz coverslip (suprasil, 0.5 mm diameter x 0.2 mm thick, Heraeus Silica & Metals Ltd., Byfleet, U.K) was placed into each petri dish and the cells were allowed to attach for three days (EMT6-S cells) or four days (EMT6-R cells) whilst incubating at 37°C, 5% CO_2 : 95% air. The medium was aspirated and replaced with medium containing VBBO, MB or TBO, and incubated for three hours, as previously described. Concentrations of drugs added were as follows : for EMT6-S cells, 5.0 μM VBBO, 25 μM MB and 10 μM TBO; for EMT6-R cells, 5.0 μM VBBO, 35 μM MB and 15 μM TBO. Following 3 hours' incubation, the cells were examined with a scanning laser confocal fluorescence microscope using a helium / neon laser at 633 nm. Untreated cells were also examined, under the same conditions, for autofluorescence, however, none was observed.

4.4 Results

4.4.1 Phototoxicity : Dark toxicity

Exposure of EMT6-S and EMT6-R cells to light alone (7.2 J cm^{-2}) did not produce cytotoxicity ($p > 0.05$) (Figure 27). However, VBBO, MB and TBO were all found to exert a photocytotoxic effect when exposed to light (7.2 J cm^{-2}) (Figures 28 & 29). Statistical analysis was carried out using the Student's t-test.

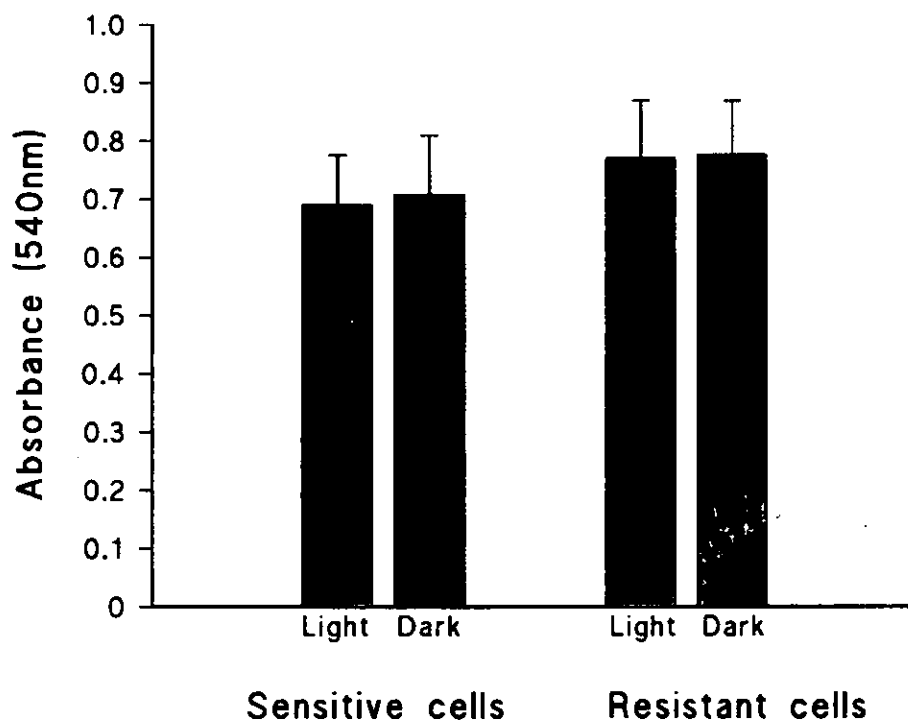


Figure 27 : Effect of light (7.2 J cm^{-2}) on EMT6-S (sensitive) and EMT6-R (resistant) cells.

Cell viability was evaluated using the MTT assay [177]. MTT is a yellow tetrazolium dye which is reduced to purple formazan crystals by live cells. The crystals are solubilised in DMSO and the absorbance read spectrophotometrically at 540 nm. Each point represents mean \pm SEM ($n \geq 11$).

All the photosensitizers were found to have some effect in reducing drug resistance in the EMT6-R cell line, in the order VBBO > TBO > MB (Figures 28b & 29b) when exposed to light (7.2 J cm^{-2}), however, VBBO and TBO were the most effective in the dark (Figures 28a & 29a). VBBO was more effective (both in the light and the dark) than *cis*-platinum. The resistant cell line (EMT6-R) required almost 100-fold more doxorubicin than the sensitive cell line to obtain the IC_{50} (Table 11). By contrast, this resistance was overcome by *cis*-platinum (Table 11). Illumination of VBBO (7.2 J cm^{-2}) resulted in a 10-fold decrease in the IC_{50} value (Table 11), which clearly indicates that VBBO is able to induce a photocytotoxic response and that it is able to kill MDR cells. EMT6-S cells line showed a similar response. The IC_{50} of VBBO for the resistant cell line, however, was 10-fold greater than for the sensitive cell line (Table 11), suggesting that efflux of the drug by the resistant cells may have led to the higher requirement for effective cytotoxicity. In the case of MB and TBO, both the resistant and sensitive cells showed approximately a 2-fold increase in susceptibility to the agent when illuminated (7.2 J cm^{-2}), but, interestingly, the levels required to overcome the resistant cell line were similar to those required for the sensitive cell line (Table 11). This suggests that there is some degree of photoactivity, but that MB and TBO are toxic in their own right and may be able to circumvent the effect of P-glycoprotein.

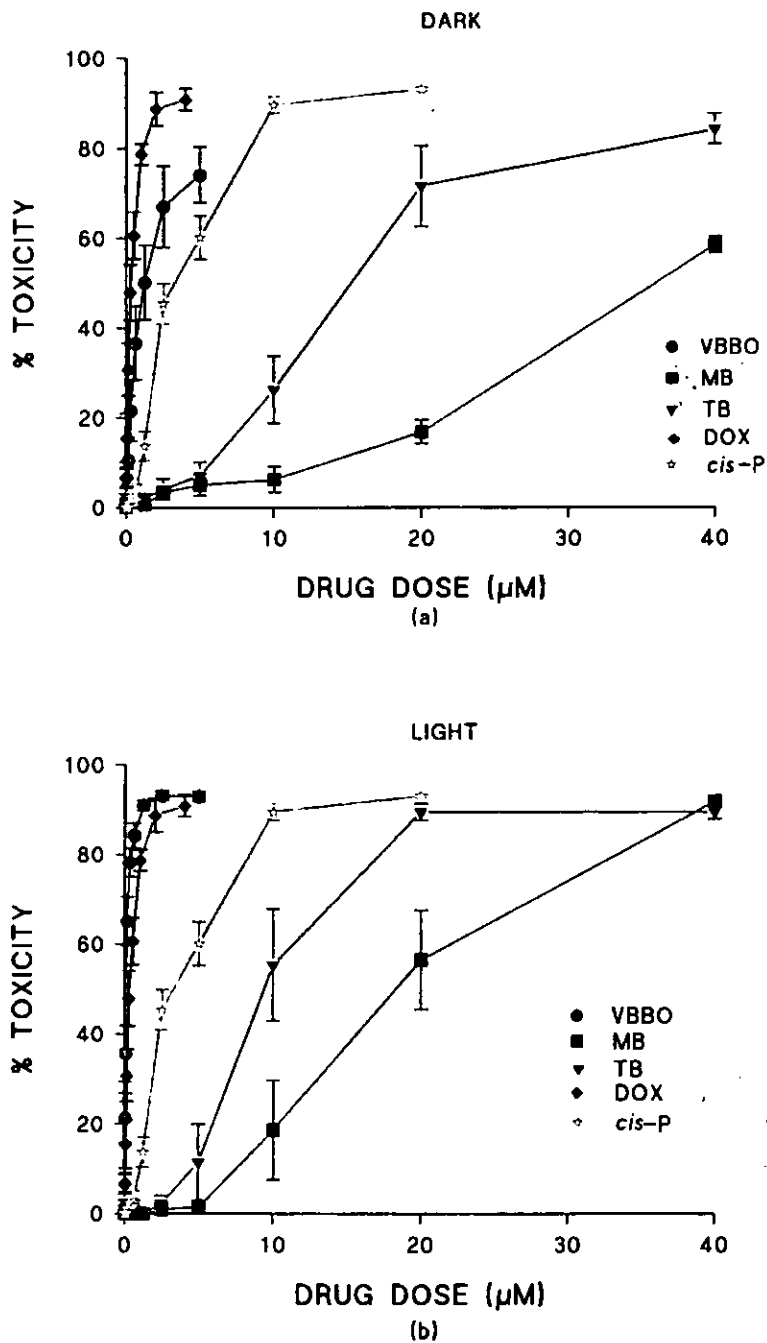


Figure 28 : Comparison of % cytotoxicity elicited by VBBO, MB, TBO, doxorubicin & cis-platinum against EMT6-S cells.

Cells (1000 / well in 96 well plates) were allowed to attach for 48 hours. Drugs (200 µl at 0 - 0.625 µM in RPMI 1640) were added to the cells and incubated for 3 hours. The cells were then rinsed with RPMI 1640 and exposed to light (7.2 J cm⁻²) (b) or kept dark (a), prior to growing on for 3 days at 37°C, 5% CO₂ : 95% air. Cytotoxicity was measured using the MTT assay. Each point represents mean ± SEM (n ≥ 6).

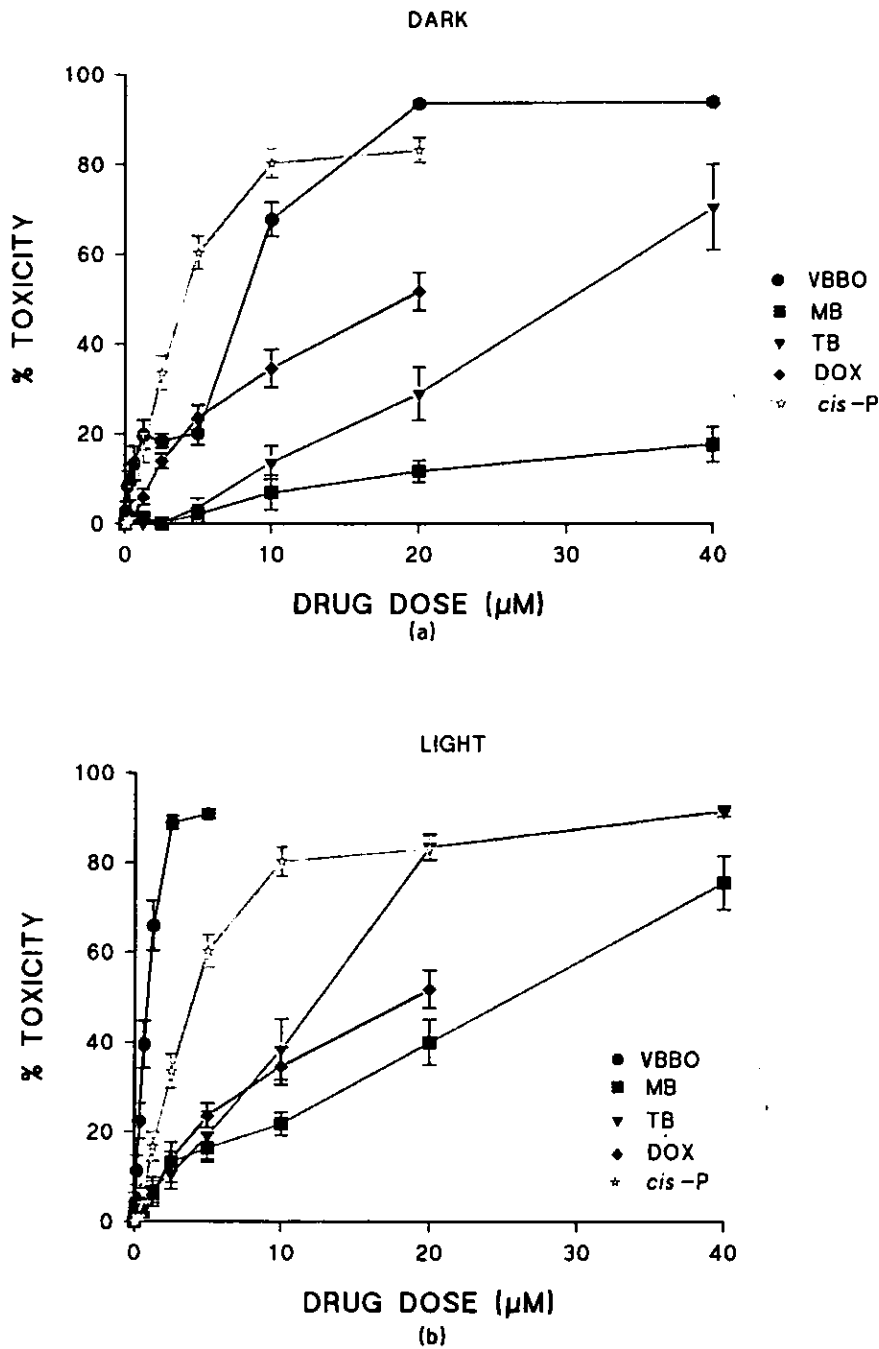


Figure 29 : Comparison of % cytotoxicity elicited by VBBO, MB, TBO, doxorubicin & cis-platinum against EMT6-R cells.

Cells (1000 / well in 96 well plates) were allowed to attach for 48 hours. Drugs (200 µl at 0 - 0.625 µM in RPMI 1640) were added to the cells and incubated for 3 hours. The cells were then rinsed with RPMI 1640 and exposed to light (7.2 J cm⁻²) (b) or kept dark (a), prior to growing on for 3 days at 37°C, 5% CO₂ : 95% air. Cytotoxicity was measured using the MTT assay. Each point represents mean ± SEM (n ≥ 6).

Table 11 : IC₅₀ values for photosensitizers, doxorubicin and *cis*-platinum.

The light enhancement factor is the ratio of light : dark IC₅₀ values. The light:dark differential is not constant, but varies at different concentrations, and for this reason has been standardised, using the IC₅₀ values, to give the LEF.

DRUG	DARK IC₅₀ (μM)	LIGHT IC₅₀ (μM)	LIGHT ENHANCEMENT FACTOR (LEF)
SENSITIVE CELLS			
VBBO	1.25	0.12	10.4
MB	36.0	17.5	2.1
TBO	16.0	9.0	1.8
Doxorubicin	0.25	0.26	1.0
<i>cis</i>-Platinum	3.6	3.6	1.0
RESISTANT CELLS			
VBBO	8.5	1.0	8.5
MB	72.0	26.0	2.8
TBO	30.0	13.0	2.3
Doxorubicin	20.0	19.0	1.0
<i>cis</i>-Platinum	3.7	3.8	1.0

4.4.2 Localisation Studies Using Confocal Scanning Laser Fluorescence Microscopy.

The brightness of the images varied considerably and in some instances the colour map was stretched. The greyscale value range (gsv) which was processed for each set of images has therefore been included in the text for comparison. Three hours' incubation with VBBO (5.0 μM) showed a similar localisation pattern in both EMT6-S and EMT6-R cells (Figures 30 & 31). However, the intensity of the dye in the sensitive cells (0-143 gsv) was greater than that seen in the resistant cells (0-235 gsv), indicating that the uptake may be slower in the resistant cell line. In both cell lines the dye was shown to localise throughout the cytoplasm of the cells, but little fluorescence was noted in the nucleus.

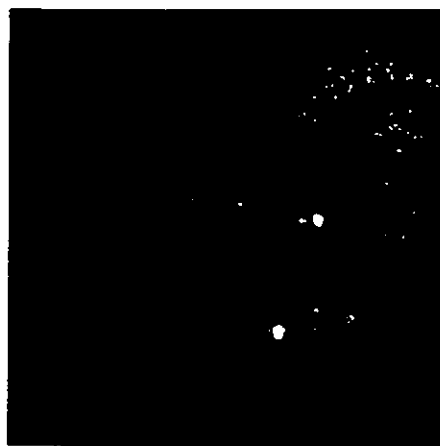
Figures 31(e) and (f) show the same cell which has been scanned twice by the confocal laser beam. The cell appears less defined with the second scan (Figure 31(f)), which may be due to a heating effect by the laser. This effect was not noted, however, when single cells were subjected to a series of scans, following localisation of VBBO over time (see section 7.4.1).

Three hours' incubation of EMT6-S and EMT6-R cells with MB at concentrations of 25 μM and 35 μM , respectively, showed very interesting results. Similar distribution of the drug was noted in both cell lines (Figures 32 & 33, gsv 0-65 & 0-120, respectively). The dye appeared to be localised within the cell cytoplasm (Figures 32(a), 33(a), (c) & (e) although one of the cells appeared to show some nuclear infiltration (Figure 33(c)). The punctate distribution of the dye in the cytoplasm, shown especially in Figures 32(a) and 33(c), suggested that the dyes may be localised within vesicles and subsequent scanning with the laser beam appeared to cause vesicle lysis (Figures 32(b), 33(b), (d) & (f)).

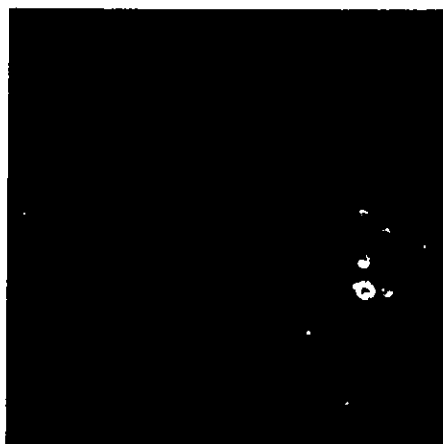
Three hours' incubation of EMT6-S and EMT6-R cells with TBO at concentrations of 10 μ M and 15 μ M, (Figures 34 & 35, respectively), again showed similar localisation patterns and similar levels of uptake in both EMT6-S and EMT6-R cell lines (gsv 0-40 & 0-78, respectively). The drug appeared to localise throughout the cytoplasm, but not in the nucleus.



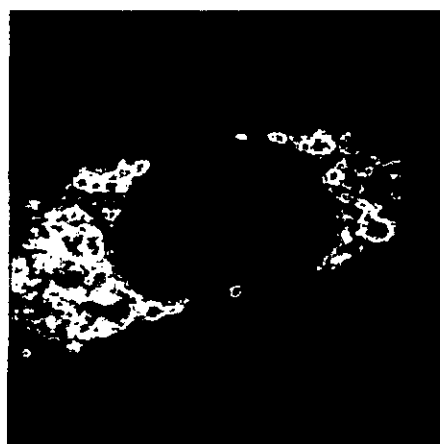
(a)



(b)



(c)



(d)



*



(e)

Figure 30 : Intracellular distribution of VBBO ($5 \mu\text{M}$) in EMT6-S cells following 3 hours' incubation, shown by confocal fluorescence microscopy. Figures (a-e) show different cells following a single scan with the laser beam. * Scale of fluorescence intensity (red-255, maximum; black-0, minimum).

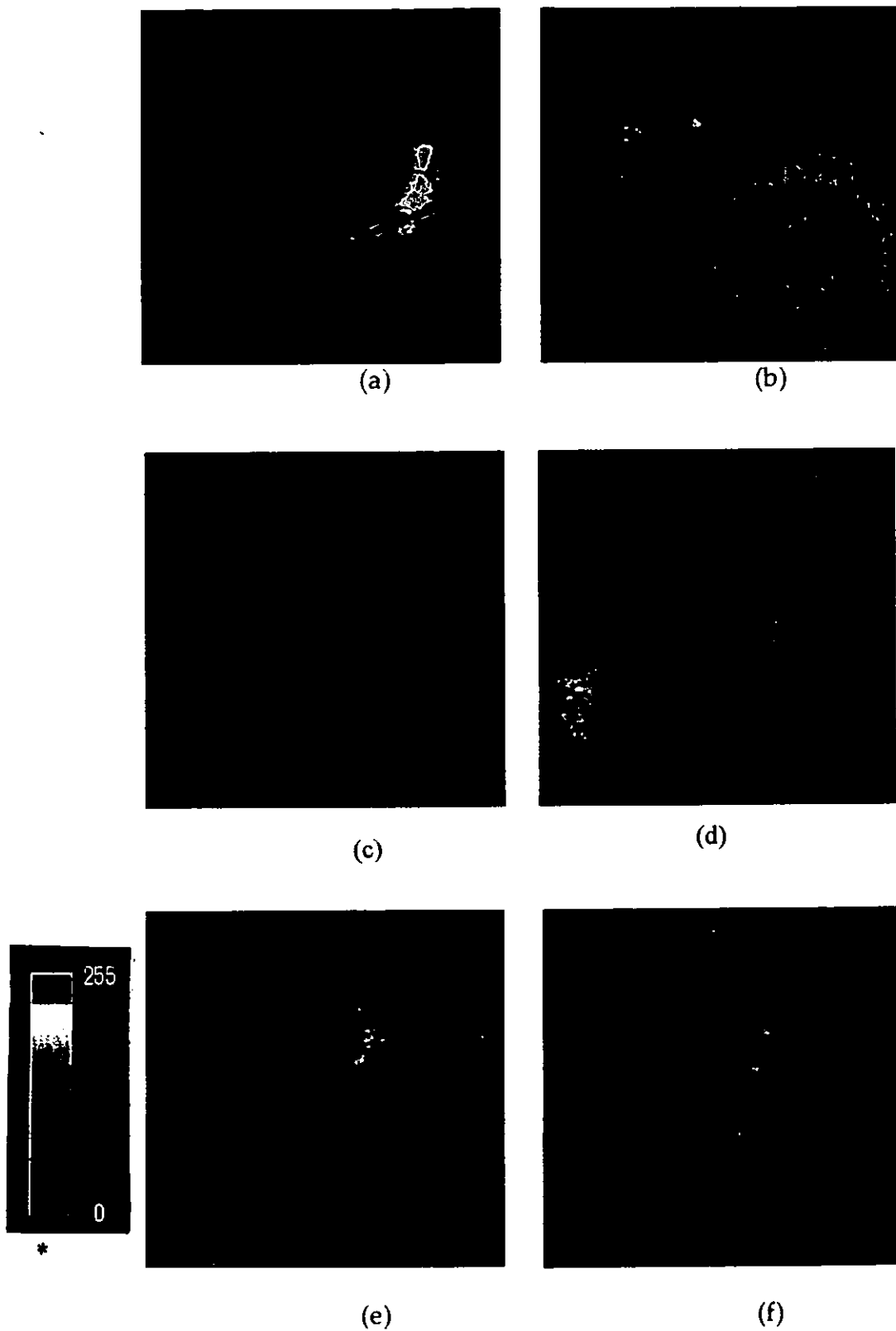
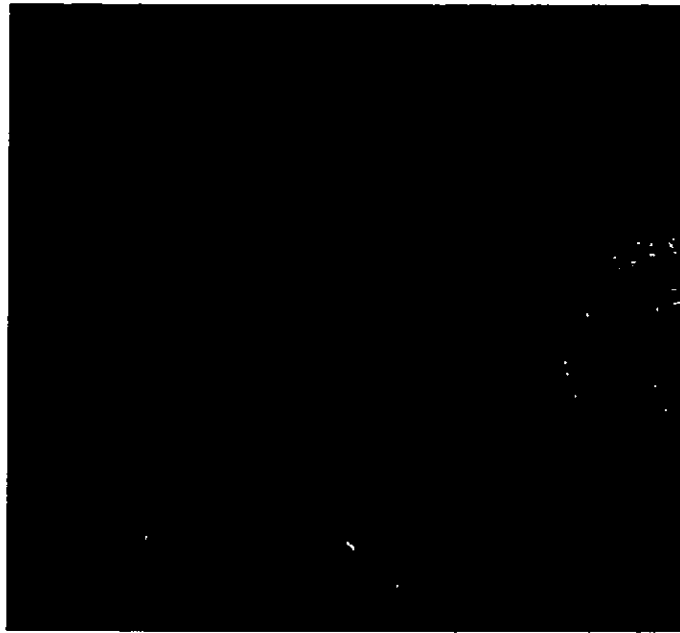
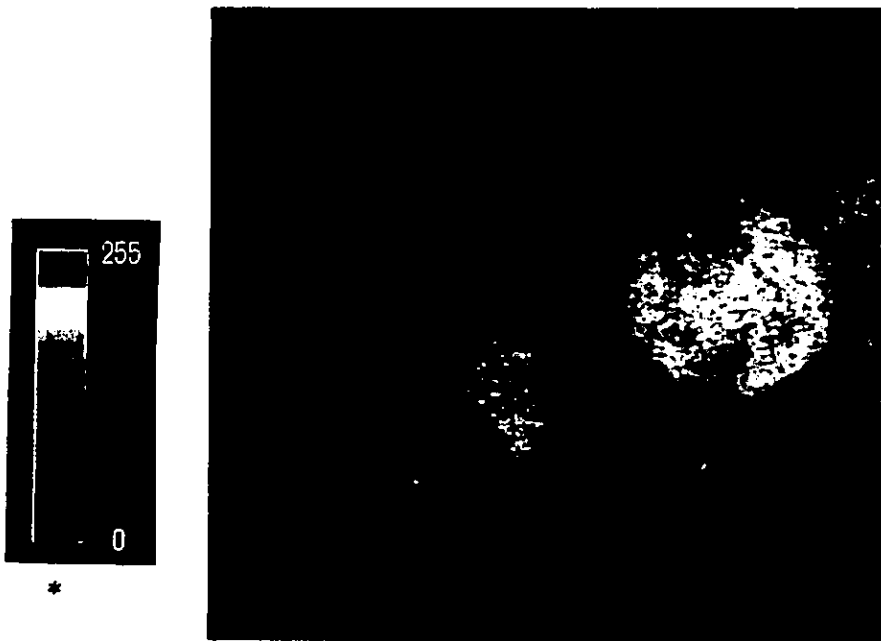


Figure 31 : Intracellular distribution of VBBO (5 μ M) in EMT6-R cells following 3 hours' incubation, shown by confocal fluorescence microscopy. Figures (a-e) show different cells following a single scan with the laser beam. Figure (f) shows the same cell as (e) following a second scan. * Scale of fluorescence intensity (red-255, maximum; black-0, minimum).

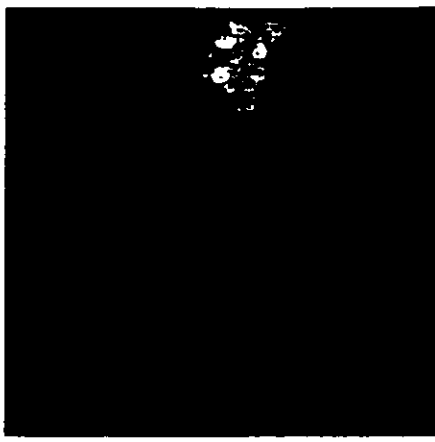


(a)

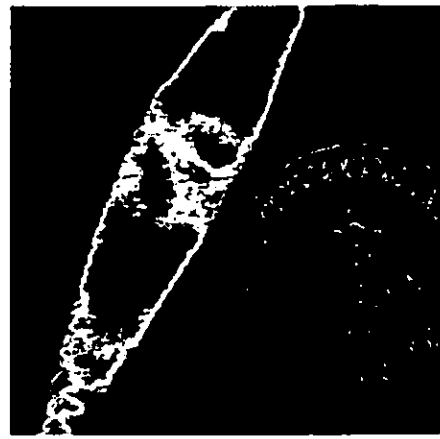


(b)

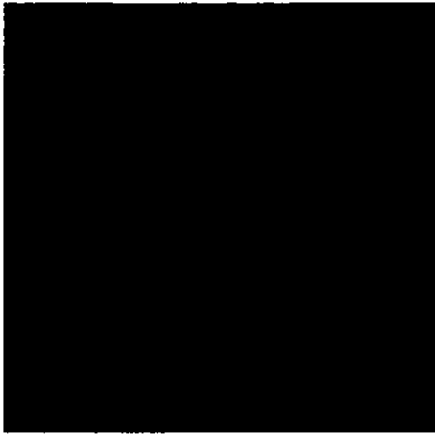
Figure 32 : Intracellular distribution of MB (25 μ M) in EMT6-S cells following 3 hours' incubation, shown by confocal fluorescence microscopy. Figures (a & b) show the same two cells following a single scan (a) and a second scan (b) with the laser beam. * Scale of fluorescence intensity (red-255, maximum; black-0, minimum).



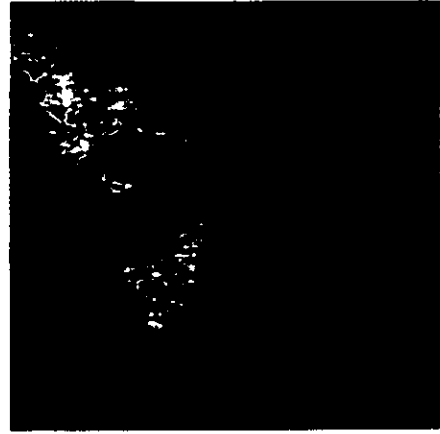
(a)



(b)



(c)



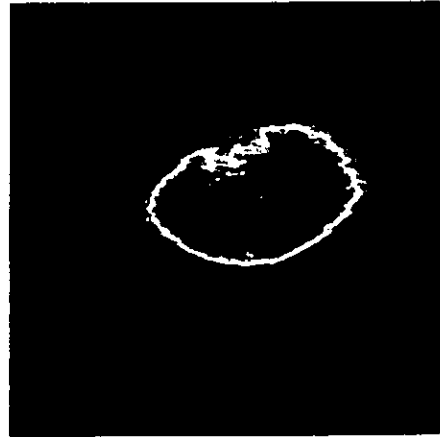
(d)



*

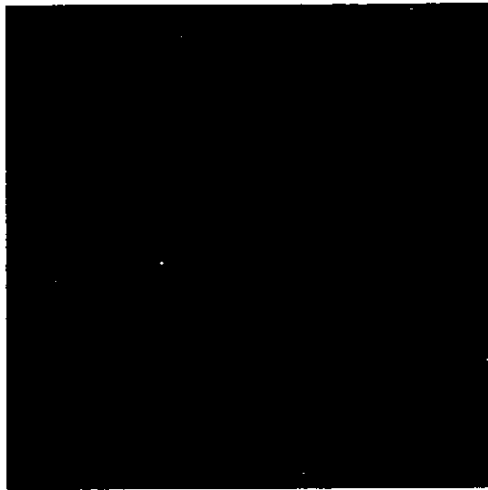


(e)

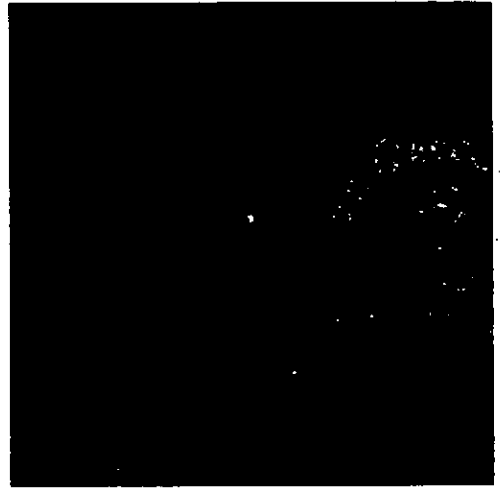


(f)

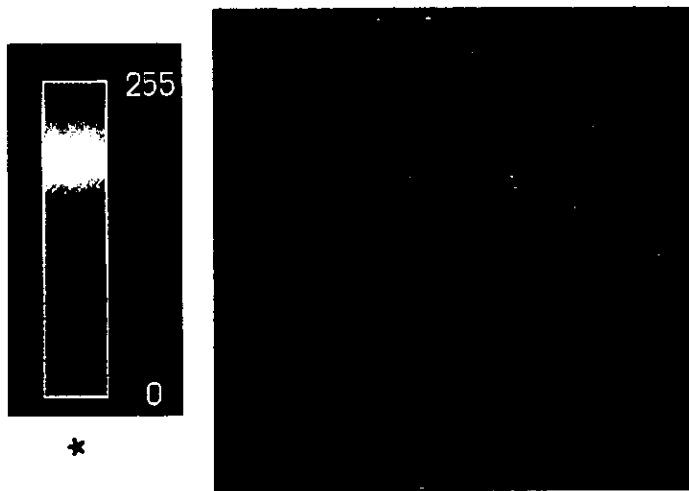
Figure 33 : Intracellular distribution of MB (35 μ M) in EMT6-R cells following 3 hours' incubation, shown by confocal fluorescence microscopy. Figures (a, c & e) show three different cells following one scan with the laser beam, and figures (b, d & f) show the same cells, respectively, following a second scan. * Scale of fluorescence intensity (red-255, maximum; black-0, minimum).



(a)



(b)

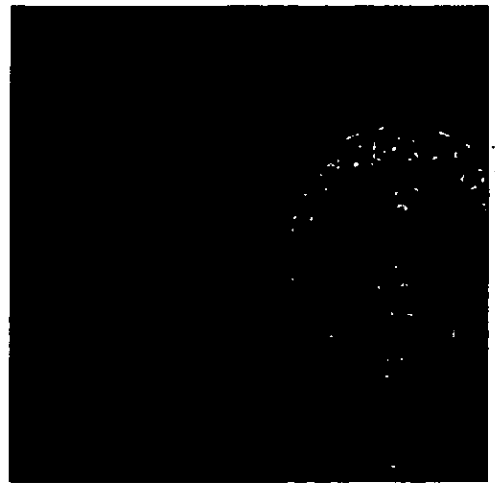


(c)

Figure 34 : Intracellular distribution of TBO (10 μ M) in EMT6-S cells following 3 hours' incubation, shown by confocal fluorescence microscopy. Figures (a - c) show three different cells following a single scan with the laser beam. * Scale of fluorescence intensity (red-255, maximum; black-0, minimum).



(a)



(b)



*



(c)

Figure 35 : Intracellular distribution of TBO (15 μ M) in EMT6-R cells following 3 hours' incubation, shown by confocal fluorescence microscopy. Figures (a - c) show the three different cells following a single scan with the laser beam. * Scale of fluorescence intensity (red-255, maximum; black-0, minimum).

4.4.3 Effect of pre-treatment of EMT6-S and EMT6-R cells with VBBO, MB or TBO on the cytotoxicity of doxorubicin.

Pre-treatment of EMT6-S and EMT6-R cells with VBBO, prior to treatment with doxorubicin, increased the efficacy of doxorubicin in each cell line by approximately two-fold (Figures 36a & b) using a concentration of approximately 1/8th of the VBBO IC_{50} value for each cell line. Since the cytotoxicity exerted by VBBO alone at this concentration is less than 10%, this is clearly a synergistic effect. A similar effect was seen in EMT6-R cells when pre-treated with MB at a concentration equivalent to 1/8th of the IC_{50} value for MB (Figure 37b), however, a lesser effect was seen in the sensitive cell line (Figure 37a), the pre-treatment inducing an increase in doxorubicin cytotoxicity of only 1.4. Pre-treatment of EMT6-S cells with TBO at a concentration of 1/8th the IC_{50} value for TBO increased the efficacy of doxorubicin by a factor of 1.8 (Figure 38a). This was increased to a factor of 3.0 in the resistant cell line (Figure 38b).

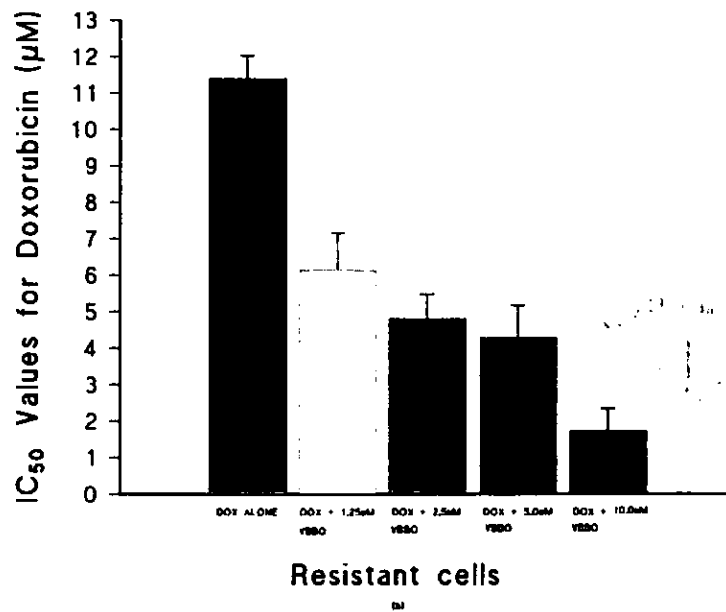
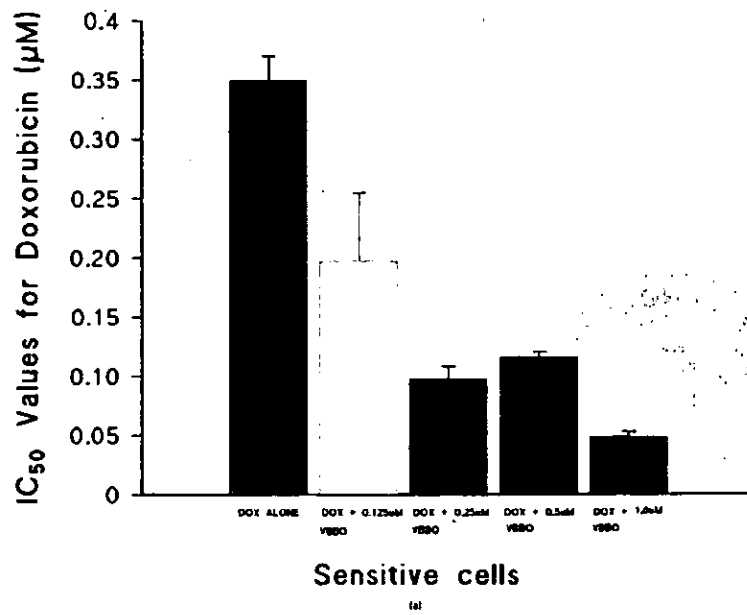


Figure 36 : Effect of pre-treatment with VBBO on IC₅₀ values for doxorubicin, with respect to EMT6-S and EMT6-R cells.

Cells (1000/well in 96 well plates) were allowed to attach for 48 hours. A single concentration of VBBO (200 µl at 1.25, 2.5, 5.0 or 10 µM for EMT6-R cells and 0.125, 0.25, 0.5 or 1.0 µM for EMT6-S cells) was added to each well and incubated for 3 hours. The cells were then rinsed with RPMI prior to the addition of doxorubicin (0 - 20.0 µM for EMT6-R cells and 0 - 2.0 µM for EMT6-S cells). Error bars represent SEMs (n ≥ 4 for EMT6-S; n ≥ 4 for EMT6-R).

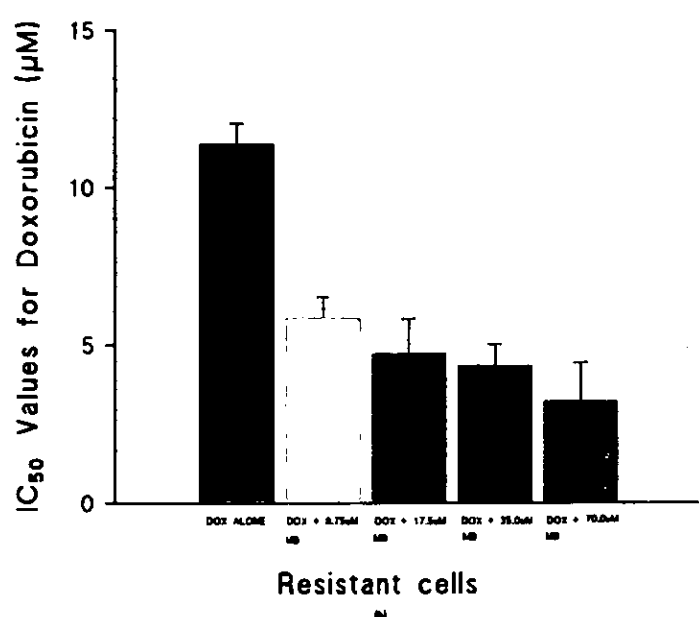
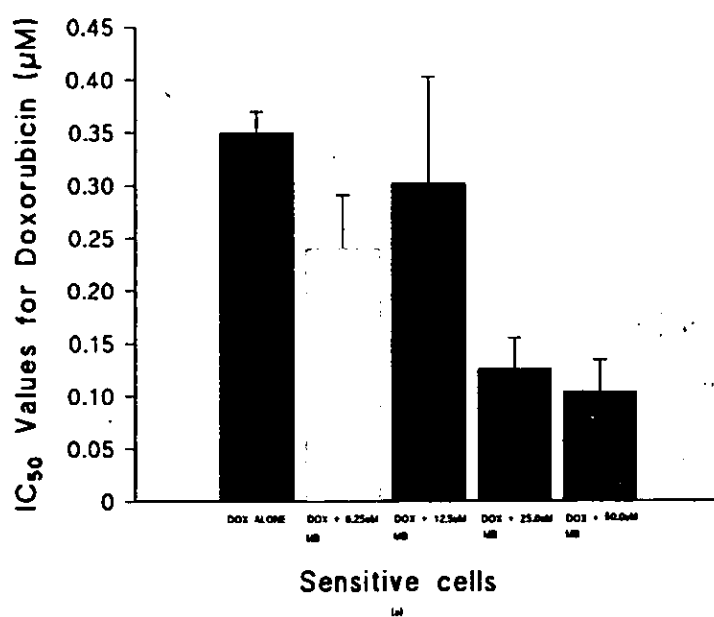


Figure 37 : Effect of pre-treatment with MB on IC₅₀ values for doxorubicin, with respect to EMT6-S and EMT6-R cells.

Cells (1000/well in 96 well plates) were allowed to attach for 48 hours. A single concentration of MB (200 µl at 8.75, 17.5, 35.0 or 70 µM for EMT6-R cells and 6.25, 12.5, 25.0 or 50.0 µM for EMT6-S cells) was added to each well and incubated for 3 hours. The cells were then rinsed with RPMI prior to the addition of doxorubicin (0 - 20.0 µM for EMT6-R cells and 0 - 2.0 µM for EMT6-S cells). Error bars represent SEMs (n ≥ 5 for EMT6-S; n ≥ 4 for EMT6-R).

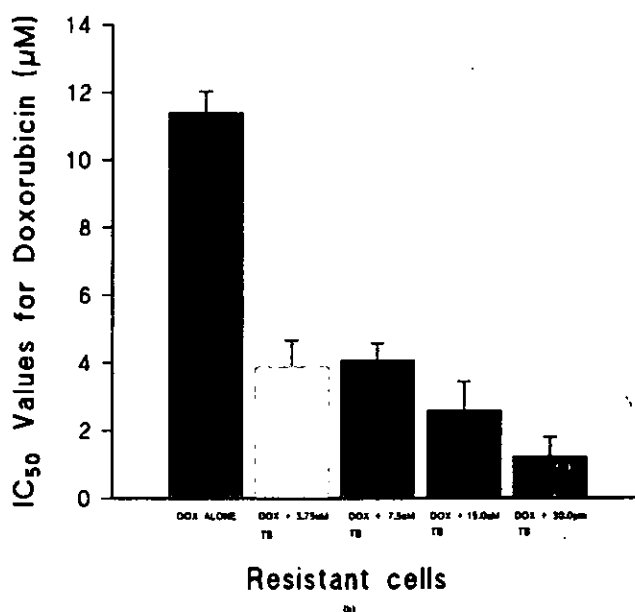
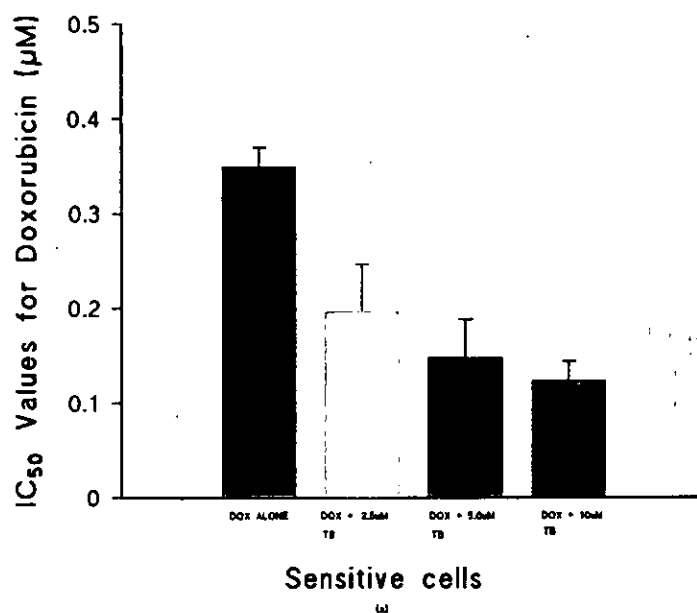


Figure 38 : Effect of pre-treatment with TBO on IC₅₀ values for doxorubicin, with respect to EMT6-S and EMT6-R cells.

Cells (1000/well in 96 well plates) were allowed to attach for 48 hours. A single concentration of MB (200 µl at 3.75, 7.5, 15.0 or 30 µM for EMT6-R cells and 2.5, 5.0, 10.0 or 20.0 µM for EMT6-S cells) was added to each well and incubated for 3 hours. The cells were then rinsed with RPMI prior to the addition of doxorubicin (0 -20.0 µM for EMT6-R cells and 0 - 2.0 µM for EMT6-S cells). Error bars represent SEMs ((n ≥ 5 for EMT6-S; n ≥ 3 for EMT6-R).

4.5 Discussion.

Each of the dyes tested was found to exert a photocytotoxic effect on EMT6-S and EMT6-R cells. The light enhancement factor (LEF), which is the ratio of IC_{50} values achieved in the light : dark, has been calculated for comparison of these effects. It should be noted that the light : dark differential is not constant, but varies at different concentrations, and for this reason has been standardised, using IC_{50} values, to calculate the LEF. VBBO was clearly the most effective photosensitizer (LEF approximately 10-fold in both cell lines), at much lower concentrations than MB or TBO. The latter two dyes were moderately photocytotoxic, showing approximately a 2-fold LEF in both cell lines. No photocytotoxic effect was noted with either *cis*-platinum or doxorubicin.

VBBO has been shown to exert higher photocytotoxicity in EMT6-S and EMT6-R cells than either MB or TBO, following three hours' incubation, which could be due to differences in uptake and/or subcellular localisation of the drugs. VBBO is highly lipophilic compared to MB and TBO (Table 11), suggesting that it is susceptible to uptake by passive diffusion, facilitating entry into the cell interior. MB and TBO are both hydrophilic, however, as previously discussed, in biological systems, neutral species are also formed which are much more lipophilic.

Previous studies have shown that VBBO binds specifically to mitochondria [132] due to the affinity of the positively charged cation for the negatively charged mitochondrial membrane. Since mitochondria in tumour cells have a higher potential gradient than normal cells, carcinoma mitochondria take up higher concentrations of cationic dyes and retain them longer than normal cells [178]. These positively charged dyes may also bind to the negatively charged phospholipid, cardiolipin, which is abundant in the mitochondrial membrane. Cañete *et al.* [128] observed that TBO localised in the cytoplasm of HeLa cells, mainly at the perinuclear level, following more than three hours' incubation. Another study [168] has also described the mitochondrial localisation

of TBO in an epidermoid carcinoma cell line. By contrast, MB has been shown to localise in lysosomes [169]. Several phenothiazinium dyes have been shown to accumulate in lysosomes due to the pH gradient, in contrast to cyanine cationic dyes, which favour mitochondrial localisation due to the potential gradient [179,180,181]. Phenothiazinium dyes can diffuse across the membrane when they are uncharged and unprotonated, however, in the low pH environment of lysosomes they become protonated and trapped in the vesicle [182]. This process depends on the pH gradient of the subcellular compartment and the ability of the dye to undergo protonation-deprotonation [183].

The localisation of the photosensitizers in this study, using confocal microscopy, support the above findings. Both VBBO and TBO showed widespread accumulation throughout the cytoplasm, which could be consistent with mitochondrial distribution. Considerably more VBBO appeared to be accumulated in both cell lines than either MB or TBO, following three hours' incubation, which suggests that the uptake of VBBO into the cell interior was more efficient than the other photosensitizers. This may be expected due to the differences in lipophilicity of the agents. Some studies have shown that MDR may be associated with differences in membrane potential of certain cell lines [184]. Impaired accumulation of a cationic cyanine dye was noted in an adriamycin-resistant Friend leukaemia cell line, and it was suggested that a decreased membrane potential was associated with MDR in this cell line [184]. Further studies should be carried out to establish any differences in membrane potential between EMT6-S and EMT6-R cells.

The results for MB were very interesting. The punctate pattern of distribution within the cytoplasm (Figures 32(a) and 33(b)) could suggest sequestration into vesicles, following three hours' incubation, which may be consistent with lysosomal localisation. Prior to incorporation into the lysosomes, it is suggested that the dye may be taken into the cells *via* pinocytosis, forming small vesicles. Most endocytotic vesicles eventually fuse with primary lysosomes and ultimately become secondary lysosomes which digest the

macromolecular contents [185]. Interestingly, subsequent scanning of both EMT6-S and EMT6-R cells containing MB resulted in what appeared to be lysis of the vesicles, with a resultant flood of MB inside the cell. It is not clear whether the vesicles were lysosomes or simply pinocytotic vesicles formed prior to their fusing with primary lysosomes. This phenomenon did not occur with the subsequent scanning of either VBBO or TBO, indicating a different subcellular localisation of MB.

Canête *et al.* [128] compared the uptake kinetics of MB and TBO in HeLa cells and found that MB displayed rapid penetration kinetics at short incubation times (less than six hours), reaching saturation after approximately six hours of treatment. TBO displayed slower kinetics at these incubation times, but its uptake appeared to equate to that of MB following twelve hours' incubation. In addition, no significant difference in cytotoxicity displayed by MB and TBO was seen at incubation times of less than three hours, but MB was found to be more effective when incubated for more than three hours. It has been shown that short incubation periods with a photosensitizer, followed by irradiation, lead to primary damage in the plasma membrane, whereas extended incubation periods of twenty four hours induce increased damage to cytoplasmic organelles and enzymes [186,187]. MB is thought to exert its photocytotoxic effects *via* DNA intercalation, however, this study did not show any nuclear localisation of the agent. This may be due to the relatively short incubation time of three hours and studies using increased incubation times should be carried out to investigate this further.

All the photosensitizers were found to have some effect in overcoming drug resistance in the EMT6-R cell line when exposed to light (7.2 J cm^{-2}) in the order VBBO>TBO>MB, however, in the dark VBBO and TBO were the most effective. *cis*-Platinum was found to be equally effective against EMT6-S and EMT6-R cells, whereas both VBBO and doxorubicin required increased drug concentration levels to overcome the resistance. However, VBBO only required approximately a 10-fold increase in concentration, in contrast to doxorubicin which required almost a 100-fold increase. These results show

that VBBO is partially able to overcome MDR in EMT6-R cells, suggesting that this partial response may be due to the drug being effluxed by Pgp or, alternatively, VBBO may be interacting in some way with Pgp. TBO and MB both showed some effect in reducing MDR in EMT6-R cells, but interestingly, the drug concentration levels required to overcome the resistance were similar (less than 2-fold) to those required for the sensitive cell line. This suggests that TBO and MB are toxic in their own right and may be able to circumvent efflux *via* Pgp.

Doxorubicin is a known substrate for Pgp whose cytotoxicity can be modified by certain chemosensitizers, such as verapamil [188,189]. This agent binds to Pgp, preventing the efflux of cytotoxic agents, with a resultant increase in intracellular drug concentration and concomitant increase in cytotoxicity [189]. In order to investigate the interaction of VBBO, MB or TBO with Pgp, the effects of pre-treatment of EMT6-S and EMT6-R cells with each of the photosensitizers, on the cytotoxicity of doxorubicin against these cell lines, were examined.

Pre-treatment of EMT6-S and EMT6-R cells with low concentrations of VBBO, MB or TBO, (equivalent to 1/8th IC₅₀ value for each photosensitizer), prior to exposure to doxorubicin, enhanced the cytotoxicity of doxorubicin in all cases. Pre-treatment with VBBO resulted in a two-fold increase in doxorubicin toxicity in both cell lines. Since the cytotoxicity exerted by VBBO alone at this concentration is less than 10%, this is clearly a synergistic effect. Pgp is known to be overexpressed in the EMT6-R cell line [5], however, doxorubicin cytotoxicity was increased in *both* cell lines, suggesting that this mechanism was independent of Pgp efflux. Studies have shown doxorubicin to localise in mitochondria and to have a 'multisite effect on the respiratory chain' [153]. Cardiolipin (CL) is an anionic phospholipid specific to the inner mitochondrial membrane and has been shown to be intimately involved in mitochondrial enzyme activity [153]. Doxorubicin is known to have strong affinity for CL [145,146], which would explain the toxic effect shown in mitochondria. Since VBBO has also been found to localise in

mitochondria, we hypothesise that the synergistic effect demonstrated by the combined use of VBBO and doxorubicin may be largely attributed to mitochondrial damage and disruption of the respiratory chain..

Pre-treatment with MB increased doxorubicin toxicity in EMT6-R cells two-fold, but had less effect on the sensitive cell line (increase x 1.4). This suggests a different mechanism of action to that of VBBO, which may involve interaction with Pgp. Pre-treatment with TBO resulted in an increase in toxicity of almost two-fold in EMT6-S cells, but this was increased to three-fold in the resistant cell line, again suggesting possible interaction with Pgp.

CHAPTER FIVE

THE EFFECT OF VERAPAMIL AND BUTHIONINE SULFOXIMINE ON THE CYTOTOXICITY OF VBBO IN EMT6 CELLS.

5.1 Abstract

VBBO is thought to exert its photocytotoxic effects *via* free radical generation. Glutathione (GSH) and related enzymes are associated with the protection of normal tissues against free-radical damage and have also been implicated in MDR. Investigations were carried out into the effect of GSH depletion in EMT6-S and EMT6-R cells on VBBO photocytotoxicity. Buthionine sulfoximine (BSO), a potent inhibitor of γ -glutamyl cysteine synthetase, inhibited GSH levels in both EMT6-S and EMT6-R cell lines in a concentration-dependent manner, although some toxicity was observed at all concentrations tested. BSO at a concentration of 10 μ M was used for subsequent experiments. The total GSH content for EMT6-R cells was found to be higher than that of EMT6-S cells, $21.84 \pm 2.54 \mu\text{g (mg protein)}^{-1}$ and $18.79 \pm 2.7 \mu\text{g (mg protein)}^{-1}$, respectively, however, this was not found to be a significant difference ($p > 0.05$). GSH depletion of EMT6-S and EMT6-R cells did not enhance the photocytotoxic effect of VBBO, suggesting that the primary site of action of VBBO is at an intracellular site not protected by GSH or that the mechanism of action is not *via* the *in situ* generation of singlet oxygen.

Verapamil is a potent inhibitor of Pgp and its presence was shown to increase the efficacy of doxorubicin by two-fold in the the sensitive cells indicating that some Pgp is present in this cell line. The eighteen-fold increase in doxorubicin efficacy seen in the resistant cell line clearly supports the overexpression of Pgp in the EMT6-R cell line, compared to that of the parental cell line. By contrast, the presence of verapamil did not increase the cytotoxicity of VBBO in either cell line.

The enhanced cytotoxic effect of doxorubicin shown against EMT6-R cells with the addition of verapamil suggests that the primary mode of action of the chemosensitizer in this cell line, which is known to overexpress Pgp, is *via* inhibition of Pgp. Since the addition of verapamil did not enhance the cytotoxicity of VBBO, this suggests that

VBBO is not effluxed by Pgp, further supporting the hypothesis that VBBO acts at a specific site within the cell.

5.2 Introduction

Pleiotropic or acquired multiple drug resistance (MDR) in cancer chemotherapy has proved to be a highly complex phenomenon which is responsible for the failure of many cancer treatments. A vast amount of research has been performed in recent years to try to elucidate mechanisms of action of MDR. Some of these mechanisms are now well-characterised, such as the so-called 'classical' MDR involving decreased intracellular drug accumulation due to the overexpression of P-glycoprotein (Pgp), a membrane-bound ATP-dependent drug efflux pump [26]. However, many examples of 'atypical' and 'non-Pgp' MDR have also been encountered [51,52]. Glutathione (GSH) and glutathione-S-transferases (GSTs) have been implicated in MDR, although there is much conflicting evidence as to their exact role [91]. Many proteins have also been found to be involved in MDR, and the recently identified multidrug resistance-associated protein (MRP) has been shown to be important, particularly with respect to its function as an efflux pump for conjugates of glutathione [57].

GSH and associated enzymes have been shown to be important in normal tissues for protection against free radical damage [58,91]. Since increased GSH levels have also been associated with MDR, several studies have investigated the depletion of GSH in drug resistant cell lines (reviewed by Moscow & Dixon [91]). Buthionine sulfoximine (BSO), a potent inhibitor of γ -glutamyl cysteine synthetase, has been shown to increase the cytotoxicity of a variety of chemotherapeutic agents [190-193]. Anthracycline antibiotics, such as doxorubicin, are known to generate free radical intermediates when metabolised, leading to toxic cellular effects [194] and since GSH depletion by the addition of BSO can increase the cytotoxicity of anthracyclines [190-194], it has been suggested that this enhancement may be due a reduction in the protective effect of GSH. VBBO is also thought to exert its photocytotoxic effects *via* free radical generation, therefore the effects of GSH depletion in EMT6-S and EMT6-R cells, by the addition of BSO, were investigated in this study.

MDR may be also modified by the addition of various hydrophobic agents, referred to as chemosensitizers or resistance modifiers [188,195-196]. Many chemosensitizers potentiate the cytotoxicity of a variety of chemotherapeutic agents by inhibiting the Pgp efflux pump, resulting in an increase in the intracellular concentration of the agents [189]. Seven main categories of resistance modifier have been described : (i) calcium channel blockers; (ii) calmodulin antagonists; (iii) noncytotoxic anthracycline and *Vinca* alkaloid analogues; (iv) steroids and hormone antagonists; (v) cyclosporins; (vi) dipyridamole; and (vii) miscellaneous hydrophobic, cationic compounds [189]. All of these agents are highly lipophilic and many are heterocyclic and positively charged, however, they share only broad structural similarities.

Verapamil, a calcium channel blocker, has been shown to be a potent inhibitor of Pgp, reversing resistance to various chemotherapeutic agents such as vincristine and doxorubicin [197,198]. The potentiation of the cytotoxicity of the agents by verapamil is also associated with the inhibition of Pgp. However, the chemosensitizing action of verapamil varies between cell lines and some cross-resistance is refractory to modulation [189]. Various theories have been postulated, such as the possibility that mutations in the *MDR1* gene [199] or post-translational modifications of Pgp [200] may alter the affinity of agents to the drug binding site(s). Similarly, Pgp may express multiple binding sites.

VBBO has been shown partially to overcome the resistance shown by EMT6-R cells [see Chapter 4], however, higher concentrations of the drug, compared to those used against the parental line, are necessary to achieve this reversal. This suggests that some VBBO may be effluxed from the cells *via* Pgp. Similarly, it has been shown that pre-treatment of EMT6-S and EMT6-R cells by VBBO, prior to treatment with doxorubicin, enhances the cytotoxicity of doxorubicin [see chapter 4]. One explanation of this result may be that VBBO interferes with the transport of doxorubicin across the cell membrane, leading to increased intracellular accumulation of doxorubicin. In order to investigate whether VBBO is a substrate of Pgp, the effects of verapamil on the cytotoxicity of

VBBO and doxorubicin against EMT6-S and EMT6-R cells were compared in this study.

5.3 Materials and Methods.

5.3.1 Chemicals.

Victoria blue BO (VBBO), and 1-octanol were purchased from Aldrich Chemicals (Gillingham, UK) and were used without further purification. MTT (3-[4,5-dimethylthiazol-2-yl]-2,5-diphenyl-2*H*-tetrazolium bromide), DMSO(dimethyl sulfoxide), verapamil, BSO (buthionine sulfoximine), sodium phosphate, sodium-EDTA (ethylenediaminetetraacetic acid), DTNB (5,5'-dithiobis-(2-nitrobenzoic acid)), NADPH and glutathione reductase (type III from *Saccharomyces cerevisiae*) were obtained from Sigma, Poole, U.K. Doxorubicin was a gift from Farmitalia Carlo Erba Ltd., St. Albans, U.K.

5.3.2 Cell Culture

The murine mammary tumour cell line (EMT6) was originally obtained from Zeneca Pharmaceuticals, Macclesfield, Cheshire. Cultures were routinely maintained at 37°C, 5% CO₂ : 95% air in RPMI 1640 culture medium (Life Technologies, Paisley, U.K.), supplemented with 10% (v/v) foetal calf serum (M.B.Meldrum Ltd., Bourne End, U.K.), 200 mM glutamine (Sigma) and penicillin/streptomycin solution at 1x10⁴ units ml⁻¹ and 10 mg ml⁻¹, respectively, in 0.9% NaCl (Sigma). Trypsin (activity 1200 BAEE units/mg solid) was obtained from Sigma.

5.3.3 Effect of BSO on glutathione levels in EMT6-S and EMT6-R cells.

4 ml aliquots of each cell line were seeded into 60 mm petri dishes at a cell density of 8×10^4 cells ml^{-1} in RPMI 1640 and incubated at 37°C , 5% CO_2 : 95% air. The EMT6-S cells were grown on for three days and the EMT6-R cells for four days, to ensure each cell line was in logarithmic phase. The medium was then removed from the petri dishes and replaced with 4 ml of either RPMI 1640 (controls) or RPMI containing various concentrations of BSO (10, 100 or 1000 μM). The cells were incubated for five hours in the absence or presence of BSO. The medium was then aspirated and the cells washed twice with 4 ml ice-cold PBS (4°C). The cells were lysed by the addition of 0.5 ml 0.6% (w/v) 5-sulfosalicylic acid (5-SA) left on ice for 40 minutes, in the dark, shaking occasionally to ensure all the cells were covered by the acid. The supernatant was then removed and used to estimate the amount of glutathione present using a modified version of the Tietze recycling assay, according to the method of Eady *et al.* [201]. In this assay, GSH is sequentially oxidised to glutathione disulphide (GSSG) by 5,5'-dithiobis-(2-nitrobenzoic acid) (DTNB) and reduced by NADPH in the presence of glutathione reductase. The rate of formation of 2-nitro-5-thiobenzoic acid (TNB) may be followed spectrophotometrically and the GSH levels determined by reference to a standard curve.

A stock buffer of 143 mM sodium phosphate and 6.3 mM sodium-EDTA (pH 7.5) was made in distilled water and used to prepare solutions of 0.3 mM NADPH, 6 mM DTNB and 50 units ml^{-1} GSH reductase. Standards of known GSH content were prepared by serial dilution in 0.6% (w/v) 5-SA and the GSH content in the samples was determined by reference to a standard curve. For each assay, a final tube was made up containing 700 μl NADPH solution, 100 μl cell extract (or GSH standard) and 100 μl distilled water. Each tube was incubated at 30°C for ten minutes before being transferred to a cuvette containing 10 μl GSH reductase. The rate of absorbance at 412 nm was measured spectrophotometrically (Pharmacia Novaspec II linked to a Kipp & Zonen chart recorder). After removing the 5-SA extract, the cell monolayer was scraped from the petri dish and dissolved in 4 ml Tris (2 M) / EDTA (0.1 M) buffer prior to protein

estimation *via* the standard Bradford assay [202]. The amount of glutathione in each cell line was then expressed as $\mu\text{g GSH (mg protein)}^{-1}$.

5.3.4 Effect of glutathione depletion on the cytotoxicity exerted by VBBO against EMT6-S and EMT6-R cells.

96 well microtitre plates were seeded with 1000 cells per well (in 200 μl RPMI 1640) and incubated at 37°C, 5% CO₂ : 95% air for 2 days. The medium was aspirated prior to the addition of 200 μl of varying concentrations of BSO (10, 100 or 100 μM) and the cells were incubated, under the same conditions as previously described, for five hours. The medium was then aspirated and the cells rinsed twice with RPMI 1640 prior to the addition of varying concentrations of VBBO (0-2 μM for EMT6-S cells; 0-20 μM for EMT6-R cells). The cells were incubated for a further three hours, rinsed twice with 200 μl RPMI and illuminated at 7.2 J cm⁻¹ or kept dark . The cells were then grown on for three days at 37°C, 5% CO₂ : 95% air. A proportion of cells was left untreated on each plate as a control. All drug dilutions were made using RPMI 1640 medium. Cytotoxicity was measured using the MTT assay as previously described in Chapter 4, section 4.3.3.

5.3.5 Effect of verapamil on the cytotoxicity exerted by doxorubicin or VBBO against EMT6-S and EMT6-R cells.

96 well microtitre plates were seeded with 1000 cells per well (in 200 μl RPMI 1640) and incubated at 37°C, 5% CO₂ : 95% air for 2 days. The medium was aspirated and 200 μl VBBO or doxorubicin were added, in varying concentrations, in the absence and presence of verapamil (7 μM). The cells were then incubated, as previously described, for 3 hours. The medium containing the drug was aspirated and the cells rinsed with 200 μl RPMI 1640, before replacing with a further 200 μl RPMI 1640. The cells were then grown on for 3 days at 37°C, 5% CO₂ : 95% air. A proportion of cells was left untreated on each plate as a control. All drug dilutions were made using RPMI 1640 medium. Cytotoxicity was measured using the MTT assay as previously described.

5.4 Results.

5.4.1 Effect of BSO on glutathione levels in EMT6-S and EMT6-R cells.

The total GSH content for EMT6-R cells was found to be higher than that of EMT6-S cells, $21.84 \pm 2.54 \mu\text{g (mg protein)}^{-1}$ and $18.79 \pm 2.7 \mu\text{g (mg protein)}^{-1}$, respectively, however, this was not found to be a significant difference ($p > 0.05$) (Student's t-test). BSO inhibited GSH levels in both EMT6-S and EMT6-R cell lines in a concentration-dependent manner (Figure 39), however, some toxicity was observed at all concentrations tested. BSO at a concentration of $10 \mu\text{M}$ was used for subsequent experiments.

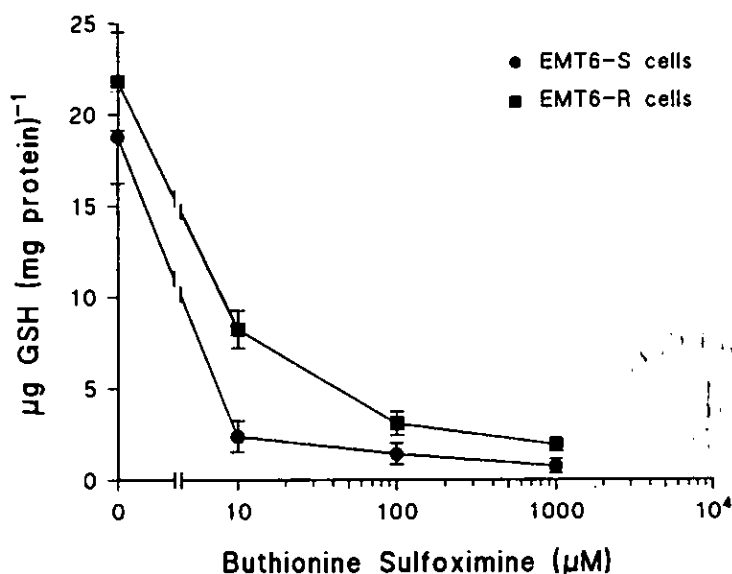


Figure 39 : Effect of Buthionine Sulfoximine (BSO) on glutathione levels in EMT6-S and EMT6-R cells

Cells (4×10^5 in 60 mm petri dishes) were grown for 3 days (sensitive cells) or 4 days (resistant cells) at 37°C , 5% CO_2 : 95% air. The cells were then incubated for 5 hours in the presence of BSO ($10^{-10^3} \mu\text{M}$). All drug dilutions were made using RPMI 1640 medium. The protein content was determined using the standard Bradford assay [202] and GSH levels were calculated using a modification of the Tietze assay [201]. Each point represents mean \pm SEM ($n \geq 5$).

5.4.2 Effect of glutathione depletion on the cytotoxicity exerted by VBBO against EMT6-S and EMT6-R cells.

On first examination, VBBO photocytotoxicity appeared to be enhanced when EMT6-S and EMT6-R cells were exposed to 10 μM BSO (Figures 40(a & b), 40(c & d), respectively), however, the combined effect was lower than the additive effect of the two agents, which are toxic in their own right. It was thus concluded that GSH depletion of EMT6-S and EMT6-R cells did not enhance the photocytotoxic effect of VBBO.

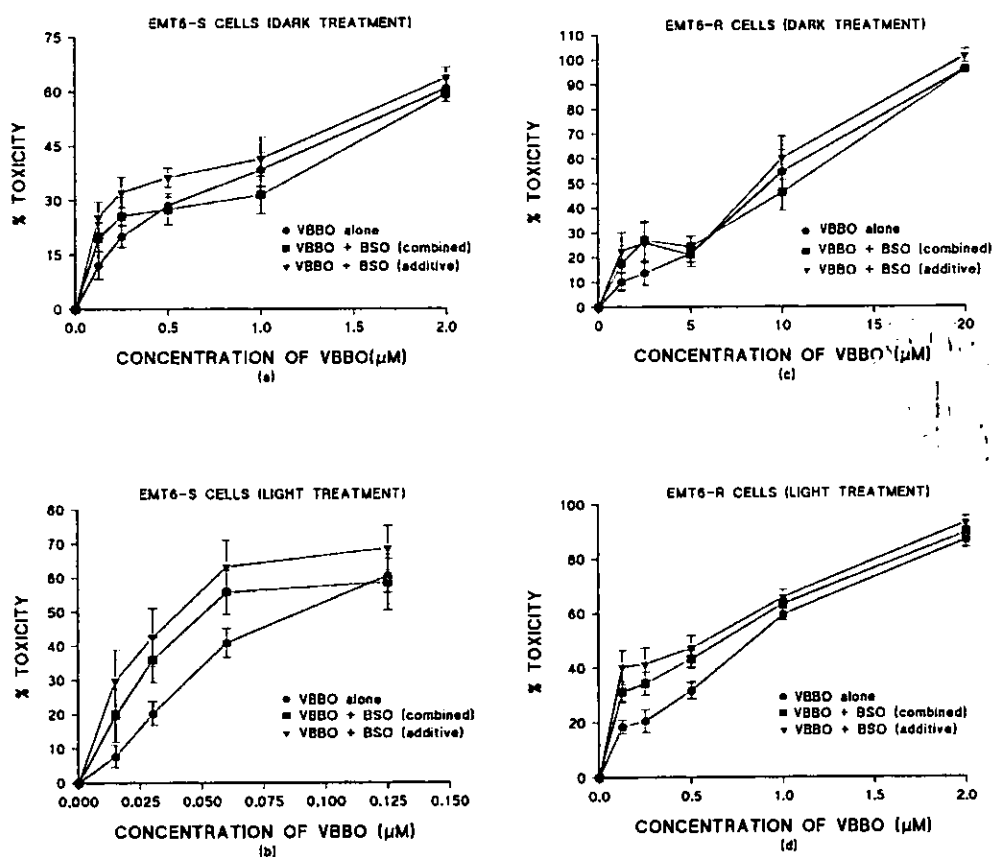


Figure 40: Effect of glutathione depletion in EMT6-S and EMT6-R cells on the photocytotoxicity of VBBO.

Cells (1000 / well in 96 well plates) were allowed to attach for 48 hours. The medium was aspirated, 200 μl BSO (10 μM) added and the cells incubated for 5 hours. The cells were then rinsed with RPMI medium and exposed to varying concentrations of VBBO for 3 hours. The VBBO was aspirated, the cells rinsed and exposed to light (7.2 J cm^{-2}) (Figures c & d) or kept dark (Figures a & b), prior to growing on for 3 days at 37°C, 5% CO_2 : 95% air. 'Combined' data refers to that of agents used in conjunction with each other, and 'additive' data refers to the addition of data obtained from separate treatment with each agent. Each point represents mean \pm SEM ($n \geq 7$).

5.4.3 Effect of verapamil on the cytotoxicity exerted by doxorubicin or VBBO against EMT6-S and EMT6-R cells.

The combined treatment of VBBO and verapamil (7 μM) on EMT6-S and EMT6-R cells did not enhance VBBO cytotoxicity in either cell line in the dark (figures 41a & b). By contrast, the IC_{50} value of doxorubicin for EMT6-S cells decreased by two-fold and for EMT6-R cells by eighteen-fold (Figures 41c & d). This suggests that VBBO does not act as a substrate for Pgp since, if this was the case, verapamil would have increased the dark toxicity of VBBO.

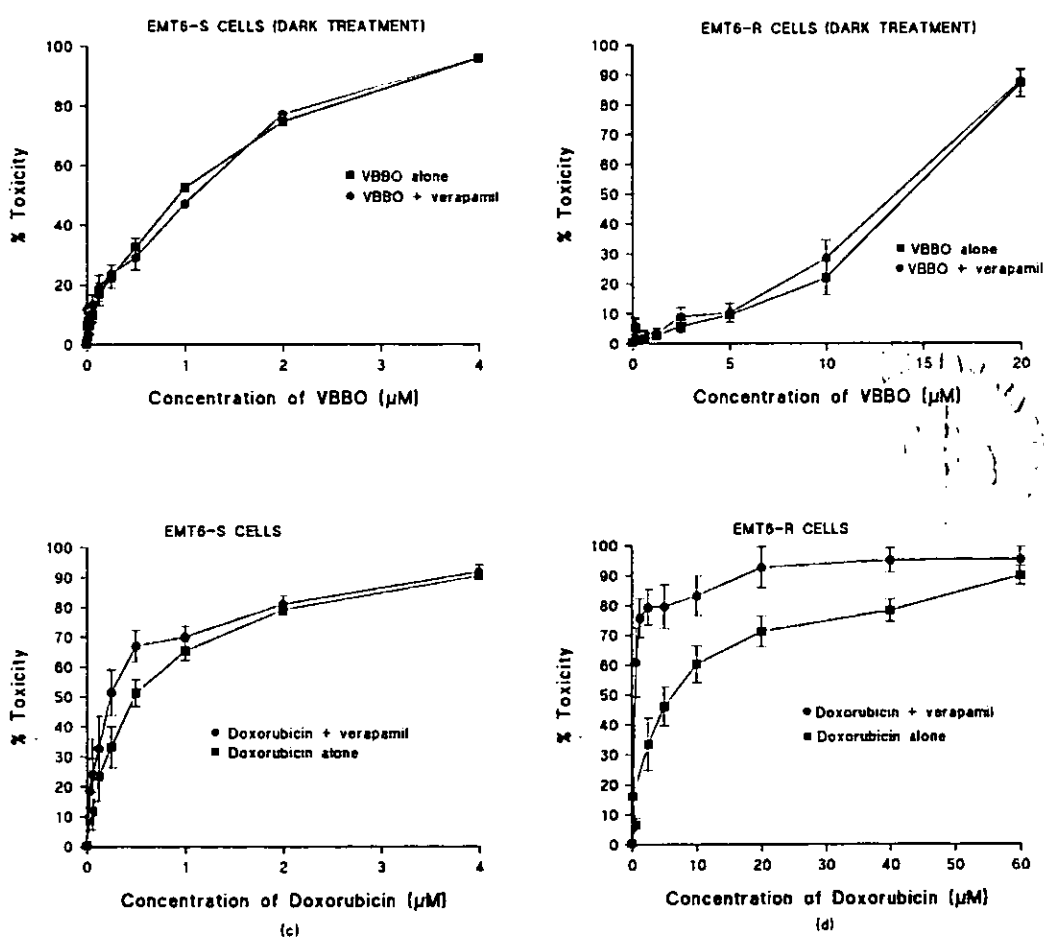


Figure 41 : Effect of verapamil on cytotoxicity exerted by VBBO or doxorubicin against EMT6-S cells (a & c, respectively) and EMT6-R cells (b & d, respectively). Cells (1000 / well in 96 well plates) were allowed to attach for 48 hours. The medium was aspirated and VBBO or doxorubicin (200 μl of varying concentrations) was added to the cells, in the absence or presence of verapamil (7 μM), and incubated for 3 hours. The cells were rinsed with 200 μl RPMI 1640, the medium replaced and the cells grown on for 3 days at 37°C, 5% CO_2 : 95% air. Each point represents mean \pm SEM ($n \geq 4$).

5.5 Discussion.

The total content of GSH present in the EMT6-R cell line was found to be higher than that of the EMT6-S cell line ($21.84 \pm 2.54 \mu\text{g (mg protein)}^{-1}$ and $18.79 \pm 2.7 \mu\text{g (mg protein)}^{-1}$, respectively), although this was not found to be significant ($p > 0.05$). This agrees with the findings of Cox [5], although a significantly higher level of GST activity in the resistant cell line was reported, compared to that of the sensitive cells ($P < 0.05$). The elevated GST activity indicates an increase in GSH turnover which may be associated with increased export of GSH conjugates [203]. It was postulated that the actual amount of GSH observed in the EMT6 cells represents a basal level of unconjugated GSH which may reflect a balance between the production of GSH and the excretion of conjugated metabolites [5]. Other studies have also failed to demonstrate a difference in basal levels of GSH between sensitive and resistant cell lines (204, 205), however, there are reports of some resistant cell lines which *do* show higher levels of GSH than their sensitive, parental cell lines [190,206,207]. Interestingly, in all these studies, depletion of GSH levels by BSO enhanced the cytotoxicity of a variety of chemotherapeutic agents.

Initially, it appeared that the photocytotoxicity of VBBO was enhanced by the addition of $10 \mu\text{M}$ BSO, particularly in the case of EMT6-S cells (Figures 40(a-d)). However, since BSO and VBBO are both toxic in their own right, the additive effect of the toxicity of the separate use of these two agents must be considered and compared to the effect exerted by BSO *combined* with VBBO. In each case, the additive effect of the agents' toxicity was greater than their combined effect (Figure 40(a-d)), and it was thus concluded that GSH depletion of EMT6-S and EMT6-R cells did not enhance the photocytotoxic effect of VBBO.

Although many studies have shown that GSH depletion leads to increased cytotoxicity of various chemotherapeutic agents [190-193], Moscow and Dixon [91] have reviewed the effects of GSH depletion on anthracycline cytotoxicity in many cell lines, and found

wide variability in results. They suggested that these discrepancies may be due to variations in intrinsic biological properties of different cell lines, or indeed to different methodologies employed. In addition, it was suggested that in cases where BSO appears to be effective in increasing cytotoxicity of an agent, the mechanism by which this occurs is not clear. Possible mechanisms include direct inhibition of the glutathione-redox cycle, other effects of glutathione depletion or toxic effects of BSO. The present study indicates that some toxicity was exerted by BSO against EMT6 cells, even at the lowest concentration used (10 μ M), following five hours' exposure to the drug. Future studies could investigate the effects of lower concentrations of BSO on the viability of EMT6-S and EMT6-R cells and on levels of glutathione depletion achieved. Lee *et al.* [192] found that BSO induced GSH depletion occurred in HEp3 cells in a concentration-dependent manner from 0.1-1.0 mM BSO, before levelling off. It was also shown that the level of GSH depletion by 1mM BSO was linear for approximately three hours, followed by first order kinetics for up to 6 hours, and then slowed significantly [192]. Interestingly, cytotoxicity induced by BSO occurred with exposure times exceeding six hours, but was not encountered with lower exposure times. Dethlefsen *et al.* [208] also reported that BSO was cytotoxic to the mouse mammary carcinoma 66 cell line when exposed for forty eight hours to 0.05 mM BSO. This cytotoxicity was not evident, however, following twenty four hours' exposure. Prolonged exposure to BSO, producing extended GSH depletion, was associated with a G₁ and G₂/M block in the cell cycle leading to a delay in cell-cycle progression and cell death in the murine 66 cells [208].

It has also been suggested that depletion of GSH levels may affect membrane permeability. Lutzky *et al.* [209] reported that BSO increased the uptake and retention of daunorubicin in an anthracycline-resistant sub-line of the HL60 human myelogenous leukaemia cell line. Crescimanno *et al.*, however, showed that doxorubicin cytotoxicity in both the wild-type Friend leukaemia cell line and a resistant sub-line was significantly increased with the addition of BSO, but that accumulation and retention of doxorubicin was unaltered [194]. Their study concluded that the status of GSH and GSH-related

enzymes plays an important role in the resistance of Friend leukaemia cells to doxorubicin.

There is clearly controversy surrounding the role of GSH and GSH-related enzymes in MDR, however, on balance, there does appear to be evidence to support the protective function of GSH against free-radical damage. Since depletion of GSH levels in EMT6-S and EMT6-R cells was not found to enhance the cytotoxicity of VBBO, this suggests that the primary site of action of VBBO is at an intracellular site not protected by GSH or that the mechanism of action is not *via* the *in situ* generation of singlet oxygen (Type II pathway) but may occur *via* a direct redox reaction between the photoexcited sensitizer and biomolecules (Type I pathway) (see section 1.4.2). VBBO is highly lipophilic ($\log P = +3.5$) and positively charged. It has been shown to localise preferentially in the mitochondria of malignant cells on the inside of the membrane, which is negatively charged [132]. Modica-Napolitano *et al.* [132] have shown the dark toxicity of VBBO to involve uncoupling of oxidative phosphorylation. By contrast, photoirradiation appears to alter the mechanism of mitochondrial toxicity exerted by VBBO, by producing specific inhibition of Respiratory Complex I. In this respect, VBBO appears to exert a more *specific* effect on cells than many other cationic photosensitizers.

Verapamil is a potent inhibitor of Pgp [189] and its presence was shown to increase the efficacy of doxorubicin, a known substrate for the transporter [189] (Figures 40c & d). A two-fold increase in the efficacy of doxorubicin was noted in the sensitive cells indicating that some Pgp is present in this cell line, however, the eighteen-fold increase in doxorubicin efficacy seen in the resistant cell line clearly supports the overexpression of Pgp in the EMT6-R cell line compared to the parental cell line [5]. By contrast, the presence of verapamil did not increase the cytotoxicity of VBBO in either cell line in the dark (Figures 40a & b) implying that VBBO is not effluxed by Pgp.

Verapamil has clearly been shown to exert its action by binding to Pgp and affecting drug efflux [189], however, Drori *et al.* [210] postulate that chemosensitizers also affect membrane permeability. Chemosensitizers are usually positively charged, hydrophobic compounds which would therefore be likely to interact with membrane lipids. Ramu *et al.* [211] showed that treatment with verapamil, dipyridamole and tamoxifen increased phosphatidylcholine synthesis in MDR cells, but not in the sensitive parental cell lines. Drori *et al.* [210], however, have shown that chemosensitizers potentiate the cytotoxicity of chemotherapeutic agents not only in resistant cell lines, but also in wild-type cells which do not express Pgp. It was postulated that the majority of chemosensitizers alter membrane fluidity, thereby increasing membrane permeability, which in turn results in the intracellular accumulation of various hydrophobic chemotherapeutic agents [210]. Other studies have also found verapamil to alter the subcellular distribution of doxorubicin within drug resistant cell lines [212,213].

Verapamil was shown to potentiate the cytotoxicity of doxorubicin two-fold in EMT6-S cells. Cox [5] also found that that addition of verapamil to EMT6-S and EMT6-R resulted in an increased accumulation of doxorubicin in both cell lines, albeit to a greater extent in the resistant cell line. This suggests that either a small amount of Pgp is present in the EMT6-S cell membranes and/or that verapamil also binds to the anionic phospholipids in the membrane thus affecting the fluidity of the membrane. The enhanced cytotoxic effect of doxorubicin shown in EMT6-R with the addition of verapamil, however, suggests that the primary mode of action of the chemosensitizer in this cell line, which is known to overexpress Pgp [5], is *via* inhibition of Pgp. Since the addition of verapamil did not enhance the cytotoxicity of VBBO, this suggests that VBBO is not effluxed by Pgp, further supporting our hypothesis that VBBO acts at a specific site within the cell.

CHAPTER SIX

UPTAKE AND CELL-KILLING ACTIVITIES OF A SERIES OF VICTORIA BLUE DERIVATIVES IN A MOUSE MAMMARY TUMOUR CELL LINE

6.1 Abstract

The triarylmethane dye Victoria blue BO (VBBO) is a known photosensitizer which has been shown to induce a cytotoxic response *in vivo*. A range of novel VBBO derivatives, with varying physicochemical properties, has been compared to VBBO, with respect both to dark toxicity and phototoxicity, on a mouse mammary tumour cell line, EMT6-S. Cells were incubated with varying concentrations (0-5.0 μM) of the dyes and either exposed to light (7.2 J cm^{-2}) or kept dark. Increased light dose (14.4 & 28.8 J cm^{-2}) had little effect on the activity of VBBO but did lead to an increase in the photocytotoxicities of the dimethylamino and morpholino derivatives, MVB and MOVb, respectively.

In respect of uptake, VBBO, PVB, and MVB showed very similar behaviour, all showing increased uptake over time. However, after two hours the rates of VBBO and PVB appeared to equilibrate, whereas that of MVB was still increasing. By contrast MOVb exhibited a much slower rate of uptake, showing little increase over three hours. It was observed that all the photosensitizers exhibited a similar trend of uptake with respect to concentration. In addition, the rate of uptake could be correlated with the lipophilicity of the agents, the most lipophilic being the most efficient.

Confocal microscopy studies showed that all the photosensitizers appeared to be distributed widely throughout the cytoplasm with considerable concentration of the dye in the perinuclear region shown by VBBO and PVB. There appeared to be very little localisation in the nucleus for VBBO and MVB, although slight fluorescence was noted. More evidence of nuclear infiltration was demonstrated with PVB and MOVb.

The chemical changes employed were shown to alter the uptake of the photosensitizers and the resulting light : dark toxicity differentials.

6.2 Introduction.

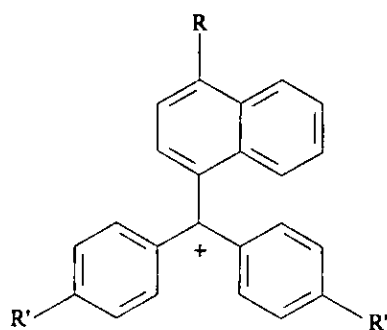
Photodynamic therapy (PDT) is now well-established and is gaining increasing acceptance in the treatment of neoplastic disorders [106]. Problems associated with first generation porphyrin photosensitizers, such as poor light absorption in the 'therapeutic window' (600-750 nm) and prolonged skin photosensitization [214], have led to the search for new and improved drugs. The requirements for a successful photosensitizing drug remain: high selectivity for malignant cells, high photosensitizing activity, low dark toxicity, lack of skin photosensitization, ease of production of pure drug and biochemical stability.

Much recent progress in drug development has been based on porphyrin derivatives and their analogues, e.g. chlorins and phthalocyanines [110-111,215]. However, photosensitizers based on commercial dyes are also of interest because of their familiar and well-established chemistries and synthetic routes. Several examples of commercial photosensitizers have been examined for photocytotoxicity : acridines [126]; phenoxazines [127]; phenothiazines [128] and xanthenes [129]. In most cases, although photocytotoxicity has been demonstrated, there has been concomitant dark toxicity. Few workers have thus far attempted to eradicate the latter by the synthesis of specifically designed photosensitizers based on commercial dyes.

One class of compounds which has received scant attention in this area is the cationic triarylmethane series. Studies have suggested that the flexibility of the ring structure of triarylmethanes causes a fast relaxation of the singlet excited electronic state, and thus a low degree of photosensitizing activity [133]. However, immobilisation of the compounds, which may occur when binding of the structure to biomolecules endows greater structural rigidity, greatly increases the photosensitizing ability. [137]. The Victoria blue series consists of triarylmethane dyes related to crystal violet, where one of the phenyl groups is replaced by 1-naphthyl. Victoria blue BO (VBBO) and Victoria blue R (VBR) (Figure 42) have been reported to exhibit photocytotoxic effects in several

mammalian cell lines, including human squamous cell carcinoma (FaDu) and human melanoma (NEL), though some dark toxicity was observed [133]. The phenylamino analogue, Victoria blue B, (VBB) (Figure 42) has also shown antitumour activity in animal systems [216].

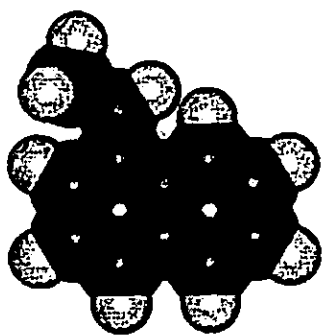
A series of compounds based on the skeleton of VBBO has been synthesised in the Department of Chemistry, UCLAN, possessing different structural features and hence varying physicochemical properties. Figure 43 shows Hyperchem representations of the naphthyl residues in the Victoria blue derivatives used in this study, showing proximities of the amine side chain protons to the naphthyl *peri*-proton (H-8). The aim of the study was to examine known and new photosensitizers for the effect of such physicochemical change upon the photodynamic selectivity, that is, high tumour cell uptake plus a high ratio of light to dark toxicity. Investigations were carried out on the photocytotoxicity / dark toxicity of three compounds having different naphthyl substitution and of one compound having a rigidified triarylmethane structure compared to VBBO, on the murine mammary tumour cell line, EMT6-S. Since the main differences in structure occur at the 4-position of the naphthyl moiety, the different substituted amino groups were used for compound indication (Figure 42). Thus the Victoria blue analogue having a pyrrolidine group in the 4-naphthyl position was denoted as PVB; the 4-dimethylamino- analogue as MVB and the 4-morpholino- analogue as MOVB. In FVB, the two substituted phenyl rings were replaced by the planar 3,6-*bis*(dimethylamino)fluoren-9-yl moiety in an effort to increase the coplanarity and the concomitant sensitizing efficiency of the system.



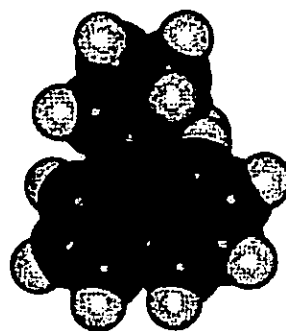
	R	R'	λ_{\max} (nm) ^a	$\log \epsilon_{\max}$ ^b	$\log P$ ^c	pK_a ^d
VBBO	NHC ₂ H ₅	N(C ₂ H ₅) ₂	612	4.58	3.5	11.0
VBR	NHC ₂ H ₅	N(CH ₃) ₂	612	4.48	1.5	9.5
VBB	NHC ₆ H ₅	N(CH ₃) ₂	612	4.55	2.8	7.7
MVB	N(CH ₃) ₂	N(C ₂ H ₅) ₂	622	4.36	2.3	8.5
MOVB		N(CH ₃) ₂	622	4.37	0.9	8.1
PVB		N(CH ₃) ₂	624	4.39	1.8	8.4

^aWavelength of maximum absorption and ^blogarithm of the extinction coefficient measured in aqueous buffer, pH 7.3; ^clogarithm of the partition coefficient between water and 1-octanol and ^dlogarithm of the equilibrium constant measured spectrophotometrically in aqueous buffer.

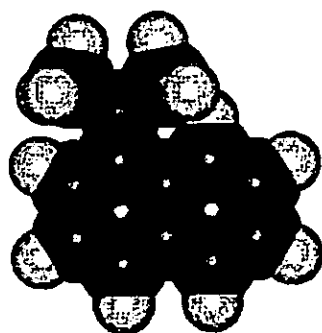
Figure 42 : Structures and physico-chemical data for Victoria blue derivatives.



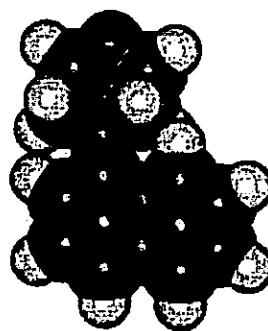
(a)



(b)



(c)



(d)

Figure 43 : Hyperchem representations of the naphthyl residues in the Victoria blue derivatives employed in this work, showing the proximities of the amine side chain protons to the naphthyl *peri*-proton (H-8) : (a) VBBO, (b) PVB, (c) MVB, (d) MOVb.

6.3 Materials and Methods

6.3.1 Chemicals

VBBO, VBR and VBB were purchased from Aldrich Chemicals (Poole, U.K.) and were used without further purification. The synthesis of new photosensitizers followed an established procedure [217]. Elemental analyses for the new photosensitizers were correct and purity was confirmed by high performance liquid chromatography and high field ^1H nmr. 1-Octanol was purchased from Merck, Lutterworth, U.K. and was used without further purification. Both the partition coefficients of the photosensitizers in a pH 7.3 phosphate buffered saline/1-octanol system [218] and their pK_a values [219] were determined spectrophotometrically using a Hewlett Packard 8452A diode array spectrophotometer. Absorption spectra are given in Figure 42. This work was performed by the Chemistry Department, UCLAN.

6.3.2 Cell Culture

The murine mammary tumour cell line (EMT6-S) was originally obtained from Zeneca Pharmaceuticals, Macclesfield, Cheshire. Cultures were routinely maintained at 37°C , 5% CO_2 : 95% air in RPMI 1640 culture medium (Life Technologies, Paisley, U.K.), supplemented with 10% (v/v) foetal calf serum (M.B.Meldrum Ltd., Bourne End, U.K), 200 mM glutamine (Sigma, Poole, U.K.) and penicillin/streptomycin solution at 1×10^4 units ml^{-1} and 10 mg ml^{-1} , respectively, in 0.9% NaCl (Sigma). Trypsin (activity 1200 BAEE units/mg solid), MTT (3-[4,5-dimethylthiazol-2-yl]-2,5-diphenyl-2H-tetrazolium bromide) and DMSO (dimethyl sulphoxide) were obtained from Sigma.

6.3.3 Characterisation of drug uptake

6.3.3.1 Absorbance Spectra

Spectral measurements on a range of dye dilutions (0-5 μM in methanol) were carried out using a Hewlett Packard 8452A diode array spectrophotometer, to check adherence to the Beer-Lambert law. The wavelength of maximum absorption in the visible region for each dye was then used for the spectrophotometric analysis of the dyes in the uptake experiment. FVB exhibited no absorption in the visible region due to rapid hydrolysis in PBS.

6.3.3.2 Drug Uptake

10 ml aliquots of EMT6-S cells were seeded into 75 cm^2 flasks at a cell density of 8×10^4 cells ml^{-1} , in RPMI 1640 medium, supplemented with 10% (v/v) foetal calf serum, 200 mM L-glutamine and penicillin/streptomycin, as previously described. The cells were then incubated at 37°C, 5% CO_2 : 95% air and grown to confluence. The medium was aspirated and replaced with varying concentrations of each dye (0-0.625 μM) and the cells incubated for a further 0.5, 1, 2, or 3 hours under the same conditions as previously described. Following incubation, the medium was aspirated from each flask and the cell monolayer removed by the addition of 1ml 0.25% (w/v) trypsin and 0.5% (w/v) EDTA (in Dulbecco's PBS). The cells were resuspended in 10 ml RPMI to neutralise the action of the trypsin and counted using an improved Neubauer haemocytometer. The cell suspension was centrifuged at 160 g for 5 minutes and the supernatant removed. The cell pellet was then rinsed twice by resuspension in PBS followed by centrifugation at 160 g for 5 minutes. The supernatant was aspirated and the cells resuspended in 1 ml methanol for 30 minutes. The cell suspension was then centrifuged at 160 g for 30 minutes. The supernatant was removed and the absorbance determined spectrophotometrically. The experiments were performed three times, in

duplicate. Specific uptake for each dye was established from a calibration curve and expressed in picomoles $(10^6 \text{ cells})^{-1}$.

6.3.4 Phototoxicity : dark toxicity experiment

The method was carried out as described in section 4.3.3.

6.3.5 Effect of variable illumination

96 well microtitre plates were set up as previously described (section 4.3.3). The cells were exposed to the various drug concentrations as before. However, in this series of experiments, the plates were illuminated for 30 minutes, 1 hour, 2 hours or kept in the dark. The photocytotoxicity : dark toxicity ratio effected by each drug was then established using the MTT assay, as previously described.

6.3.6 Localisation Studies Using Confocal Microscopy.

2 ml aliquots of EMT6-S and EMT6-R cells were seeded at a cell density of 1×10^4 cells ml^{-1} into 35 mm petri dishes (Falcon, Fahrenheit Laboratories, Rotherham, U.K.) in RPMI 1640 medium, supplemented with 10% (v/v) foetal calf serum, 200 mM L-glutamine and penicillin / streptomycin, as previously described. A sterile quartz coverslip (suprasil, 0.5 mm diameter \times 0.2 mm thick, Heraeus Silica & Metals Ltd., Byfleet, U.K) was placed into each petri dish and the cells were allowed to attach for three days (EMT6-S cells) or four days (EMT6-R cells) whilst incubating at 37°C, 5% CO_2 : 95% air. The medium was aspirated and replaced with medium containing a 5 μM concentration of VBBO, PVB, MVB or MOVV, and incubated for three hours, under conditions previously described. Following 3 hours' incubation, the cells were examined with a scanning laser confocal fluorescence microscope using a helium / neon laser at 633 nm. Untreated cells were also examined for autofluorescence, but none was found.

6.4 Results

6.4.1 Absorbance Spectra

With the exception of FVB, all the dyes absorbed maximally in the red wavelength region (Figure 42). The absorption spectrum of FVB showed no absorption in the visible region due to the spontaneous hydrolysis of this compound in PBS, thus an acceptable standard curve, and hence uptake values, could not be obtained. Log P values and pK_a values for all the Victoria blue photosensitizers dealt with in this work appear in Figure 42.

6.4.2 Drug Uptake

The initial uptake of VBBO, MVB and PVB over one hour was found to be very similar (Figure 44), with that of VBBO and MVB equilibrating after approximately two hours. The uptake of PVB between one and two hours appeared to be slightly lower than VBBO and MVB, but then increased between two and three hours, reaching a similar level to VBBO and PVB after three hours. MOVV showed a much lower rate of uptake than the other three dyes, increasing slowly over three hours (Figure 44). Control experiments showed there to be no artifactual binding of the dye to the plastic petri dishes.

VBBO, PVB, MVB and MOVV all showed a good correlation between drug concentration and cellular uptake after three hour's incubation (Figure 45). The uptake / dose trend was similar for all four drugs tested, and followed the order of efficacy VBBO > PVB > MVB > MOVV. This corresponded to the lipophilicity of the agents, with VBBO being the most lipophilic. At very low concentrations (< 0.156 μ M), the uptake of MVB appeared to be lower than that of the other three drugs.

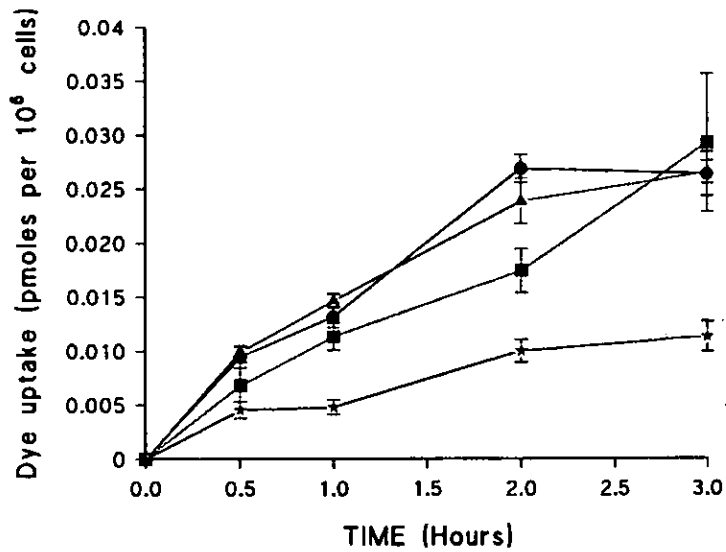


Figure 44 : Uptake curves of Victoria blue derivatives by EMT6 cells: VBBO (●), PVB (■), MVB (▲), MOVB (+). Dyes (at 0.625 μ M in RPMI 1640) were added to the cells, and cellular dye concentrations were determined at different time intervals after incubation at 37°C, 5% CO₂ 95% air. Each point represents mean \pm SEM (n=3).

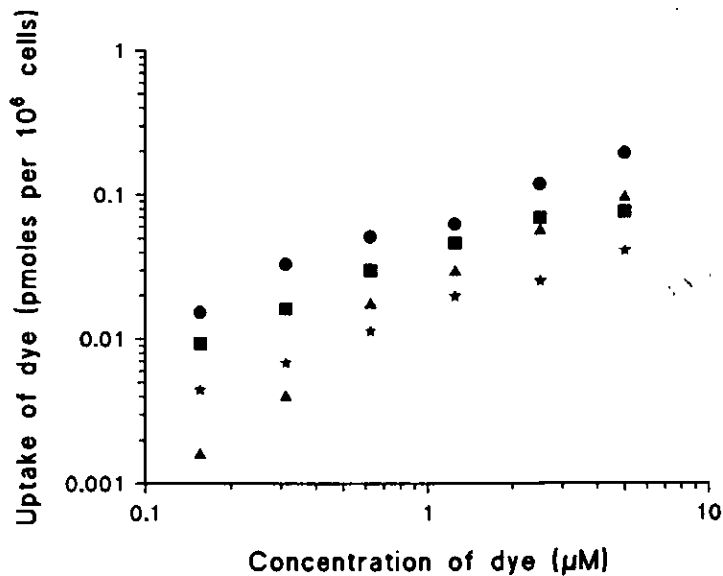


Figure 45 : Uptake curves for Victoria blue derivatives. VBBO (●),PVB (■), MVB (▲), MOVB (+). Dyes (0.156–5.0 μ M) in RPMI 1640 were added to the cells and incubated for 3 hours at 37°C, 5% CO₂ : 95% air. Cellular retention of the dye at each concentration was calculated.

6.4.3 Mean cytotoxicity following 3 hours' incubation

VBBO gave the greatest differential between light and dark cytotoxicity at all concentrations, with the optimum differential seen between 0.156 μM and 0.312 μM (Figure 46(a)). The results for the Victoria blue derivatives indicated that they all gave a lower photocytotoxic response than VBBO thus decreasing the light/dark differential (Figures 46 (b), (c) & (d)).

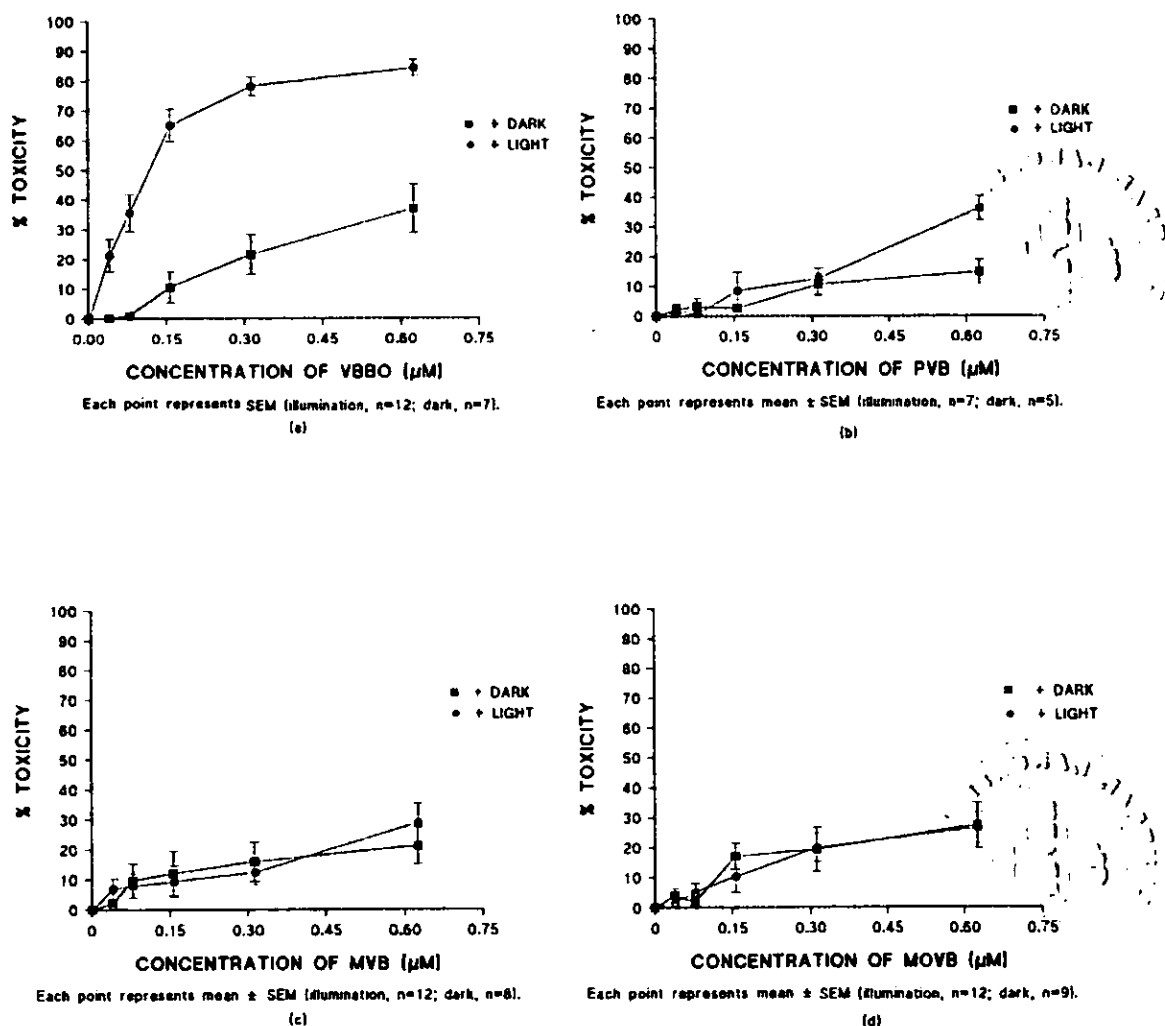


Figure 46 : % cytotoxicity on EMT6-S cells elicited by Victoria blue derivatives following illumination : (a) VBBO; (b) PVB; (c) MVB; (d) MOVB.

Cells (1000 / well in 96 well plates) were allowed to attach for 48 hours. Drugs (200 μl at 0 - 0.625 μM in RPMI 1640) were added to the cells and incubated for 3 hours. The cells were then rinsed with RPMI and exposed to light (7.2 J cm^{-2}), prior to growing on for 3 days at 37°C, 5% CO_2 : 95% air.

The IC₅₀ values for the light and dark toxicities of each compound are shown in Table 12. The light enhancement factor (LEF) is the ratio of light : dark IC₅₀ values. The light : dark toxicity ratio is not constant, but varies with differing concentrations and for this reason has been standardised using the IC₅₀ values. The light dose used was 7.2 J cm⁻².

Table 12 : IC₅₀ values / Light Enhancement Factor for Victoria Blue derivatives.
The light enhancement factor (LEF) is the ratio of light : dark IC₅₀ values.

Drug	IC ₅₀ (μM) / Dark	IC ₅₀ (μM) / Light	LEF
VBBO	1.19	0.12	9.9
PVB	3.37	1.26	2.7
MVB	2.35	1.24	1.9
MOVB	2.22	1.79	1.2

6.4.4 Effect of variable illumination

Increasing the light dose above 7.2 J cm⁻² produced no enhancement in the cytotoxicity induced by 0.625 μM VBBO. By contrast, cytotoxicity induced by PVB increased following further illumination, although this was not a linear response (Figure 47). The greatest change in the photocytotoxic response produced by PVB was seen when the light dose was increased to 14.4 J cm⁻², with a further, smaller increase seen at 28.8 J cm⁻². This shows that PVB is inherently a better photosensitizer than MVB and MOVB. PVB was less effective overall compared to VBBO at equimolar doses. Similarly, the cytotoxicity induced by MVB was enhanced when the light dose was increased to 14.4 J cm⁻², but illumination at 28.8 J cm⁻² gave no further increase. MVB was also less effective overall compared to VBBO. MOVB was not appreciably phototoxic at physiological concentrations, and increased light dose did not enhance this. FVB was found to hydrolyse rapidly in medium and hence was ineffective as a photosensitizer with visible light.

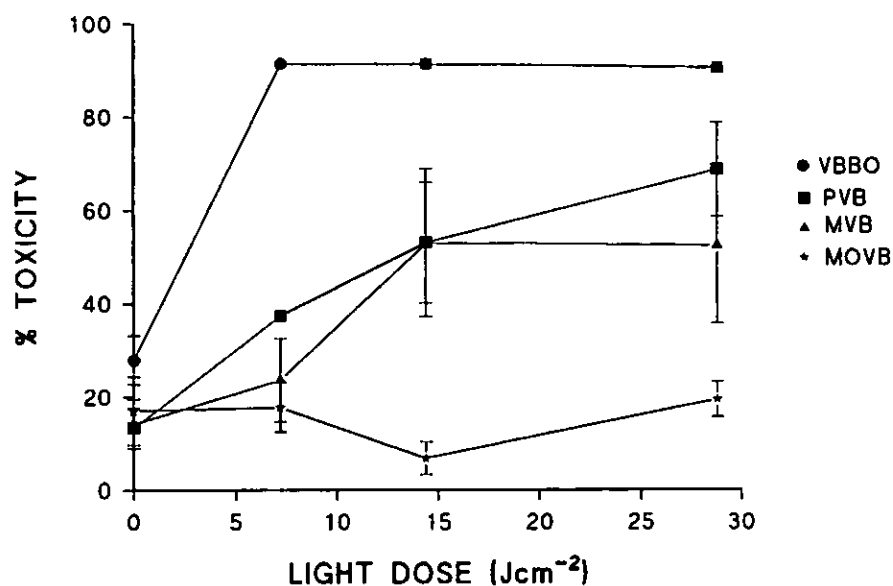
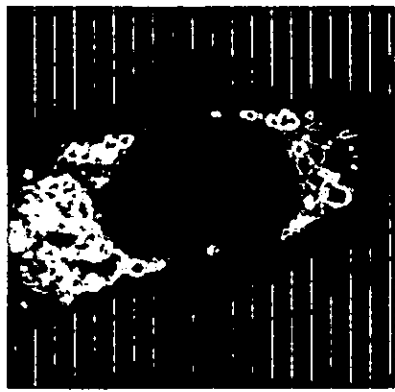


Figure 47 : Effects of variable light dose on the % cytotoxicity elicited by Victoria blue derivatives against EMT6-S cells.

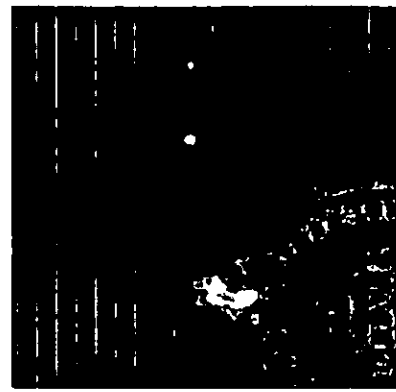
Cells (1000 / well in 96 well plates) were allowed to attach for 48 hours. Drugs (200 μ l at a concentration of 0.625 μ M in RPMI 1640) were added to the cells and incubated for 3 hours. The cells were then rinsed with RPMI and exposed to various light doses (7.2 - 28.8 J cm⁻²), prior to growing on for 3 days at 37°C, 5% CO₂ : 95% air. Each point represents mean \pm SEM (n \geq 4).

6.4.5 Localisation Studies Using Confocal Microscopy.

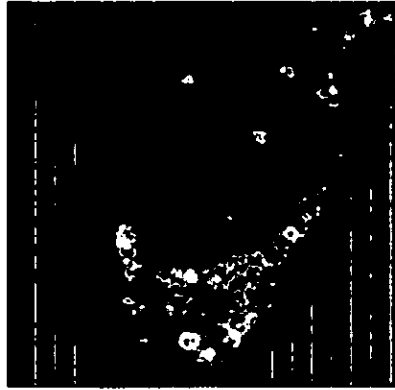
Figures 48 (a & b) show two different cells treated with 5 μ M VBBO. The dye appeared to be distributed widely throughout the cytoplasm in a punctate pattern, which may be consistent with the distribution of mitochondria. There appeared to be very little fluorescence in the nucleus. Figures 48 (c & d), (e & f) and (g & h) show different cells incubated for three hours with PVB, MVB and MOVb, respectively, all at a concentration of 5 μ M. They all showed a similar intracellular localisation to VBBO in that the dyes were distributed widely throughout the cytoplasm, however, figures 48 (c) (PVB) and 48(g) (MOVb) suggested some nuclear infiltration.



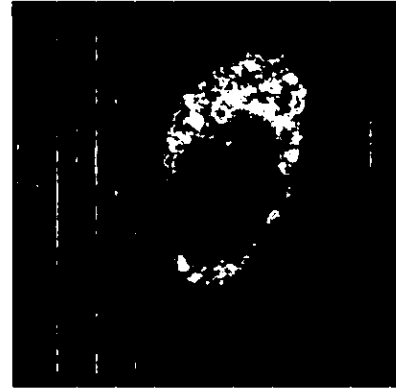
(a)



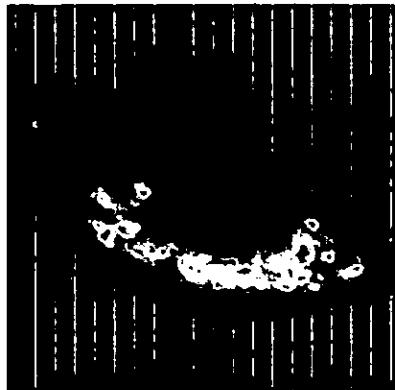
(b)



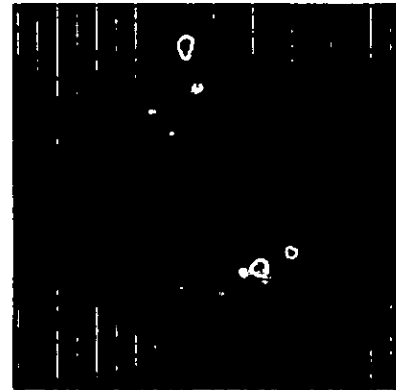
(c)



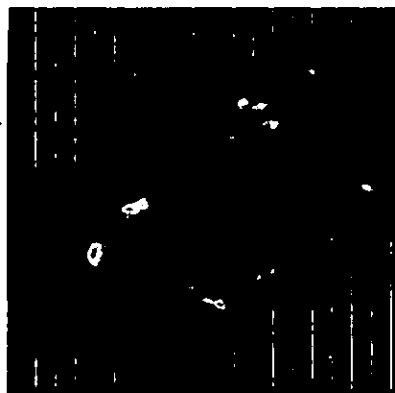
(d)



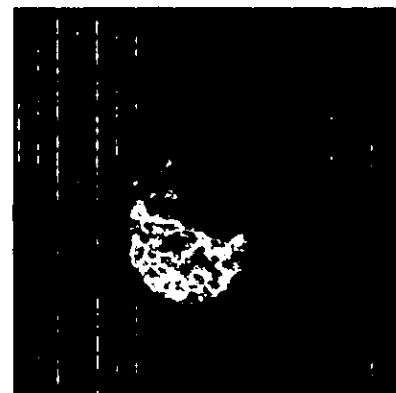
(e)



(f)



(g)



(h)

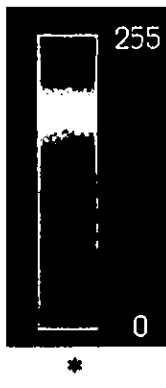


Figure 48 : Intracellular distribution of (a) & (b) VBBO, (c) & (d) PVB, (e) & (f) MVB & (g) & (h) MOVB, all at a concentration of 5 μ M, in EMT6-S cells following 3 hours' incubation, shown by confocal microscopy. Figures (a) - (h) show different cells following a single scan with the laser beam. * Scale of fluorescence intensity (red-255, maximum;black-0, minimum).

6.5 Discussion

The compounds under discussion can exist in several forms in aqueous media (Figure 49). Triarylmethane dyes are well known to react with water to give non-planar, neutral carbinol compounds (Figure 49(b)) [219]. This situation is further complicated for the Victoria blue series in that it is also possible for a secondary amino group attached to the naphthyl residue to become deprotonated, again giving a neutral compound - the Homolka Base (Figure 49(c)). Only the ionised (blue) species (Figure 49(a)) is photoactive but the neutral forms are expected to exert some influence on pharmacological activity.

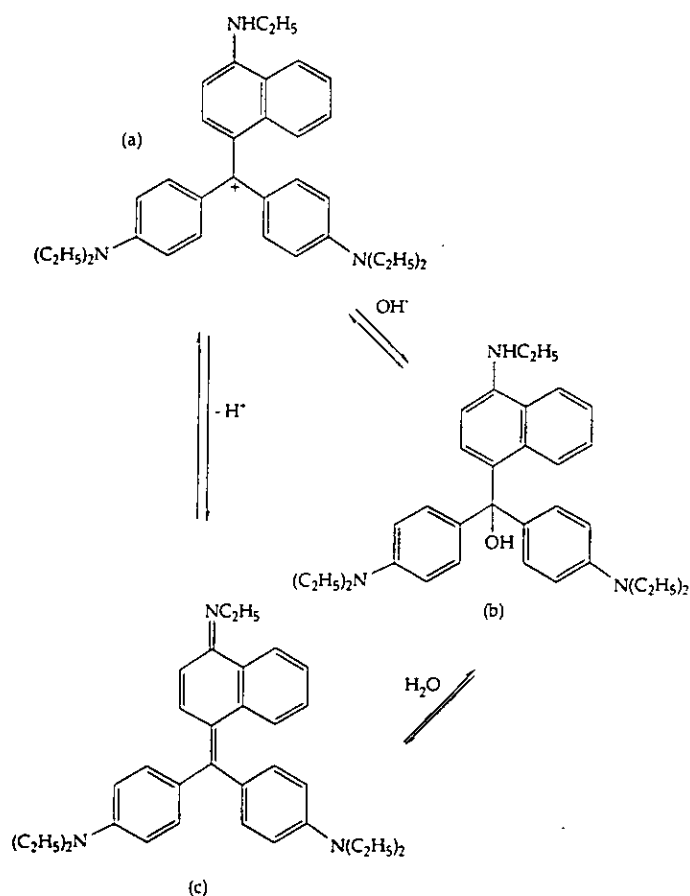


Figure 49 : Interaction of VBBO with water.

The derivatives investigated can exist in several forms in aqueous media giving non-planar neutral carbinol compounds (b). In the Victoria blue series, the secondary amine group can also be deprotonated forming the Homolka base (a neutral compound) (c). Only the ionised (blue) series (a) is photoactive, but the neutral forms are expected to exert some influence on pharmacological activity.

It is possible to relate the uptake trends of the photosensitizers to their respective $\log P$ and pK_a values. Thus a highly lipophilic species such as VBBO exhibited a high level of uptake and was retained inside the cell, probably in the mitochondria [167]. As the lipophilicity of the series decreases it may be that uptake becomes increasingly difficult, or that the more hydrophilic members were removed more efficiently from the cell by an efflux mechanism. This is supported by the fact that all the drugs showed a similar trend in their uptake / dose profiles, in the order of efficacy VBBO > PVB > MVB > MOVB, which correlated with their levels of lipophilicity.

On consideration of the rates of uptake, VBBO, PVB, and MVB showed very similar behaviour (Figure 44), all showing increased uptake over time. After two hours, the rates of VBBO and MVB appeared to equilibrate, whereas that of PVB was still increasing. By contrast MOVB exhibited a much slower rate of uptake, increasing slowly over three hours. This may suggest a more rapid uptake-efflux mechanism, presumably facilitated by the more hydrophilic nature of MOVB.

Victoria blue BO exhibits significant dark toxicity indicating interaction with a sensitive target site. Indeed, VBBO is known to localise in mitochondria and also has a similar $\log P / pK_a$ profile to that of the sulfur analogue of Nile blue [210] which may indicate lysosomal activity. A lack of organelle specificity would explain the lower dark toxicities and lower phototoxicities of the Victoria blue derivatives compared to that of VBBO. Confocal microscopy studies showed that VBBO appeared to be distributed widely throughout the cytoplasm (Figure 48), which may be consistent with the distribution of mitochondria. Considerable concentration of the dye in the perinuclear region is also shown (Figure 48(a)), also supporting this hypothesis. There appeared to be very little localisation in the nucleus, although slight fluorescence was evident. PVB, MVB and MOVB also showed widespread cytoplasmic distribution (Figures 48(c & d), (e & f), (g & h), respectively), however, there was more evidence of nuclear infiltration in PVB and MOVB.

Both VBBO and PVB exhibited considerable phototoxicity in the EMT6-S tumour cell line, whereas neither MVB nor MOVB was effective in this respect. Triarylmethyl cations such as VBBO are non-planar, minimising steric repulsions within the molecule by adopting a propeller-like shape. This lack of coplanarity of the aromatic rings accounts for the absence of photosensitizing activity in chemical tests. It has been stated that the cellular photosensitizing activity of the Victoria blue series is due to enforced molecular coplanarity by interaction with biomolecules [136]. To explain the different phototoxicities observed it is therefore necessary to look more closely at the molecular structures involved. For efficient photosensitizing activity it is necessary for there to be efficient interaction between the lone pair of electrons on the amino nitrogens and the remainder of the molecule.

MVB and MOVB both have a lack of coplanarity between the amine group attached to the naphthyl residue because of repulsion between the hydrogens of the amino group and the *peri* hydrogen naphthyl ring of (H-8). This lack of coplanarity is well known to decrease photosensitizing ability in other systems [221]. It is expected that PVB will suffer to a lesser extent from this repulsion because of the small size of the pyrrolidinyl ring. Thus a degree of coplanarity will exist with a concomitant increase in photosensitizing ability compared to MVB and MOVB. VBBO shows the highest photosensitizing ability of the series which may occur because the N-ethyl group is able to adopt a configuration which minimises the repulsions mentioned above, that is, a high degree of coplanarity exists between the amine and naphthyl moieties. The greater photosensitizing efficacy of PVB compared to MVB and MOVB was demonstrated by the larger increases in cytotoxicity seen with PVB on increasing the light dose (Figure 47).

As mentioned previously, VBBO is much more phototoxic than VBR. If the above argument is followed, it would be expected that VBR, having the same aminonaphthyl moiety as VBBO (dimethylaminophenyl rather than diethylaminophenyl moieties) would exhibit a similar degree of phototoxicity. That this is not the case may indicate that the

intracellular localisation of VBR is quite different, that is, that it exerts its photosensitizing effect at sites which are less likely to lead to cell death.

It must be emphasised that no photosensitizing activity for these compounds using standard *in vitro* chemical tests, that is, singlet oxygen generation efficiency *via* quenching with 1,3-diphenylisobenzofuran, was demonstrated in this study. Such activity is only apparent from biological testing.

The importance of a secondary amino group in a series of cationic photosensitizers has been reported previously for Nile Blue and its congeners [221]. Nile Blue is a planar molecule, whereas there is a lack of coplanarity between the naphthyl moiety and the remainder of the molecule in the Victoria Blue series. Here, the presence of the secondary amino group in 4-position of the naphthalene ring appears to be of even greater significance as regards photosensitizing ability. The presence of a tertiary amino group, unless small, in this position inhibits efficient photosensitizing activity due to a lack of coplanarity between the amino group itself and the naphthyl residue. However, as with the majority of drugs, this single factor does not govern drug efficacy. Although photosensitizing ability is obviously important, it is the combination of this with other physicochemical properties which dictates activity. The present work has shown that, in common with other types of photosensitizer, Victoria blue derivatives have specific cellular sites of action. Photosensitizing ability becomes important only once these sites are reached and the cellular/organelle uptake and kinetics involved are governed by factors such as $\log P$ and pK_a .

CHAPTER SEVEN

INTRACELLULAR LOCALISATION STUDIES OF DOXORUBICIN AND VICTORIA BLUE BO IN EMT6-S AND EMT6-R CELLS USING CONFOCAL MICROSCOPY

7.1 Abstract

The subcellular localisation of doxorubicin and VBBO in EMT6-S and EMT6-R cells was studied, using confocal microscopy, in order to investigate their sites of action. In cells which had been treated with doxorubicin (10 μ M) for ninety minutes, prior to recovery for forty minutes in drug-free medium, the pattern of distribution differed between EMT6-S cells and EMT6-R cells. Doxorubicin was found to localise mainly in the nucleus of the sensitive cell line, whereas no nuclear involvement was seen in the resistant cells. The drug was also effluxed more rapidly from EMT6-R cells than EMT6-S cells. A study following the accumulation of doxorubicin at various time intervals over one hour in EMT6-S cells showed that the drug clearly interacts with both the plasma membrane and the nucleus.

In contrast to doxorubicin, the intracellular distribution of VBBO in both cell lines was similar, although uptake of the drug appeared slower in the resistant cell line. The pattern of localisation of VBBO was found to be markedly different to that of doxorubicin in EMT6 cells. VBBO was clearly localised throughout the cytoplasm, in a punctate pattern, which may be consistent with the widespread distribution of mitochondria. A more apical pattern of accumulation was noted in the EMT6-R cell line. No interaction with the plasma membrane was evident. These results indicate that the main modes of action for the two drugs differ markedly, suggesting interaction with both the membrane and the nucleus in the case of doxorubicin, but possibly mitochondrial involvement for VBBO.

7.2 Introduction

The subcellular localisation of the triarylmethane dyes VBBO, PVB, MVB and MOVB and the phenothiazinium dyes MB and TBO in EMT6 cells have been studied by confocal microscopy in order to investigate their sites of action (chapters four and six). The intracellular distribution of doxorubicin is also of interest due to its widespread use in the treatment of cancer [176] and to extensive studies into its mode of action. The mechanisms by which doxorubicin exerts its cytotoxicity have proved to be very complex and several theories have been proposed. Doxorubicin is known to act mainly by intercalation with DNA and interaction with nucleic acids and nuclear components, such as DNA topoisomerase II [143,222]. In addition, doxorubicin has been shown to be cytotoxic without entering the cell [144] and this cytotoxicity does not necessarily correlate with DNA damage or inhibition of DNA synthesis [144]. Recent studies have shown that the mechanism of action may be directly related to drug-membrane interactions and particularly to drug lipid-interactions (145,146, section 2.1).

Phospholipids are extremely important in transmembrane signalling. Most attention has been focussed on the role of phosphatidylinositols (in particular, phosphatidylinositol bisphosphate (PIP₂)) in this process [223], however, there is growing evidence that phosphatidylcholine, sphingomyelin and their metabolites are also important mediators of signal transduction [224]. Tritton *et al.* [143] postulate that doxorubicin exerts its cytotoxicity by interacting with, and damaging the functions of, both the plasma membrane and nuclear DNA. They argue that, for cytotoxicity to occur, the activation of the protein kinase C (PKC) pathway, following membrane perturbation, is crucial for signal transduction between the cell surface and the nucleus. Figure 50 shows the proposed scheme by which doxorubicin cytotoxicity may occur.

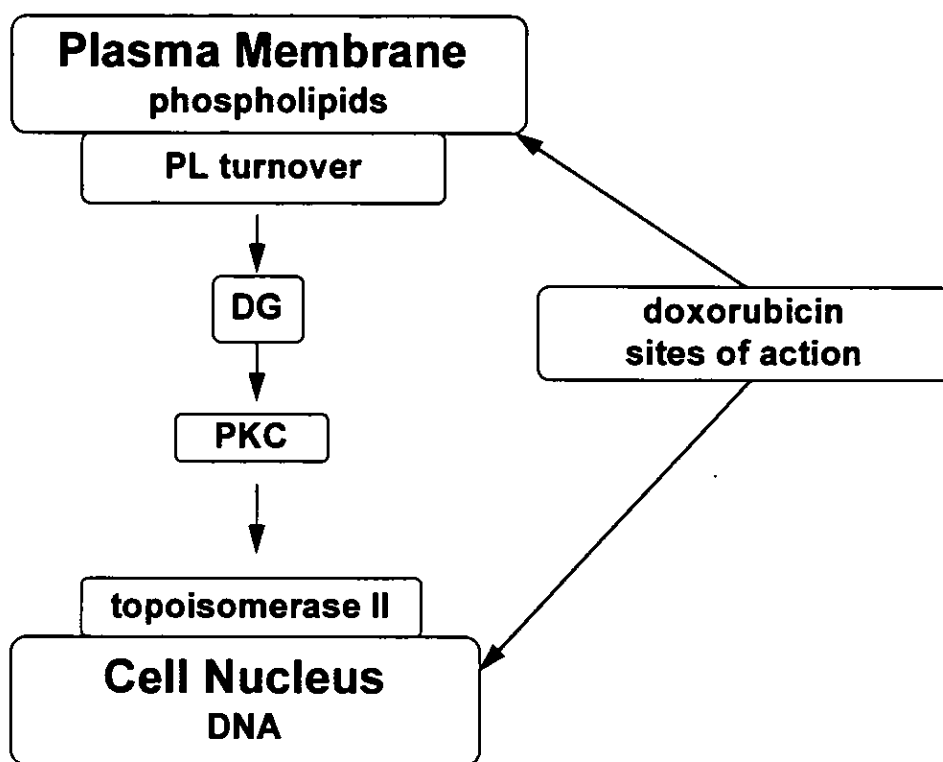


Figure 50 : Schematic diagram showing proposed mechanism of doxorubicin cytotoxicity.

Doxorubicin interacts with both the cell nucleus and nuclear DNA thereby damaging their functions. In order for cytotoxicity to occur, membrane perturbation and the subsequent activation of the PKC pathway is necessary for signal transduction to take place between the cell surface and the nucleus. PL - phospholipid; DG - diacylglycerol; PKC - protein kinase C. (Adapted from Tritton [143]).

Doxorubicin has been shown to interact with other subcellular targets, such as the cytoskeleton [225] and studies using cultured tumour cells displaying MDR characteristics have also demonstrated alterations in intracellular drug accumulation and distribution [81,82,226], further adding to the complexity of the drug's action.

MDR appears to be multifactorial with many different mechanisms contributing to the MDR phenotype. In addition to the mechanisms discussed in previous chapters, another important phenomenon associated with MDR is an altered subcellular drug distribution [82]. Various fluorescence studies have demonstrated that the development of MDR is associated with a relative shift of doxorubicin or daunorubicin fluorescence from the nucleus to the cytoplasm [81,82,227,228]. Schuurhuis *et al.*, [228] argue that this

phenomenon may make an important contribution to the resistance displayed against anthracyclines by MDR cells.

The aim of this study was to examine the intracellular localisation of doxorubicin and VBBO by confocal microscopy, over time, in EMT6 cells and to compare their subcellular distribution.

7.3 Materials and Methods

7.3.1 Localisation Studies Using Scanning Laser Confocal Microscopy

7.3.1.1 Time course studies

2 ml aliquots of EMT6-S and EMT6-R cells were seeded at a cell density of 1×10^4 cells ml^{-1} into 35 mm petri dishes (Falcon, Fahrenheit Laboratories, Rotherham, U.K.) in RPMI 1640 medium, supplemented with 10% (v/v) foetal calf serum, 200 mM L-glutamine (Sigma, Poole, U.K.) penicillin/streptomycin solution at 1×10^4 units ml^{-1} and 10 mg ml^{-1} , respectively, in 0.9% NaCl (Sigma). A sterile quartz coverslip (suprasil, 0.5 mm diameter x 0.2 mm thick, Heraeus Silica & Metals Ltd., Byfleet, U.K) was placed into each petri dish and the cells were allowed to attach for three days (EMT6-S cells) or four days (EMT6-R cells) whilst incubating at 37°C, 5% CO₂ : 95% air. A coverslip with attached EMT6-S cells was placed in a flow cell which was adapted for use with the confocal microscope by fixing to a microscope slide. RPMI 1640 medium was added to the cells by the use of an attached syringe and the cells were examined for autofluorescence. The medium was then replaced with RPMI 1640 medium containing 10 μM doxorubicin and images were taken using a scanning laser confocal fluorescent microscope at various intervals over the period of one hour. The microscope was fitted with an argon ion laser at 488 nm. This procedure was repeated for both EMT6-S and EMT6-R cells using VBBO at a concentration of 5 μM , but using a helium neon laser at

633 nm. Unfortunately, due to time constraints, no time course images of EMT6-R cells in the presence of doxorubicin were obtained.

7.3.1.2 Intracellular localisation of doxorubicin in treated EMT6-S and EMT6-R cells, following recovery in drug-free medium

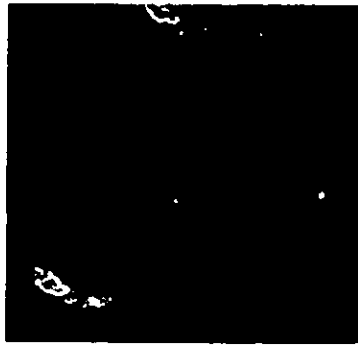
The cells were grown as previously described in 7.2.1.1, however, in this study EMT6-S and EMT6-R cells were initially treated with doxorubicin for 1.5 hours, followed by incubation in drug-free medium.

The medium was aspirated from the petri dishes and replaced with medium containing doxorubicin (10 μ M), and the cells incubated for 1.5 hours, under conditions previously described. The cells were rinsed with RPMI 1640 medium and incubated for a further forty minutes. The cells were then examined with a scanning laser confocal fluorescence microscope fitted with an argon ion laser at 488 nm.

7.4 Results

7.4.1 Time course studies

Doxorubicin was taken up rapidly by EMT6-S cells and could be seen in the plasma membrane and nucleus after only two minutes (Figure 51 (a)). Localisation in the plasma membrane and nucleus increased with time up to ten minutes, however, very little drug was seen in the cytoplasm. There also appeared to be apical concentration of doxorubicin in the plasma membrane of the cell (Figures 51 (a - g). Figures 51 (c & d) show considerable accumulation in the plasma membrane, but subsequent images show this concentration to diminish (Figures 51 (e - h). The nuclear accumulation appeared to be slightly reduced after fifteen minutes (Figure 51(e)), and continued to diminish over forty minutes (Figure 51(h)).



(a) + 2 min



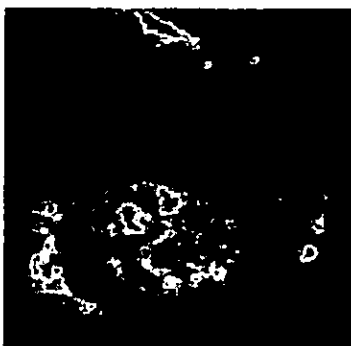
(b) + 4 min



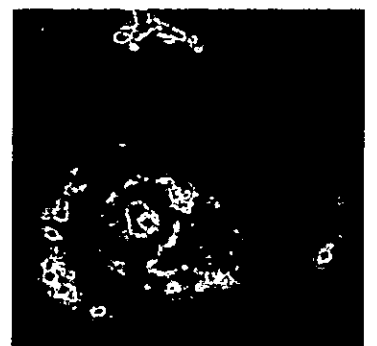
(c) + 6 min



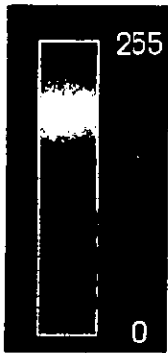
(d) + 10 min



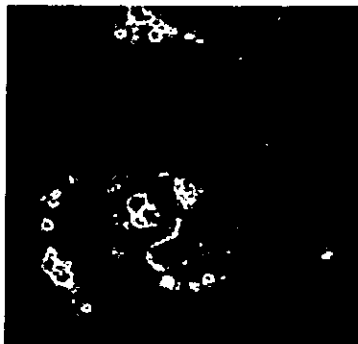
(e) + 15 min



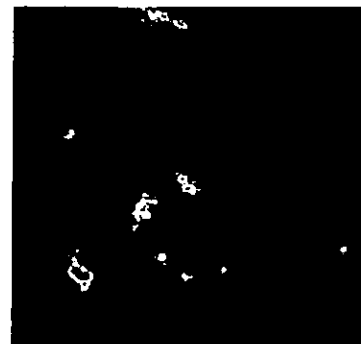
(f) + 20 min



*



(g) + 30 min

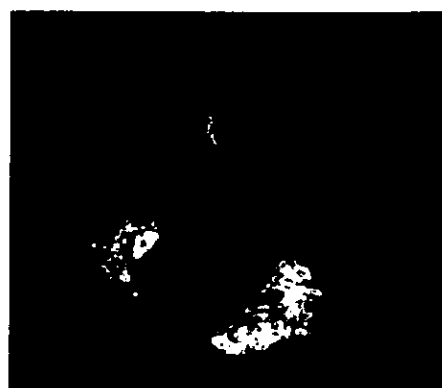


(h) + 40 min

Figure 51 : Intracellular distribution of doxorubicin (10 μ M) in EMT6-S cells shown by confocal microscopy. A single cell was imaged at various time intervals (indicated below each figure) following the addition of doxorubicin. * Scale of fluorescence intensity (red-255, maximum; black-0, minimum).

By contrast, localisation of VBBO in EMT6-S cells was markedly different to that of doxorubicin. Once again, the drug was taken up rapidly by the cells and could clearly be seen after four minutes (Figure 52 (a)). The concentration of drug in the cell increased marginally over the next eleven minutes (Figures 52 (b - c)) and remained constant until sixty minutes when a slight decrease was noted (Figures 52 (d - g)). VBBO was clearly localised throughout the cytoplasm, in a punctate pattern which may be consistent with the widespread distribution of mitochondria. Some diffuse fluorescence was evident in the nuclear region after eight minutes (Figure 52 (b)), however, this did not appear to increase over time (Figures 52 (b - g)). Interestingly, no interaction with the plasma membrane was shown.

Uptake of VBBO by the resistant cells appeared to be slower than in the sensitive cells (Figures 53 (a-h)) with an increase in accumulation of the drug seen over forty minutes (Figures 53 (a - f)). The concentration did not appear to change between forty and sixty minutes (Figures 53 (f & g)). VBBO was again seen to be localised throughout the cytoplasm, however, there did appear to be an apical concentration of the drug in these cells, which may indicate localisation within the Golgi apparatus or mitochondria. Weak, diffuse fluorescence appeared in the nuclear region after eight minutes (Figure 53 (b)) increasing somewhat over twenty five minutes (Figures 53(b - e)), however, the main area of localisation was the cytoplasm. In common with EMT6-S cells no interaction with the plasma membrane was seen.



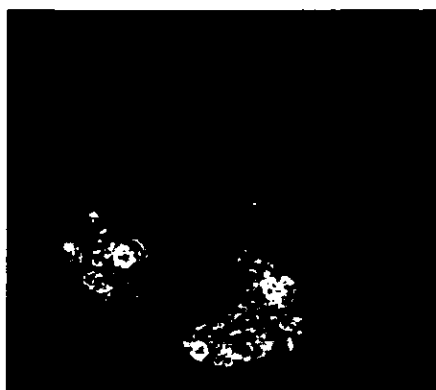
(a) + 4 minutes



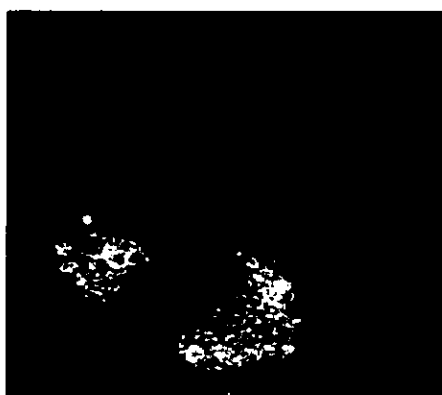
(b) + 8 minutes



(c) + 15 minutes



(d) + 21 minutes



(e) + 30 minutes



(f) + 46 minutes



*

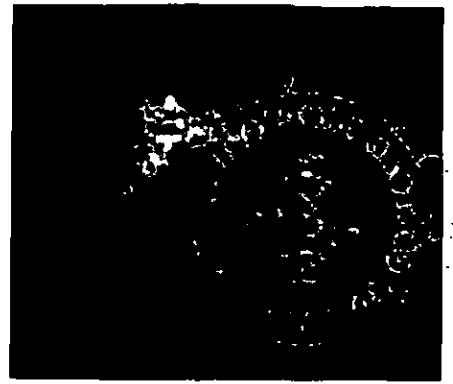


(g) + 60 minutes

Figure 52: Intracellular distribution of VBBO (5 μ M) in EMT6-S cells, shown by confocal fluorescence microscopy. A single cell was imaged at various time intervals (indicated below each figure) following the addition of VBBO. * Scale of fluorescence intensity (red-255, maximum; black-0, minimum).



(a) + 1 minute



(b) + 8 minutes



(c) + 12 minutes



(d) + 17 minutes



(e) + 25 minutes



(f) + 40 minutes



*



(g) + 60 minutes

Figure 53: Intracellular distribution of VBBO (5 μ M) in EMT6-R cells, shown by confocal fluorescence microscopy. A single cell was imaged at various time intervals (indicated below each figure) following the addition of VBBO. * Scale of fluorescence intensity (red-255, maximum; black-0, minimum).

7.4.2 Intracellular localisation of doxorubicin in treated EMT6-S and EMT6-R cells, following recovery in drug-free medium

Nuclear localisation of doxorubicin in the EMT6-S cell line was clearly visible forty minutes after rinsing the cells with RPMI 1640 (Figures 54 (a - f)) and some cytoplasmic distribution was also seen (Figures 54 (b - e)). No evidence of localisation in the plasma membrane was noted. EMT6-R cells showed very little fluorescence at all, in fact the intensity was increased x 10 to image the cells compared to that used with EMT6-S cells. Weak fluorescence was seen in the cytoplasm, in a punctate pattern (Figures 55 (a - f)) but no nuclear accumulation was noted.

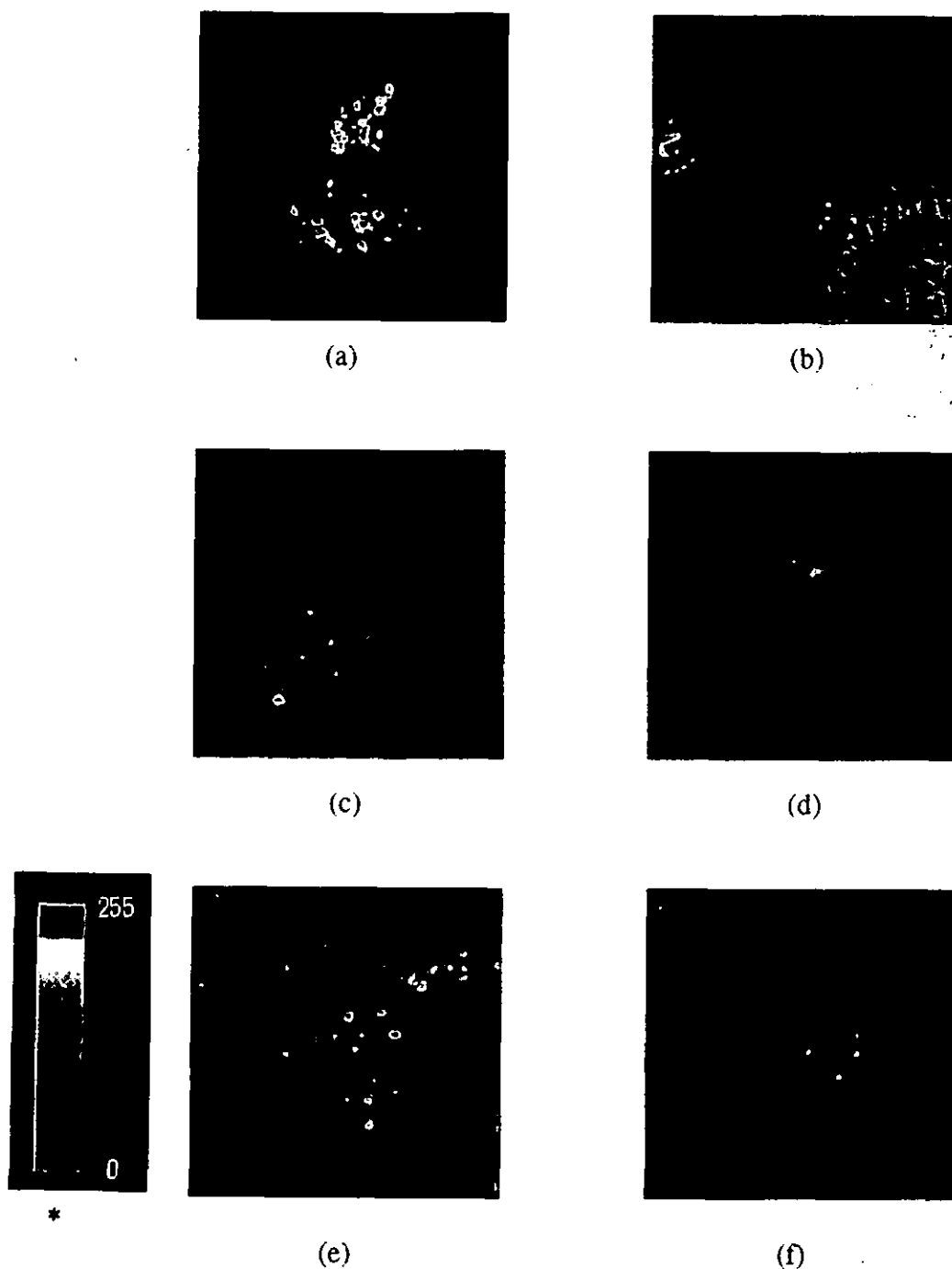
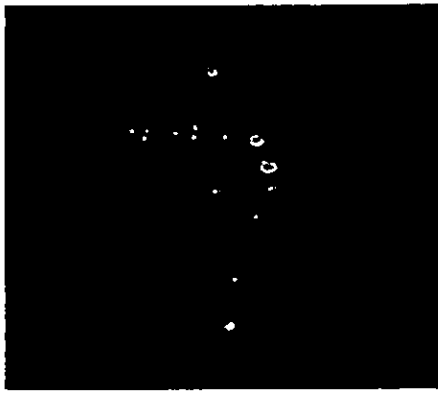


Figure 54: Intracellular distribution of doxorubicin in EMT6-S cells following exposure to 10 μ M doxorubicin for 2 hours, prior to rinsing with RPMI 1640 medium. Cells were imaged by confocal fluorescence microscopy 40 minutes after rinsing. Figures (a-f) show different cells following a single scan with the laser beam. * Scale of fluorescence intensity (red-255, maximum; black-0, minimum).



(a)



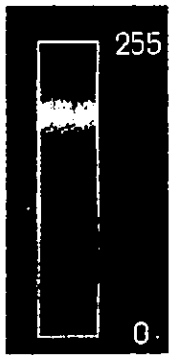
(b)



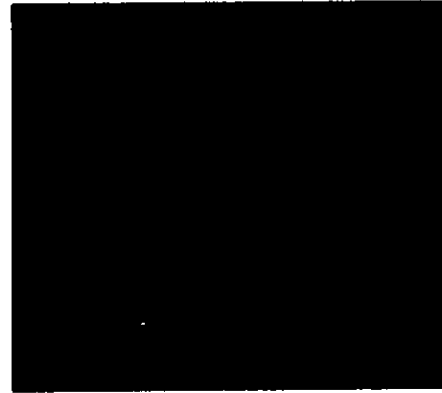
(c)



(d)



(e)



(f)

*

Figure 55 : Intracellular distribution of doxorubicin in EMT6-R cells following exposure to 10 μ M doxorubicin for 2 hours, prior to rinsing with RPMI 1640 medium. Cells were imaged by confocal microscopy 40 minutes after rinsing. Figures (a-f) show different cells following a single scan with the laser beam. * Scale of fluorescence intensity (red-255, maximum; black-0, minimum).

7.5 Discussion

Doxorubicin was rapidly taken up by EMT6-S cells, with the drug clearly localising in the plasma membrane and nucleus after only two minutes (Figure 51 (a)). The drug continued to accumulate in the plasma membrane and nucleus for up to ten minutes, however, very little fluorescence was noted in the cytoplasm. This supports the mechanism of action put forward by Tritton *et al.* [143] who propose that perturbation of the membrane induces subsequent signal transduction *via* diacylglycerol and protein kinase C, leading to interaction with the nucleus. There also appeared to be apical concentration of doxorubicin in the plasma membrane (Figures 51(a - g)). Considerable accumulation of doxorubicin in the plasma membrane was evident up to ten minutes, although after this time the localisation changed. The nuclear accumulation did not appear to increase, therefore it must be assumed that the doxorubicin diffused out of the cell into the surrounding medium. Less nuclear accumulation was seen after fifteen minutes and very little fluorescence was noted in the plasma membrane or cytoplasm.

Meschini *et al.* [229] studied the intracellular localisation of doxorubicin in M14 human melanoma cells and in MCF-7 human breast cancer cells (both sensitive and resistant cell lines). Following one hours' treatment with $1 \mu\text{g ml}^{-1}$ doxorubicin, they found that the drug was localised in the nuclei of the parental cell lines with only weak cytoplasmic fluorescence seen in some cells. This is in good agreement with the findings of the present study. They also examined cells which had previously been exposed to doxorubicin but were then allowed to recover for seventy one hours in a drug-free medium. Complete efflux of doxorubicin from the nucleus was shown, with occasional fluorescent vesicular structures localised to perinuclear regions in the cytoplasm. Other workers [213,230,231] have suggested that doxorubicin diffuses across the membrane and binds to anionic vesicles which are transported back to the cell surface *via* microtubules. Studies by Meschini *et al.* [229] support this hypothesis, and they suggest that the accumulation of doxorubicin in the perinuclear region may indicate binding to pre-lysosomes and the Golgi apparatus since these organelles are associated with the

transport of secretory vesicles to the cell surface [81,232]. Since the present study only examined cells one hour after recovery in drug-free medium, realistic comparisons can not be made. Further studies should be performed to examine the effects of longer recovery periods on the intracellular localisation of doxorubicin in EMT6-S and EMT6-R cells.

MDR is often associated with decreased intracellular drug accumulation [25,26], frequently due to the overexpression of the energy-dependent drug efflux pump, Pgp, in the plasma membrane of resistant cells (see section 1.3.1). EMT6-R cells have previously been shown to efflux doxorubicin *via* the Pgp pump [5], thus comparison of the intracellular distribution of doxorubicin in EMT6-S and EMT6-R cells is highly relevant. Several workers have shown that MDR can be associated with altered intracellular drug accumulation and localisation [226,233,234]. Schuurhuis *et al.* [82] have suggested that, in addition to drug efflux, Pgp may be involved in the relocalisation of drugs by pumping them into other cellular organelles away from their cytotoxic targets.

Unfortunately, due to time constraints, a time course following doxorubicin accumulation in EMT6-R cells was not performed. EMT6-R cells were, however, examined following ninety minutes' treatment with doxorubicin prior to forty minutes' recovery time in drug-free medium. The drug appeared to have been effluxed efficiently by the cells, since very little fluorescence was seen (Figures 55 (a - e)). Indeed, the intensity of the images had to be increased x 10, compared to that used for EMT6-S cells, in order to visualise the localisation of the drug. Weak fluorescence was observed in the cytoplasm of the cells, in a punctate pattern (Figures 55 (a - e)), but no nuclear accumulation was observed. Meschini *et al.* [229] also found a lack of nuclear accumulation in MCF-7 DX (resistant) cells, however, there was extensive cytoplasmic localisation. A direct comparison with their study cannot be made, since the distribution of doxorubicin in recovered EMT6-R cells was not investigated.

A clear difference was seen in intracellular doxorubicin accumulation between EMT6-S and EMT6-R cells. It would be beneficial to study the distribution of doxorubicin in EMT6-R cells over time, in the presence of doxorubicin, to confirm the lack of nuclear accumulation which is evident in the recovered EMT6-R cells. Other studies have also found distinct differences between localisation of doxorubicin in a variety of sensitive and resistant cell lines [81,226,229]. Meschini *et al.* [229] also examined the effect of the resistance modifier, verapamil, on the subcellular distribution of doxorubicin in MCF-7 DX cells. The intracellular concentration of the drug was increased and it appeared to localise in a specific area close to the nucleus. This supports a recent study by Rutherford and Willingham [235] who identified the accumulation of anthracycline molecules in the *trans*-Golgi system of resistant cells which were also treated with verapamil.

Doxorubicin is also known to localise in mitochondria and to exert some cytotoxicity *via* damage to the electron transfer chain in mitochondria [153,236]. Mitochondria are known to localise preferentially in the perinuclear region of many cultured cells [229], therefore, the distribution of doxorubicin in this area could be attributed to mitochondrial binding. It is surprising, however, if this were the case, that cytoplasmic localisation is not evident in EMT6-S cells when in contact with doxorubicin.

The intracellular distribution of VBBO was found to be markedly different to that of doxorubicin. VBBO was taken up extremely rapidly, with intense fluorescence evident after only four minutes, increasing only marginally up to fifteen minutes. The concentration of the drug appeared to be constant up to sixty minutes when a slight decrease was noted. VBBO was clearly distributed widely throughout the cytoplasm, in a punctate pattern, which may be consistent with the distribution of mitochondria. Very little evidence of nuclear localisation was seen. In contrast to doxorubicin, no interaction between VBBO and the plasma membrane was demonstrated.

The resistant cell line initially appeared to show slower uptake of VBBO than the parental line, with a more gradual increase in cellular accumulation. Equilibration was

seen at forty minutes, compared to fifteen minutes in EMT6-S cells. Although similar distribution of the drug was seen throughout the cytoplasm in EMT6-R cells to that of EMT6-S cells, there appeared to be an apical concentration of doxorubicin in the resistant line. Very little nuclear association was observed and no interaction with the plasma membrane.

This study suggests that the intracellular localisation of VBBO may be consistent with mitochondrial distribution in EMT6 cells, in agreement with other workers who have previously shown localisation of the dye in the mitochondria of tumour cells [132,167]. Interestingly, little difference was found between the intracellular distribution of VBBO in EMT6-S and EMT6-R cells, in contrast to that of doxorubicin. This is reflected in the results obtained in a previous study (Chapter 4) which showed that EMT6-R cells required almost 100-fold more doxorubicin to overcome the resistance compared to EMT6-S cells, whereas only a 10-fold increase in concentration was required for VBBO. Previous studies have also shown that VBBO does not appear to be effluxed by, or interact with, Pgp (Chapter 5), which is supported by the lack of membrane localisation shown by VBBO in EMT6 cells.

These results indicate that the main modes of action for the two drugs, VBBO and doxorubicin, differ markedly, suggesting interaction with both the membrane and the nucleus in the case of doxorubicin, but of possible mitochondrial involvement for VBBO.

CHAPTER EIGHT

CLOSING DISCUSSION

8.1 Closing Discussion and Future Studies

The development of a prokaryotic model to investigate anthracycline-membrane interactions which could subsequently be related to the eukaryotic system has several potential advantages to researchers. Bacterial systems are relatively inexpensive to use and rapid results may be obtained, thus providing an effective screening model. Synthetic membrane systems are available, however, a bacterial model provides an *in vivo* comparison. The development of the *E.coli* plasma membrane system, using the mutant strain HDL11 in which the membrane phospholipid content can be manipulated, appeared to be an ideal vehicle for such a model. Ultimately, of course, a eukaryotic model in which the phospholipid content could be manipulated, perhaps based on a yeast system, would give a more realistic representation of interactions occurring in mammalian tumour cells.

Unfortunately, the attempts to develop a prokaryotic model system for studying anthracycline-membrane interactions which could be related to eukaryotic cells did not prove to be entirely successful, since induction of phosphatidylglycerol synthesis in the HDL11 strain did not markedly increase the cytotoxic effects of doxorubicin. However, the suggestion that the wild-type MRE600 cells appear to develop a resistance mechanism to counteract the effects of doxorubicin is very interesting, since it may involve efflux mechanisms similar to those employed by eukaryotic cells displaying the MDR phenotype. This offers great potential for future research, but is beyond the scope of this study.

Eukaryotic cells *in vivo* have been employed by many researchers to investigate drug interactions and mechanisms related to cancer chemotherapy, thus the next logical step in the study was to characterise a suitable mammalian cell line. The mouse mammary tumour cell line, EMT6, has been used widely in such investigations and was chosen to investigate membrane-based effects relating to MDR. Comparisons were made between the drug-sensitive parental cell line, EMT6-S and the drug-resistant sub-line, EMT6-R.

Some studies have indicated differences in the structural order of lipids and alterations in the lipid content of certain cell lines compared to their drug-resistant sub-lines [161,162]. Comparison of the percentage of the total fatty acid composition showed there to be no significant difference between the two EMT6 cell lines ($p > 0.05$) with the exception of linoleic acid (18:2), where the level appeared to be higher in the resistant cell membranes ($p = 0.05$) and no difference was detected in the phospholipid profile. It must be emphasised, however, that this was a preliminary investigation. Since no apparent differences were demonstrated, further investigations were not pursued, due to time constraints. Future studies may be employed to perform more specific techniques.

To probe potential changes in membrane composition upon the onset of MDR, the EMT6 cell lines were characterised with respect to a range of cytotoxic agents having varying log P values and hence potentially variable levels of membrane interaction and/or cellular localisation. Photodynamic therapy is relatively new in the field of cancer chemotherapy, but offers great potential for eradication of MDR cells, in particular as an adjunct to surgery or for the treatment of inoperable cancers. To this end, the agents investigated were based on cationic commercial dyes with photosensitizing potential, and their cytotoxicity was compared to that of the more conventional anti-cancer drugs, doxorubicin and *cis*-platinum.

VBBO was found to be the most effective photosensitizer against EMT6-S and EMT6-R cells (LEF approximately 10-fold in both cell lines), at much lower concentrations than MB or TBO. The latter two dyes were moderately photocytotoxic (LEF approximately 2-fold in both cell lines), but no photocytotoxicity was noted for doxorubicin or *cis*-platinum. The higher photocytotoxicity exerted by VBBO than either MB or TBO may be due to differences in their subcellular localisation. As previously discussed, VBBO is highly lipophilic compared to MB and TBO, which may facilitate cellular uptake. The present studies, using confocal microscopy, suggest that more VBBO was accumulated within both EMT6-S and EMT6-R cells following three hours' incubation than either MB or TBO. This may be explained by the differing lipophilicity of the agents. Future

studies should be carried out to compare the specific uptake of each of the agents. Similarly, longer incubation periods could be investigated since other studies have suggested that increased incubation times lead to more effective cytotoxicity exerted by MB and TBO [128, 186, 187].

VBBO and TBO have been shown in previous studies to localise in the mitochondria [128, 132, 168], whereas MB has shown a different distribution, suggested to be lysosomal [169]. The results of this study appear to support these findings. Both VBBO and TBO showed widespread accumulation throughout the cytoplasm which may be consistent with the distribution of mitochondria. By contrast, MB appeared to localise in a punctate pattern throughout the cytoplasm, suggesting that the dye may be sequestered into vesicles such as lysosomes.

cis-Platinum was effective at equimolar concentrations in both EMT6-S and EMT6-R cells, and was therefore not susceptible to MDR in this cell line. By contrast, doxorubicin required almost a 100-fold increase in concentration in order to reach the IC₅₀ level in EMT6-R cells compared to that of the parental cells. The results for the photosensitizers were very interesting. VBBO was shown to be partially effective at overcoming MDR, requiring approximately a 10-fold increase in concentration for the EMT6-R cells, compared to the sensitive cells. Doxorubicin is known to be pumped out of the resistant cells *via* the membrane-bound drug efflux pump, Pgp [26]. The resulting decrease in intracellular doxorubicin thus renders the agent less effective. Since VBBO was shown to be only partially effective against EMT6-R cells, it was postulated that some of the drug may be effluxed *via* Pgp.

The phenothiazinium dyes, MB and TBO, were moderately photocytotoxic, but interestingly, the main cytotoxic effect appeared to be due to the dark toxicity of the agents. Both the dyes showed some effect in overcoming MDR, however, the drug concentration levels required were similar (less than 2-fold) to those required to reach

the IC₅₀ value in the sensitive cells. This suggests that MB and TBO are toxic in their own right and may be able to circumvent efflux *via* Pgp.

In order to investigate possible interaction of the photosensitizers with Pgp, the effects of pre-treatment with each of the agents, prior to exposure to doxorubicin, were studied. Since doxorubicin is a known substrate for Pgp, any interaction of the photosensitizers with Pgp would be expected to increase the cytotoxicity of doxorubicin due to the increased cellular accumulation of the drug. The resistant cell line has previously been shown to overexpress Pgp compared to the parental cell line [5], therefore a greater increase in doxorubicin toxicity would be expected in the resistant cells, following pre-treatment with the agents. Pre-treatment with the dyes led to increased doxorubicin cytotoxicity in all cases. Since very low concentrations of the dyes were used (equivalent to 1/8th of the IC₅₀ values for each agent) accounting for less than 10% toxicity alone, it was reasoned that a synergistic effect had occurred.

Pre-treatment with VBBO induced a similar increase in doxorubicin cytotoxicity in *both* cell lines which suggests that this result was independent of Pgp efflux. Time course studies following the uptake of VBBO in both EMT6-S and EMT6-R cells showed VBBO to be rapidly accumulated in the cytoplasm, but no localisation in the membrane. VBBO has been shown to localise in the mitochondria of various cells and it is suggested that this is the main site of cytotoxic action [132]. Doxorubicin is also known to bind to mitochondria and to exert toxic effects upon the respiratory chain [153]. We hypothesise that the synergistic effect demonstrated by the combined treatment of VBBO and doxorubicin may be largely attributed to mitochondrial damage and disruption of the respiratory chain.

Pre-treatment of EMT6 cells with MB induced a 2-fold increase in doxorubicin cytotoxicity in the resistant cell line, but only a 1.4-fold increase in the sensitive cells, suggesting a different mechanism of action to that of VBBO, which may involve interaction with Pgp. Similarly, pre-treatment with TBO induced an increase in almost

2-fold in EMT6-S cells, but this was increased to 3-fold in the resistant cells. This again suggests a different mode of action to VBBO, possibly involving interaction with Pgp.

VBBO was found to be the most effective photosensitizer against EMT6-S and EMT6-R cells in this study. Further investigations into its mode of action were therefore pursued. Pre-treatment of the EMT6 cell lines with VBBO suggested that the dye was not acting as a substrate for Pgp. This was confirmed by the use of the chemosensitizer, verapamil. Verapamil is a potent inhibitor of Pgp and has been shown to increase the cytotoxicity of doxorubicin by binding to Pgp. This leads to increased cellular accumulation with a concomitant increase in cytotoxicity. The combined treatment of verapamil and doxorubicin resulted in a 2-fold increase in doxorubicin cytotoxicity in the sensitive cell line but an 18-fold increase in the resistant cell line. This result clearly supports the overexpression of Pgp in the EMT6-R cells compared to that in the parental cells. By contrast, the presence of verapamil did not enhance the cytotoxicity of VBBO in either cell line.

VBBO is thought to exert its photocytotoxic effects *via* free radical generation. Glutathione and related enzymes are known to be protective of free radical damage in normal tissues [58, 91] thus it was reasoned that depletion of GSH may lead to increased cytotoxicity of VBBO. GSH levels were depleted in both cell lines by the addition of BSO, however, the photocytotoxicity of VBBO was not found to be increased. This suggests that VBBO may be acting at an intracellular site not protected by GSH or that the mechanism of action is not *via* the *in situ* generation of singlet oxygen.

PDT shows great potential for the treatment of cancer, however, there are many drawbacks associated with drugs currently available. Consequently, there is a constant search for new and improved drugs. To this end, we examined a series of compounds based on the skeleton of VBBO, possessing different structural features and hence varying physicochemical properties. The chemical changes employed were shown to alter uptake of the photosensitizers and resulting light : dark toxicity differentials.

Unfortunately, none of the compounds proved to be as effective as VBBO against EMT6-S cells. The rate of uptake for VBBO, MVB and PVB appeared to be very similar, whereas that of MOVB was slower. The uptake/dose trend was also similar for all four drugs tested and correlated to the levels of lipophilicity of the agents, VBBO being the most lipophilic.

Confocal microscopy studies showed similar localisation of the derivatives to that of VBBO, that is, throughout the cytoplasm of the EMT6-S cells, although PVB and MOVB showed more evidence of nuclear infiltration. It would be useful to perform time course studies, using confocal microscopy, on each of the derivatives to compare the pattern and rate of uptake to that of VBBO. This study suggests that, in common with other types of photosensitiser, VBBO derivatives have specific sites of action. Photosensitizing ability becomes important only once these sites are reached and the cellular/organelle uptake and kinetics are governed by such factors as $\log P$ and pK_a .

Studies following the accumulation of VBBO at various time intervals over one hour in both EMT6-S cells and EMT6-R cells showed similar localisation of the drug in both cell lines, although uptake appeared to be slower in the resistant cells. VBBO was localised throughout the cytoplasm in a punctate pattern which may correlate with the distribution of mitochondria, however, there was little evidence of nuclear involvement. Similarly, no interaction with the plasma membrane was noted. By contrast, a time course study following the accumulation of doxorubicin in EMT6-S cells over one hour found the intracellular distribution of doxorubicin to be quite different to that of VBBO. There was clear evidence of interaction with both the plasma membrane and the nucleus. This supports the theory by Tritton *et al.* that doxorubicin exerts its action by interacting with, and damaging the functions of, both the plasma membrane and nuclear DNA [143]. In cells which had been treated with doxorubicin (10 μM) for ninety minutes, prior to recovery in drug-free medium for forty minutes, doxorubicin was found to localise mainly in the nucleus of the sensitive cells, whereas no nuclear involvement was seen in the resistant cells. The drug also appeared to have been effluxed more rapidly from the

resistant cells than the sensitive cells. These results indicate that the main modes of action for the two drugs differ considerably, suggesting interaction with both the membrane and the nucleus in the case of doxorubicin, whereas VBBO appears to act at a specific site within the cell.

References.

- [1] Vile, R. (1990). Cancer and Oncogenes. *Inside Science*, **32** :1-5.
- [2] Varmus, H. and Weinberg, R.A. (1993). Genes and the Biology of Cancer. *Scientific American Library*, New York.
- [3] Franks, L.M. and Teich, N.M. (Eds.) (1995). In *Introduction to the Cellular and Molecular Biology of Cancer* (2nd. Ed.). Oxford University Press Inc., New York.
- [4] Liotta, L. (1992). Cancer Cell Invasion and Metastasis. *Scientific American*, **266** : 54 - 57.
- [5] Cox, C. (1993). *In Vitro* Studies on the Cellular Mechanisms of Resistance to Cytotoxic Compounds With Special Reference to Multidrug Resistance and Cancer Chemotherapy. *PhD Thesis*, University of Central Lancashire, U.K.
- [6] Ruddon, R. (1995). In *Cancer Biology* (3rd Ed.), Oxford University Press Inc., New York.
- [7] Coghlan, A. (1996). Blood clotting drug lays siege to tumours. *New Scientist*, **2052** : 25.
- [8] Vogt, P.K. (1993). Cancer Genes. *The Western Journal of Medicine*, **158** : 273-278.
- [9] MacDonald, F. and Ford, C.H.J. (1991). In *Oncogenes and Tumour Suppressor Genes*. BIOS Scientific Publishers Ltd., Oxford, U.K.
- [10] Shaw, I. and Jones, H. (1994). Mechanisms of non-genotoxic carcinogenesis. *TIPS*, **15** : 89-93.

- [11] Ames, B.N., McCann, J. and Yamasaki, E. (1975). Methods for detecting carcinogens and mutagens with the Salmonella / mammalian-microsome mutagenicity test. *Mutation Research*, **31** : 347-64.
- [12] Ames, B.N. (1983). Dietary carcinogens and anti-carcinogens. Oxygen radicals and degenerative diseases. *Science*, **221** : 1256-1264.
- [13] Cavenee, W.K. and White, R.L. (1995). The Genetic Basis of Cancer. *Scientific American*, **272** : 50-57.
- [14] Clayson, D.B. (1989). Can a mechanistic rationale be provided for non-genotoxic carcinogens identified in rodent bioassays? *Mutat. Res.*, **221** : 53-67.
- [15] Grasso, P. (1991). Role of persistent nongenotoxic tissue-damage in rodent cancer and relevance to humans. *Ann. Rev. Pharmacol. Toxicol.*, **31** : 253-287.
- [16] Weinberg, R. (1996). How Cancer Arises. *Scientific American*, **275** : 32-47.
- [17] Friend, S.H., Bernards, R., Rogelj, S., Weinberg, R.A., Rapaport, J.M., Albert, D.M. and Dryja, T.P. (1986). A human DNA segment with properties of the gene that predisposes to retinoblastoma and osteosarcoma. *Nature*, **323** : 643-646.
- [18] Culotta, E. and Koshland, D.E. (Jnr.) (1993). p53 Sweeps Through Cancer Research. *Science*, **262** : 1958-1959.
- [19] Marx, J. (1993). How p53 Suppresses Cell Growth. *Science*, **262** : 1644-1645.
- [20] Kamb, A.,Gruis, N.A. & Fieldhaus, J. (1994). A cell cycle regulator potentially involved in genesis of tumour types. *Science*, **264** : 436 - 440.

- [21] Schimke, R.T. (1984). Gene amplification, drug resistance and cancer. *Cancer res.*, **44** : 1735-1742.
- [22] Schneider, E. and Cowan, K.H. (1994). Multiple drug resistance in cancer therapy. *The Medical Journal of Australia*, **160** : 371-373.
- [23] Bellamy, W.T., Dalton, W.S. and Dorr, R.T. (1990). The clinical relevance of multidrug resistance. *Cancer Invest.*, **8** : 547-562.
- [24] Tannock, I. and Hill, R.P. (Eds.) (1987). In *The Basic Science of Oncology* (1st Ed.), Pergamon Press, U.S.A.
- [25] Kartner, N. and Ling, V. (1989). Multidrug Resistance in Cancer. *Scientific American*, **260** : 26-33.
- [26] Gottesman, M.M. and Pastan, I. (1988). Resistance to multiple chemotherapeutic agents in human cancer cells. *TIPS*, **9** : 54-91.
- [27] Rome, L.H. (1995). Multidrug Resistance : Locked in the Vault? *Nature Medicine*, **1** : 527.
- [28] Gottesman, M.M. and Pastan, I. (1993). Biochemistry of Multidrug Resistance Mediated by the Multidrug Transporter. *Ann. Rev. Biochem.*, **62** : 385-427.
- [29] Bradley, G., Naik, M & Ling, V. (1989). P-glycoprotein expression in multidrug-resistant human ovarian carcinoma cell lines. *Cancer Res.*, **49** : 2790-96.
- [30] Shen, D.W., Fojo, A., Chin, J.E., Roninson, I.B., Richert, N. Pastan., I. & Gottesman, M.M. (1986). Human multidrug-resistant cell lines : increased *mdr1* expression can precede gene amplification. *Science*, **232** : 643-645.

- [31] Chen, C.J., Chin, J.E., Ueda, K., Clark, D.P., Pastan, I., Gottesman, M.M. & Roninson, I.B. (1986). Internal duplication and homology with bacterial transport proteins in the MDR1 (P-glycoprotein) gene from multidrug-resistant human cells. *Cell*, **47** : 381-89.
- [32] Gerlach, J.H., Endicott, J.A., Juranka, P.F., Henderson, G., Sarangi, F., Deuchars, K.L. & Ling, V. (1986). Homology between P-glycoprotein and a bacterial haemolysin transport protein suggests a model for multidrug resistance. *Nature*, **324** : 485-489.
- [33] Gros, P., Croop, J. & Housman, D. (1986). Mammalian multidrug resistance gene : Complete cDNA sequence indicates strong homology to bacterial transport proteins. *Cell*, **47** : 371-80.
- [34] Ambudkar, S.V., Lelong, I.H., Zhang, J., Cardarelli, C.O., Gottesman, M.M. & Pastan, I. (1992). Partial purification and reconstitution of the human multidrug-resistance pump : characterisation of the drug-stimulatable ATP hydrolysis. *Proc. Natl. Acad. Sci., USA*, **89** : 8472-76.
- [35] Yoshimura, A., Kuwazuru, Y., Sumizawa, T., Ichikawa, M., Ikeda, S., Uda, T. & Akiama, S. (1989). Cytoplasmic orientation and two-domain structure of the multidrug transporter, p-glycoprotein, demonstrated with sequence-specific antibodies. *J. Biol. Chem.*, **264** : 16282-91.
- [36] Bellamy, W.T. (1996). P-Glycoproteins and Multidrug Resistance. *Annual Review of Pharmacology and Toxicology*, **36** : 161-183.
- [37] Zhang, J.T. & Ling, V. (1991). Study of membrane orientation and glycosylated extracellular loops of mouse P-glycoprotein by in vitro translation. *J. Biol. Chem.*, **266** : 18224-32.

- [38] Zhang, J.T., Duthie, M. & Ling, V. (1993). Membrane topology of the N-terminal half of the hamster P-glycoprotein molecule. *J.Biol. Chem.*, **268** : 15101-10.
- [39] Skach, W.R., Calayag, M.C. & Lingappa, V.R. (1993). Evidence for an alternative model of human P-glycoprotein structure and biogenesis. *J.Biol. Chem.*, **268** : 6903-8.
- [40] Juranka, P.F., Zastawny, R.L. & Ling, V. (1989). P-glycoprotein : Multidrug-resistance and a superfamily of membrane-associated transport proteins. *FASEB J.*, **3** : 2583-2592.
- [41] Higgins, C.F. & Gottesman, M.M. (1992). Is the multidrug transporter a flippase? *Trends Biochem. Sci.*, **17**: 18-21.
- [42] Leveille, C.R. and Moore, A.S. (1993). Multiple Drug Resistance. *Advances in Veterinary Science and Comparative Medicine.*, **37** : 31-59.
- [43] Gottesman M.M. (1993). How cancer cells evade chemotherapy : Sixteenth Richard and Hinda Rosenthal Foundation Award Lecture. *Cancer Res.*, **53** : 747-754.
- [44] Spiers, A.S.D. (1994). Multiple drug resistance, the MDR Gene, and the Law of Maximum Perversity as it applies to oncology : an hypothesis. *Haematological Oncology*, **12**, 155-161.
- [45] Valverde, M.A., Diaz, M., Sepulveda, F.V., Gill, D.R., Hyde, S.C. and Higgins, C.F. (1992). Volume-regulated chloride channels associated with the human multidrug-resistance p-glycoprotein. *Nature*, **355** : 830-833.

- [46] Wang, X., Wall, D.M., Parkin, J.D., Zalcborg, J.R. and Kemm, R. (1994). P-glycoprotein expression in classical multi-drug resistant leukaemia cells does not correlate with enhanced chloride channel activity. *Clinical and Experimental Pharmacology and Physiology*, **21** : 101-108.
- [47] Viana, F., Van-Acker, K., De-Greef, C., Eggermont, J., Raeymaekers, L., Droogmans, G. & Nilius, B. (1995). Drug-transport and volume-activated chloride channel functions in human erythroleukaemia cells : relation to expression level of P-glycoprotein. *J.Membrane. Biol.* **145** :87-98.
- [48] McClean, S. and Hill, B.T. (1992). An overview of membrane, cytosolic and nuclear proteins associated with the expression of resistance to multiple drugs *in vitro*. *Biochim. Biophys. Acta*, **114** : 107-127.
- [49] Liu, L.F. (1989). DNA topoisomerase poisons as antitumour drugs. *Ann. Rev. Biochem.*, **58** : 351-375.
- [50] Danks, M.K., Schmidt, C.A. Cirtain, M.C., Suttle, D.P. & Beck, W.T. (1988). Altered catalytic activity of and DNA cleavage by DNA topoisomerase II from human leukaemic cells selected for resistance to VM-26. *Biochem.*, **27** : 8861-8869.
- [51] Haber, M., Norris, M.D., Kavallaris, M., Bell, D.R., Davey, R.A., White, L. and Stewart, B.W. (1989). Atypical multi-drug resistance in a therapy induced drug resistant human leukaemia cell line (LALW-2) : Resistance to vinca alkaloids independent of p-glycoprotein. *Cancer res.* **49**, 5281-87.
- [52] Slapak, C.A., Daniel, J.C. and Levy, S.B. (1990). Sequential emergence of distinct resistant phenotypes in murine erythroleukaemia cells under adriamycin selection : Decreased anthracycline uptake precedes increased p-glycoprotein expression. *Cancer res.* **50**, 7895-7901.

- [53] Cole, S.P.C., Bhardwa, G., Gerlach, J.H., Mackie, J.E., Grant, C.E., Almquist, K.C., Stewart, E.U., Duncan, A.M.V. and Deeley, R.G. (1992). Overexpression of a transporter gene in a multidrug-resistant human lung cancer cell-line. *Science*, **258** : 1650-1654.
- [54] Leier, I., Jedlitschky, G., Buchholtz, U., Cole, S.P., Deeley, R.G. & Keppler, D. (1994). The MRP gene encodes an ATP-dependent export pump for leukotriene C4 and structurally related conjugates. *J. Biol. Chem.*, **269** : 27807 - 10.
- [55] Holló, Z., László, H., Hegedüs, T. & Sarkadi, B. (1996). Transport properties of the multidrug resistance-associated protein (MRP) in human tumour cells. *FEBS letters*, **383** : 99-104.
- [56] Krishnamachary, N. & Center, M.S. (1993). The MRP gene associated with a non-P-glycoprotein multidrug resistance encodes a 190-kDa membrane bound glycoprotein. *Cancer res.*, **53** : 3658-3661.
- [57] Müller, M., Meiler, C., Zaman, G.J.R., Borst, P., Scheper, R.J., Mulder, N.H., de Vries, E.G.E. & Jansen, P.L.M. (1994). Overexpression of the gene encoding the multidrug resistance-associated protein results in increased ATP-dependent glutathione S-conjugate transport. *Proc. Natl. Acad. Sci.*, **91** :13033-13037.
- [58] Müller, M., de Vries, E.G.E., & Jansen, P.L.M. (1996). Role of multidrug resistance protein (MRP) in glutathione S-conjugate transport in mammalian cells. *Journal of Hepatology*, **24** :100-108.
- [59] Leier, I., Jedlitschky, G., Buchholtz, U., Center, M., Cole, S.P.C., Deeley, R.G. & Keppler, D. (1996). ATP-dependent glutathione disulphide transport mediated by the MRP gene-encoded conjugate export pump. *Biochemical Journal*, **314** : 433-437.

[60] Nooter, K., Westerman, A.M., Flens, M.J., Zaman, G.J.R., Scheper, R.J., Vanwingerden, K.E., Burger, H., Oostrum, R., Boersma, T., Sonneveld, P., Gratama, J.W., Kok, T., Eggeremont, A.M.M., Bosman, F.T. & Stoter, G. (1995). Expression of the multidrug resistance-associated protein (MRP) gene in human cancers (1). *Clinical Cancer Research*, **1** : 1301-1310.

[61] Nooter, K. & Stoter, G. (1996). Molecular mechanisms of multidrug-resistance in cancer. *Pathology Research and Practice*, **192** : 768-780.

[62] Chuman, Y., Sumizawa, T., Takebayashi, Y., Niwa, K., Yamada, K., Haraguch., Furukawa, T., Akiyama, S. & Aikou, T. (1996). Expression of the multi-drug resistance-associated protein (MRP) in human colorectal, gastric and non-small-cell lung carcinomas. *International Journal of Cancer*, **66** : 274-279.

[63] Bordow, S.B., Haber, M., Madafiglio, J., Cheung, B., Marshall, G.M. & Norris, M. (1994). Expression of the multidrug resistance-associated protein (MRP) gene correlates with amplification and overexpression of the *N-myc* oncogene in childhood neuroblastoma. *Cancer Res.*, **54** : 5036-5040.

[64] Izquierdo, M.A., van der Zee, A.G.J., Vermorken, J.B., van der Valk, P., Beliën, J.A.M., Giaccone, G., Scheffer, G.L., Flens, M.J., Pinedo, H.M., Kenemans, P., Meijer, C.J.L.M., de Vries, E.G.E. & Scheper, R.J. (1995). Drug Resistance-Associated Marker Lrp for Prediction of Response to Chemotherapy and Prognosis in Advanced Ovarian Carcinoma. *J. Natl. Cancer Inst.*, **87** : 1230-1235.

[65] Izquierdo, M.A., Shoemaker, R.H., Flens, M.J., Scheffer, G.L., Wu, L., Prather, T. & Scheper, R.J. (1996). Overlapping Phenotypes of Multidrug-Resistance Among Panels of Cancer-Cell Lines. *International Journal of Cancer*, **65** : 230-237.

- [66] Izquierdo, M.A., Scheffer, G.L., Flens, M.J., Shoemaker, R.H., Rome, L.H. & Scheper, R.J. (1996). Relationship of LRP-human major vault protein to *in vitro* and clinical resistance to anticancer drugs. *Cytotechnology*, **19** : 191-197.
- [67] Scheffer, G.L., Wijngaard, P.L.J., Flens, M.J., Izquierdo, M.A., Slovak, M.L., Pinedo, H.M., Meijer, C.J.L.M., Clevers, H.C. and Scheper, R.J. (1995). *Nature Medicine* **1** : 578-582.
- [68] Slovak, M.L., Peley Ho, J., Cole, S.P.C., Deeley, R.G., de Vries, EG/E., Broxterman, H.J., Scheffer, G.L. & Scheper, R.J. (1995). The LRP gene encoding a major vault protein associated with drug resistance maps proximal to MRP on chromosome 16 : evidence that chromosome breakage plays a key role in MRP or LRP gene amplification. *Cancer Res.*, **55** : 4214-4219.
- [69] Scheper, R.J., Broxterman, H.J., Scheffer, G.L., Kaaijak, P., Dalton, W.S., van Heijningen, T.H.M., van Kalken, C.K., Slovak, M.L., de Vries, E.G.E., van der Valk, P., Meijer, C.J.L.M. & Pinedo, H.M. (1993). Overexpression of a 110 kD vesicular protein in a non-P-glycoprotein mediated multidrug resistance. *Cancer Res.*, **53** : 1475-1479.
- [70] Flens, M.J., Izquierdo, M.A., Scheffer, G.L., Fritz, J.M., Meijer, C.J.L.M., Scheper, R.J. & Zaman, G.J.R. (1994). Immunochemical detection of MRP in human multidrug-resistant tumour cells by monoclonal antibodies. *Cancer Res.*, **54** : 4557-4563.
- [71] Shao, Y, de Giuli, R., Wyler, B. & Lehnert, M. (1995). Overexpression of MDR1/P-glycoprotein and MRP but not LRP is mutually exclusive in multidrug resistant human myeloma cells selected with doxorubicin. *Proc. Am. Ass. Cancer Res.*, **36** : (abst. 2006).

- [72] Schadendorf, D., Makki, A., Stahr, C., Vandyck, A., Wanner, R., Scheffer, G.L., Flens, M.J., Scheper, R. & Henz, B.M. (1995). Membrane-Transport Proteins Associated With Drug-Resistance Expressed In Human-Melanoma. *American Journal of Pathology*, **147** : 1545-1552.
- [73] Izquierdo, M.A., Scheffer, G.L., Flens, M.J., Giaccone, G., Broxterman, H.J., Meijer, C.J.L.M., & Scheper, R.J. (1996). Broad distribution of the multidrug resistance-related vault protein LRP in normal human tissues and tumours. *Am. J.Pathol.*, **148** : 837-887.
- [74] Flens, M.J., Zaman, G.J.R., van der Valk, P., Izquierdo, M.A., Schroeijers, A.B., Scheffer, G.L., van der Groep, P., Haas, M., Meijer, C.J.L.M. & Scheper, R.J. (1996). Tissue distribution of the multidrug resistance-associated protein (MRP). *Am. J.Pathol.*, **148** : 1237-1247.
- [75] Vasu, S.K., Kedersha, N.L. & Rome, L.H. (1993). cDNA cloning and disruption of the major vault protein alpha gene (*mvpA*) in *Dictyostelium discoideum*. *J. Biol. Chem.* **268** : 15356-15360.
- [76] Kickhoeffer, V.A. & Rome, L.H. (1994). The sequence of a cDNA encoding the major vault protein from *Rattus norvegicus*. *Gene*, **151** : 257-260.
- [77] Kedersha, N.L. and Rome, L.H. (1986). Isolation and characterisation of a novel ribonucleoprotein particle : Large structures contain a single species of small RNA. *J. Cell Biol.* **103** : 699-709.
- [78] Rome, L.H., Kedersha, N. & Chugani, D. (1991). Unlocking vaults : organelles in search of a function. *Trends Cell Biol.*, **1** : 47-50.

[79] Kedersha, N.L., Heuser, J.E., Chugani, D.C. & Rome, L.H. (1991). Vaults 111. Vault ribonucleoprotein particles open up into flower-like structures which have octagonal symmetry. *J. Cell Biol.*, **112** : 225-235.

[80] Chugani, D.C., Rome, L.H. and Kedersha, N. (1993). Localisation of vault particles to the nuclear pore complex. *J. Cell Sci.*, **106** : 23-29.

[81] Gervasoni, J.E., Fields, S.Z., Krishna, S., Baker, M.A., Rosado, M., Thurisamy, K., Hindenburg, A.A. & Taub, R.N. (1991). Subcellular distribution of daunorubicin in P-glycoprotein-positive and -negative drug-resistant cell lines using laser-assisted confocal microscopy. *Cancer Res.*, **51** : 4955-4963.

[82] Schuurhuis, G.J., Broxterman, H.J, de Lange, J.H.M., Pinedo, H.M., van Heijningen, T.H., Kuiper, C.M., Scheffer, G.L., Scheper, R.J., van Kalken, C.K., Baak, L., & Lankelma, J. (1991). Early multidrug resistance defined by changes in intracellular doxorubicin distribution, independent of P-glycoprotein. *Br. J. Cancer*, **64** : 857-861.

[83] Clynes, M. (1993). Cellular Models for Multiple Drug Resistance in Cancer. *In Vitro Cell Dev. Biol.*, **29A** : 171-179.

[84] Hoban, P.R., Robson, C.N., Davies, S.M., Hall, A.G., Cattan, A.R., Hickson, I.D. & Harris, A.L. (1992). Reduced topoisomerase II and elevated alpha class glutathione-S-transferase expression in a MDR CHO cell line highly cross-resistant to mitomycin C. *Biochem. Pharmacol.*, **43** : 685-693.

[85] Mannervik, B., Awasthi, Y.C., Board, P.G., Hayes, J.D., Di Illio, C., Ketterer, B., Listowsky, I., Morgenstern, R., Muramatsu, M., Pearson, W., Pickett, C.B., Sato, K., Widersten, M. & Wolf, C.R. (1992). Nomenclature for glutathione transferases. *Biochem. J.*, **282** : 305-308.

[86] Ali-Osman, F., Stein, D. & Renwick, A. (1990). Glutathione expression in BCNU-resistant human malignant astrocytoma cell lines. *Cancer Res.*, **50** : 6976-6980.

[87] Lau, D.H., Lewis, A.D., Ehsan, M.N. & Sikic, B.I. (1991). Multifactorial mechanisms associated with broad cross-resistance of ovarian carcinoma cells selected by cyanomorpholino doxorubicin. *Cancer Res.*, **51** : 5181-5187.

[88] Batist, G., Tulpule, A., Sinha, B., Katki, A.G., Myers, C.E. & Cowan, K.H. (1986). Overexpression of a novel anionic glutathione transferase in MDR in human breast cancer cells. *J.Biol. Chem.*, **261** : 15544-15549.

[89] Cole, S.P., Downes, H.S., Mirski, S.E. & Clements, D.J. (1990). Alterations in glutathione and glutathione-related enzymes in a MDR small cell lung cancer cell line. *Mol. Pharmacol.*, **37** : 192-197.

[90] Wang, Y., Teicher, B.A., Shea, T.C., Holden, S.A., Rosbe, K.W., Alachi, A. & Henner, W.D. (1989). Cross-resistance and GSH-pi levels among four human melanoma cell lines selected for alkylating agent resistance. *Cancer Res.*, **49** : 6185-6192.

[91] Moscow, J.A. & Dixon, K.H. (1993). Glutathione-related enzymes, glutathione and multidrug resistance. *Cytotechnology*, **12** : 155-170.

[92] Nakagawa, K., Saijo, N., Tsuchida, S., Sakai, M., Tsunokawa, Y., Yokota, J., Muramatsu, M., Sato, K., Terada, M. & Tew, K.D. (1990). Glutathione S-transferase pi as a determinant of drug resistance in transfectant cell lines. *J. Biol. Chem.* **265** : 4296-301.

[93] Singh, S.V., Nair, S., Ahmad, H., Awasthi, Y.C. & Krishan, A. (1989). Glutathione-S-transferases and glutathione peroxidases in doxorubicin-resistant murine leukaemic p388 cells. *Biochem. Pharmacol.*, **38** : 3505-3510.

- [94] Wolf, C.R., Macpherson, J.S. & Smyth, J.F. (1986). Evidence for the metabolism of mitoxantrone by microsomal glutathione transferases and 3-methylcholanthrene-inducible glucuronosyl transferases. *Biochem. Pharmacol.*, **35** : 1577-1581.
- [95] Fairchild, C.R., Moscow, J.A., O'Brien, E.E. & Cowan, K.H. (1990). Multidrug resistance in cells transfected with human genes encoding a variant P-glycoprotein and glutathione-S-transferase-pi. *Mol. Pharmacol.*, **37** : 801-809.
- [96] Black, S.M., Beggs, J.D., Hayes, J.D., Batoszek, A., Muramatsu, M., Sakai, M & Wolf, C.R. (1990). Expression of human glutathione S-transferases in *Saccharomyces cerevisiae* confers resistance to the anticancer drugs adriamycin and chlorambucil. *Biochem. J.* **268** : 309-315.
- [97] Moscow, J.A., Townend, A.J. & Cowan, K.H. (1989). Elevation of pi class glutathione S-transferase activity in human breast cancer cells by transfection of the GST pi gene and its effect on sensitivity to toxins. *Mol. Pharmacol.*, **36** : 22-28.
- [98] Lehnert, M. (1994). Multidrug resistance in human cancer. *Journal of Neuro-oncology*, **22** : 239-243.
- [99] Ford, J.M. and Hait, W.N. (1990). Pharmacology of drugs that alter MDR in cancer. *Pharmacol. Rev.*, **42** : 155-199.
- [100] Sonneveld, P., Durie, B. & Lockhorst, H. (1992). Modulation of MDR multiple myeloma by cyclosporin. *Lancet*, **340** : 255-259.
- [101] Mickisch, G.H. (1993). Current status and future directions of research on multidrug resistance. The impact of modern biotechnology. *Urol. Res.*, **21** : 79-81.

- [102] Henderson, B. and Dougherty, T.J. (1992). How does photodynamic therapy work? *Photochem. Photobiol.*, **55** : 145-157.
- [103] Edelson, R. (1988). Light-activated drugs. *Scientific American*, **259** : 68-75.
- [104] van Hillegesberg, R., Kort, W.J. and Wilson, J.H.P. (1994). Current Status of Photodynamic Therapy in Oncology. *Drugs*, **48** : 510-527.
- [105] von Tappeiner, H. & Jesionek, A. (1903). Therapeutische Versuche mit fluoreszierenden Stoffen. *Muenchener Medizinische Wochenschrift*, **47** : 2042-4.
- [106] Brown, S.B. and Truscott, G. (1993). New light on cancer therapy. *Chem. Brit.*, **29** : 955-958.
- [107] Wilson, B.C. and Patterson, M.S. (1986). The physics of photodynamic therapy. *Phys. Med. Biol.*, **4** : 327-360.
- [108] Diamond, I., Granelli, S.G., McDonagh, A.F., Nielson, S., Wilson, C.B. and Jaenicke, R. (1972). Photodynamic Therapy of Malignant Tumours. *Lancet*, December Issue, 1175-1176.
- [109] Dougherty, T.J., Grindey, G.B. & Fiel, R. (1975). Photoradiation Therapy II : cure of animal tumours with haematoporphyrin and light. *J. Natl. Cancer Inst.*, **55** : 115-21.
- [110] Montforts, F.P., Meier, A., Scheurich, G., Haake, G. and Bats, J. (1992). Chlorins designed for photodynamic tumour therapy and as model systems for photosynthesis. *Angew. Chem. Int. Ed.*, **31**: 1592-1594.

- [111] Boyle, R.W., Leznoff, C.C. and van Lier, J.E. (1993). Biological activities of phthalocyanines-XVI. Tetrahydroxy- and tetraalkylhydroxy zinc phthalocyanines. Effect of alkyl chain length on *in vitro* and *in vivo* photodynamic activities. *Br. J. Cancer*, **67** : 1177-1181.
- [112] Imato, I. (1993). Hope for a Magic Bullet That Moves at the Speed of Light. *Science*, **262** : 32-33.
- [113] Foote, C.S. (1990). Chemical Mechanisms of Photodynamic Action. *SPIE*, **6**,115-126.
- [114] Moan, J., Johannessen, J.V., Christensen, T., Espevik, T. & McGhie, J.B. (1982). Porphyrin-sensitized photoinactivation of human cells *in vitro*. *Am. J. Pathol.* **109** : 184-192.
- [115] Dubbelman, T.M.A.R. & VanSteveninck, J. (1984). Photodynamic effect of haematoporphyrin-derivative on transmembrane transport systems of murine L929 fibroblasts. *Biochim. Biophys. Acta* **771** : 201-7.
- [116] Perring, L.C. & Dubbelman, T.M.A.R. (1994). Fundamentals of photodynamic therapy : cellular and biochemical aspects. *Anti-Cancer Drugs*. **5** : 139-46.
- [117] Kawanishi, S., Inoue, S. & Sano, S. (1986). Photodynamic guanine modification by haematoporphyrin is specific for single-stranded DNA with singlet oxygen as a mediator. *J. Biol. Chem.*, **260** : 6090-5.
- [118] Perring, L.C., Keirse, M.J.N.C. & VanSteveninck, J. (1993). Calcium mediated PGE₂ induction reduces haematoporphyrin derivative-induced cytotoxicity of T24 human bladder transitional carcinoma cells *in vitro*. *Biochem. J.* **292** : 237-40.

- [119] Jolles, C.J., Ott, M.J., Straight, R.C. & Lynch, D.H. (1988). Systemic immunosuppression induced by peritoneal photodynamic therapy. *Am. J. Obstet. Gynaecol.* **158** : 1446.
- [120] Gomer, C.J., Ferrario, A., Hayashi, N., Rucker, N., Szirth, B.C. and Murphree, A.L. (1988). Molecular, Cellular and Tissue Responses Following Photodynamic Therapy. *Lasers in General Surgery and Medicine*, **8** : 450-463.
- [121] Saul, H. (1993). New light on cancer treatment. *New Scientist*, **139** : 17.
- [122] Orth, K., Rück, A., Staresen, A. and Beger, H.G. (1995). Intraluminal treatment of inoperable oesophageal tumours by intralesional photodynamic therapy with methylene blue. *Lancet*, **345** : 519-20.
- [123] D'Halewin, M.A. & Baert, L. (1995). Long-term results of whole bladder wall photodynamic therapy (PDT) for multifocal carcinoma in situ of the bladder. *Urology*, **45** : 763-7.
- [124] Wilson, B.C. (1989). Photodynamic Therapy : light delivery and dosage for second-generation photosensitizers. *Photosensitizing Compounds : their Chemistry, Biology and Clinical Use*, Wiley, Chichester (Ciba Foundation Symposium 146), 60-77.
- [125] Roberts, D.J.H. & Cairnduff, F. (1995). Photodynamic therapy of skin cancer : a review. *British Journal of Plastic Surgery*, **48** : 360-370.
- [126] Iwamoto, Y., Yoshioka, H and Yanagihara, Y. (1987). Singlet oxygen producing activity and photodynamic biological effects of acridine compounds. *Chem. Pharm Bull.*, **35**, 2478-2483.

- [127] Cincotta, L., Foley, J.W., Maceachern, T., Lampros, E. and Cincotta, A.H. (1994). Novel photodynamic effects of a benzophenoxazine on two different murine sarcomas. *Cancer Res.*, **54**, 1249-1258.
- [128] Cañete, M., Villanueva, A. and Juarranz, A. (1993). Uptake and photo-effectiveness of two thiazines in HeLa cells. *Anti-Cancer Drug Design.*, **8**, 471-477.
- [129] Melloni, E. Dasdia, T., Fava, G., Rocca, G., Zunino, F. and Marchesini, R. (1988). *In vitro* photosensitizing properties of Rhodamine 123 on different human tumour cell lines. *Photochem. Photobiol.*, **48**, 311-314.
- [130] Lewis, M.R., Goland, P.P. & Sloviter, H.A. (1946). Selective action of certain dyestuffs on sarcomata and carcinomata. *Anat. Rec.* **96** : 201-220.
- [131] Summerhayes, I.C., Lampidis, T.J., Bernal, S.D., Nadakavukaren, K.K., Shephard, E.L. & Chen, L.B. (1982). Unusual retention of rhodamine 123 by mitochondria in muscle and carcinoma cells. *Proc. Natl. Acad.Sci. U.S.A.* **79** : 5292-5296.
- [132] Modica-Napolitano, J.S., Joyal, J.L., Ara, G., Oseroff, A.R. & Aprille, J.R. (1990). Mitochondrial toxicity of cationic photosensitizers for photochemotherapy. *Cancer Res.* **50** : 7876-7881.
- [133] Wadwa, K., Smith, S. and Oseroff, A.R. (1988). Cationic Triarylmethane Photosensitizers for Selective Photochemotherapy : Victoria Blue-BO, Victoria Blue-R and Malachite Green. *SPIE*, **997**, 154-160.
- [134] Moan, J. & Berg, K. (1992). Photochemotherapy of Cancer : Experimental Research. *Photochemistry and Photobiology*, **55** : 931-948.

- [135] Shea, C.R., Chen, N., Wimberly, J. & Hasan, T. (1989). Rhodamine dyes as potential agents for photochemotherapy of cancer in human bladder carcinoma cells. *Cancer Res.*, **49** : 3961-3965.
- [136] Oster, G. In *Luminescence of Organic and Inorganic Materials*. (1955). Wiley and Sons, U.K.
- [137] Oster, G. (1955). Dye binding to high polymers. *J. Polymer. Sci.*, **36** :235-44.
- [138] Browning, C.H. (1964). In *Experimental Chemotherapy 2*. (Eds. Schnitzer & Hawking), Academic Press, New York,
- [139] Viola, A., Hadjur, C., Jeunet, A. & Julliard, M. (1996). Electron-paramagnetic-resonance evidence of the generation of superoxide (O-2(center-dot-)) and hydroxyl ((OH)-O-(center-dot)) radicals by irradiation of a new photodynamic therapy photosensitizer Victoria blue BO. *J. Photochem. Photobiol. B.*, **32** : 49-59.
- [140] Wainwright, M. (1996). Non-Porphyrin Photosensitizers in Biomedicine. *Chemical Society Reviews*, **25** : 351-359.
- [141] Wilson, M. (1993). Photolysis of oral bacteria and its potential use in the treatment of caries and peridontal disease. *Journal of Applied Bacteriology*, **75** : 299-306.
- [142] Carter, S.K. (1975). Adriamycin - A Review. *Journal of the National Cancer Institute*, **55** : 1265-1273.
- [143] Tritton, T.R. (1991). Cell Death in Cancer Chemotherapy : The Case of Adriamycin. In *Apoptosis : The Molecular Basis of Cell Death*, Tomei, D. and Cope, F. (Eds.), Cold Spring Harbor Laboratory Press, Cold Spring Harbor. New York, U.S.A.

- [144] Tritton, T.R. and Yee, G. (1982). The anticancer agent adriamycin is actively cytotoxic without entering cells. *Science*, **217** : 248-250.
- [145] de Wolf, F.A., Maliepaard, M., van Dorsten, F., Berguis, I., Nicolay, K. & de Kruijff, B., (1991). Comparable interaction of doxorubicin with various acidic phospholipids results in changes of lipid order and dynamics. *Biochimica et Biophysica Acta*, **1096** : 67-80.
- [146] de Wolf, F.A., Staffhorst, R.W.H.M., Smits, H.P., Onwezen, M.F. & de Kruijff, B. (1993). Role of Anionic Phospholipids in the Interaction of Doxorubicin and Plasma Membrane Vesicles : Drug Binding and Structural consequences in Bacterial Systems. *Biochemistry*, **32** : 6688-6695.
- [147] Kusters, R., Dowhan, W. & de Kruijff, B. (1991). Negatively charged phospholipids restore prePhoE translocation across phosphatidylglycerol-depleted *Escherichia coli* inner membranes *J.Biol.Chem.*, **266** : 8659-62.
- [148] Raetz, C.R.H. (1978). Enzymology, Genetics and Regulation of Membrane Phospholipid Synthesis in *Escherichia coli*. *Microbial Reviews*, **42** : 615-659.
- [149] Asai, Y., Katayose, Y., Hikita, C., Ohta, A. and Shibuya, I. (1989). Suppression of the lethal effect of acidic phospholipid deficiency by defective formation of the major outer-membrane lipoprotein in *Escherichia coli*. *J.Bacteriol.*, **171** : 6867-6869.
- [150] Harris, F., Chatfield, L.K. and Phoenix, D. A. (1995). Depletion of anionic phospholipids has no observable effect on the anchoring of penicillin binding protein 5 to the inner membrane of *Escherichia coli*. *FEMS Microbiology Letters*, **129** : 215-220.

- [151] Bligh, E.G. and Dyer, W.J. (1959). A Rapid Method of Total Lipid Extraction and Purification. *Canadian Journal of Biochemistry and Physiology*, **37** : 911-917.
- [152] Rolph, C.E. & Goad, L.J. (1991). Phosphatidyl biosynthesis in celery cell suspension cultures with altered sterol compositions. *Physiol. Plant.* **83** : 605-610.
- [153] Goormatigh, E. and Ruyschaert, J.M. (1984). Anthracycline Glycoside-Membrane Interactions. *Biochimica et Biophysica Acta*, **779** : 271-288.
- [154] Short, S.A. and White, D.C. (1971). Metabolism of Phosphatidylglycerol. Lysylphosphatidylglycerol and Cardiolipin of *Staphylococcus aureus*. *J.Bacteriol.*, **108** : 219-226.
- [155] Spratt, B.G. (1994). Resistance to Antibiotics Mediated by Target Alterations. *Science*, **264** : 388-393.
- [156] Burns, C.P., North, J.A., Petersen, E.S. & Ingram, L.S. (1988). Subcellular distribution of doxorubicin : comparison of fatty acid modified and unmodified cells. *Proc. Soc. Biol. Med.* **188** : 455-460.
- [157] Lewis, K. (1994). Multidrug resistance pumps in bacteria : variations on a theme. *TIBS*, **19** : 119-123.
- [158] Ouellette, M., Légaré, D. and Papadopoulou, B. (1994). Microbial multidrug resistance ABC transporters. *TIBS*, **2** : 407-410.
- [159] Morgan, S.J. & Darling, D.C. (1993). In *Animal Cell Culture.*, BIOS Scientific Publishers Ltd., Oxford, U.K.

- [160] Lockwood, A.P.M. & Lee, A.G. (1984). In *The Membranes of Animal Cells* (3rd Ed.), Edward Arnold (Publishers) Ltd., London, U.K.
- [161] Ramu, A., Glaubiger, D., Magrath, I.T. & Joshi, A. (1983). Plasma Membrane Lipid Structural Order in Doxorubicin-sensitive and -resistant P388 cells. *Cancer Res.*, **43** : 5533-5537.
- [162] Ramu, A., Glaubiger, D., & Weintraub, H. (1984). Differences in Lipid Composition of Doxorubicin-Sensitive and -Resistant P388 Cells. *Cancer Treatment Reports*, **68** : 637-642.
- [163] Rockwell, S.C., Kallman, R.F. and Fajardo, L.F. (1972). Characteristics of a serially-transplanted mouse tumour and its tissue culture-adapted derivative. *J.Natl. Cancer Inst.*, **49** :735-749.
- [164] Blazek, R., Schmitt, K., Krafft, U. & Hadding, U. (1990). Fast and simple procedure for the detection of cell culture mycoplasmas using a single monoclonal antibody. *Journal of Immunological Methods*, **131** : 203-212.
- [165] Kamla, V., Henrich, B. & Hadding, U. (1992). Species differentiation of mycoplasmas by EF-Tu specific monoclonal antibodies. *Journal of Immunological Methods*, **147** : 73-81.
- [166] Hamilton, R.J. & Hamilton, S. (Eds.) (1992). In *Lipid Analysis : A Practical Approach*, IRL Press at Oxford University Press, Oxford, U.K.
- [167] Fiedorowicz, F., Galindo, J.R., Julliard, M., Mannoni, P. and Chanon, M. Efficient photodynamic action of Victoria Blue BO against the human leukemic cell lines K-562 and TF-1. (1993). *Photochem. Photobiol.*, **58**, 356-361

- [168] Darzynkiewicz, Z., & Carter, S.P. (1988). Photosensitizing effect of the tricyclic heteroaromatic cationic dyes pyronin Y and toluidine blue O (tolonium chloride). *Cancer Research*, **48** :1295-1299.
- [169] Rück, A., Köllner, T., Dietrich, A., Strauss, W. & Schneckenburger, H. (1992). Fluorescence formation during photodynamic therapy in the nucleus of cells incubated with cationic and anionic water-soluble photosensitizers. *Journal of Photochemistry and Photobiology, B: Biology*, **12** : 403-412.
- [170] Ito, T. & Kobayashi, K. (1977). A survey of *in vivo* photodynamic activity of xanthenes, thiazines and acridines in yeast cells. *Photochem. Photobiol.*, **26**, 581-587.
- [171] Yu, D.S., Chang, S.Y. & Ma, C.P. (1993). The effect of methylene blue-sensitized photodynamic treatment on bladder cancer cells : a further study on flow cytometric basis. *The Journal of Urology*, **149**, 1198-1201.
- [172] Twentyman, P.R. (1993). Non-P-glycoprotein mediated MDR. *Cancer Topics*, **9**, 46-47.
- [173] Posada, J., Vichi, P. & Tritton, T.R. (1989). Protein kinase C in Adriamycin action and resistance in mouse sarcoma 180 cells. *Cancer Res.* **49**, 6634-6639.
- [174] Tewey, K.M., Rowe, T.C., Yand, L., Halligan, B.D. & Liu, L.F. (1984). Adriamycin-induced DNA damage mediated by mammalian DNA topoisomerase II. *Science*, **226**, 466.
- [175] Goodman, J. & Hochstein, P. (1977). *Biochem. Biophys. Res. Commun.* **77**, 797-802.

- [176] Goodman Gilman, A., Rall, T.W. Nies, A.S. & Taylor, P. (Eds.) (1991). In *Goodman's & Gilman's The Pharmacological Basis of Therapeutics* (8th Ed., Vol. II), Pergamon Press, Oxford, U.K.
- [177] Carmichael, J., DeGraf, W.G, Gazdar, A.F., Minna, J.D. & Mitchell, J.B. (1987). Evaluation of a tetrazolium-based semiautomated colourimetric assay : assessment of chemosensitivity testing. *Cancer Res.*, **47** : 936-942.
- [178] Oseroff, A.R., Ohuoha, D., Ara, G., McAuliffe, D., Foley, J. & Cincotta, L. (1986). Intramitochondrial dyes allow selective in vitro photolysis of carcinoma cells. *Proc. Natl. Acad. Sci.*, **83** : 9729-9733.
- [179] Zdolsek, J.M., Olssen, G.M. & Brunk, U.T. (1990). Photooxidative damage to lysosomes of cultured macrophages by acridine orange. *Photochem. Photobiol.*, **51** : 67-76.
- [180] Lin, C.W., Shulock, J.R., Kirley, S.D., Cincotta, L. & Foley, J.W. (1991). Localisation and mechanism of uptake of Nile blue photosensitizers in tumour cells. *Cancer Res.*, **51** : 2710-2719.
- [181] Lin, C.W., Shulock, J.R., Kirley, S.D., Bachelder, C.M., Flotte, T.J., Sherwood, M.E., Cincotta, L. & Foley, J.W. (1992). Lysosomes as the primary cellular target of photodynamic action initiated by Nile blue photosensitizers. *Proc. Am. Ass. Cancer Res.*, **33** : 501.
- [182] de Duve, C., de Barse, T., Poole, B., Trouet, A., Tulkens, P. & van Hoff, F. (1974). Lysosomotropic agents. *Biochem. Pharmacol.*, **23** : 2495-2531.
- [183] Diwu, Z. & Lown, J.W. (1994). Phototherapeutic potential of alternative photosensitizers to porphyrin. *Pharmac. Ther.*, **66** : 1-35.

- [184] Hassman, M., Valet, G.K., Tapiero, H., Trevorrow, K. & Lampidis, T.J. (1989). Membrane potential differences between Adriamycin-sensitive and -resistant cells as measured by flow cytometry. *Biochem. Pharmacol.*, **38** : 305-312.
- [185] Alberts, B., Bray, D., Lewis, J., Raff, M., Roberts, K. & Watson, J.D. (1983). In *Molecular Biology of the Cell*, Garland Publishing Inc., New York, USA.
- [186] Gomer, C.J., Rucker, N., Ferrario, A. & Wong, S. (1989). Properties and applications of photodynamic therapy. *Radiation Research*, **120** : 1-18.
- [187] Chapman, J.D., Stobbe, C.C., Annfield, M.R., Santus, R., Lee, J. & McPhee, M.S. (1991). Oxygen dependency of tumour cell killing 'in vitro' by light-activity. *Radiation Research*, **126** : 73-79.
- [188] Tsuruo, T., Iida, H., Noriji, M., Tsukagoshi, S. & Sakurai, Y. (1983). Circumvention of vincristine and adriamycin resistance *in vivo* and *in vitro* by calcium influx blockers. *Cancer Res.*, **43** : 2905-2910.
- [189] Ford, J.M. & Hait, W.N. (1993). Pharmacologic circumvention of multidrug resistance. *Cytotechnology* **12** : 171-212.
- [190] Hamilton, T.C., Winker, M.A., Louie, K.G., Batist, G., Behrens, B.C., Tsuruo, T., Grotzinger, K.R., McKoy, W.M., Young, R.C. & Ozols, R.F. (1985). Augmentation of Adriamycin, melphalan and cisplatin cytotoxicity in drug-resistant and -sensitive human ovarian carcinoma cell lines by buthionine sulphoximine mediated glutathione depletion. *Biochem. Pharmacol.*, **34** : 2583-2586.
- [191] Ozols, R.F. (1985). Pharmacological reversal of drug resistance in ovarian cancer. *Semin. Oncol.*, **7** : 7-11.

- [192] Lee, F.Y.F., Vessey, A.R. & Siemann, D.W. (1988). Glutathione as a Determinant of Cellular Response to Doxorubicin. *NCI Monogr.*, **6** : 211-215.
- [193] Russo, A., Carmichael, J., Friedman, N., DeGraff, W., Tochner, Z., Glatstein, E. & Mitchell, J.B. (1986). The Roles of Intracellular Glutathione in Antineoplastic Chemotherapy. *Int. J. Radiation Oncology Biol. Phys.*, **12** : 1347-1354.
- [194] Crescimanno, M., Borsellino, N., Leonardi, V., Flandina, C., Flugy, A., Rausa, L. & D'Alessandro, N. (1994). Effect of Buthionine Sulfoximine on the Sensitivity to Doxorubicin of Parent and MDR Tumour Cell Lines. *Journal of Chemotherapy*, **6** : 343-348.
- [195] Skovsgaard, T. (1978). Mechanisms of resistance to daunorubicin in resistant Ehrlich ascites tumour cells. *Cancer Res.*, **38** : 1783-1791.
- [196] Tsuruo, T., Iida, H., Tsukagoshi, S. & Sakurai, Y. (1981). Overcoming of vincristine resistance in P388 leukaemia cells *in vivo* and *in vitro* through enhanced cytotoxicity of vincristine and vinblastine by verapamil. *Cancer Res.*, **41** : 1967-1972.
- [197] Tsuruo, T., Iida, H., Tsukagoshi, S. & Sakurai, Y. (1982). Increased accumulation of vincristine and Adriamycin in drug-resistant P388 tumour cells following incubation with calcium antagonists and calmodulin inhibitors. *Cancer Res.*, **42** : 4730-4733.
- [198] Tsuruo, T., Iida, H., Tsukagoshi, S. & Sakurai, Y. (1983). Potentiation of vincristine and Adriamycin in human hematopoietic tumour cell lines by calcium antagonists and calmodulin inhibitors. *Cancer Res.*, **43** : 2267-2272.

- [199] Choi, K., Chen, C., Kriegler, M. & Roninson, I.B. (1988). An altered pattern of cross-resistance in multidrug-resistant human cells results from spontaneous mutations in the *mdr1* (P-glycoprotein) gene. *Cell*, **53** : 519-529.
- [200] Hait, W.N. & Aftab, D.T. (1992). Rational design and preclinical pharmacology of drugs for reversing multidrug resistance. *Biochem. Pharmacol.*, **43** : 103-107.
- [201] Eady, J.J., Orta, T., Dennis, M.F., Stratford, M.R.L. & Peacock, J.H. (1995). Glutathione determination by the Tietze enzymatic recycling assay and its relationship to cellular radiation response. *British Journal of Cancer*, **72** : 1089-1095.
- [202] Robyt, J.F. & White, B.J. (1987). In *Biochemical Techniques Theory and Practice*. Brooks/Cole Publishing Company, California.
- [203] Dethmers, J.K. & Meister, A. (1981). Glutathione export by human lymphoid cells : Depletion of glutathione by inhibition of its synthesis decreases export and increases sensitivity to irradiation. *Proc. Natl. Acad. Sci. (USA)*, **78** : 7492-7496.
- [204] Batist, G., Tulpule, A., Sinha, B.K., Katki, A.G., Myers, C.E. & Cowan, K.H. (1986). Overexpression of a novel anionic glutathione transferase in multidrug-resistant human breast cancer cells. *J. Biol. Chem.*, **261** : 15544-15549.
- [205] Nair, S., Singh, S.V., Samy, T.S.A. & Krishan, A. (1990). Anthracycline resistance in murine leukaemic P388 cells : Role of drug efflux and glutathione related enzymes. *Biochem. Pharmacol.*, **39** : 723-728.
- [206] Suzukake, K., Petro, B.J. & Vistica, D.T. (1982). Reduction in glutathione content of L-Pam resistant L1210 cells confers drug sensitivity. *Biochem. Pharmacol.*, **31** : 121-124.

- [207] Russo, A., & Mitchell, J.B. (1985). Potentiation and protection of doxorubicin cytotoxicity by cellular glutathione modulation. *Cancer Treat. Rep.*, **69** : 1293-1296.
- [208] Dethlefsen, L.A., Biaglow, J.E., Peck, V.M. & Ridinger, M.S. (1986). Toxic Effects of Extended Glutathione Depletion by Buthionine Sulfoximine on Murine Mammary Carcinoma Cells. *Int. J Radiation Oncology Biol. Phys.*, **12** : 1157-1160.
- [209] Lutzky, J., Astor, M.B., Taub, R.N., Baker, M.A., Bhalla, K., Gervasoni, J.E., Rosado, M., Stewart, V., Krishna, S. & Hindenburg, A.A. (1989). Role of glutathione and dependent enzymes in anthracycline-resistant HL60/AR cells. *Cancer Res.*, **49** : 4120-4125.
- [210] Drori, S., Eytan, G.D. & Assaraf, Y.G. (1995). Potentiation of anti-cancer drug cytotoxicity by multidrug-resistance chemosensitizers involves alterations in membrane fluidity leading to increased membrane permeability. *Eur. J. Biochem.* **228** : 1020-1029.
- [211] Ramu, A., Ramu, N. & Rosario, L.M. (1991). Circumvention of multidrug resistance in P388 cells is associated with a rise in the cellular content of phosphatidylcholine. *Biochem. Pharmacol.* **41** : 1455-1461.
- [212] Willingham, M.C., Cornwell, M.M., Cardarelli, C.O., Gottesman, M.M. & Pastan, I. (1986). Single cell analysis of daunomycin uptake and efflux in multidrug-resistant and -sensitive KB cells : Effects of verapamil and other drugs. *Cancer Res.*, **46** : 5941-5946.
- [213] Hindenburg, A.A., Baker, M.A., Gleyzer, E., Stewart, V.J., Case, N., Taub, R.N. (1987). Effect of verapamil and other agents on the distribution of anthracyclines and on the reversal of multidrug resistance. *Cancer Res.*, **47** : 1421-1425.

- [214] Weshaupt, K.R, Gomer, C.J. & Dougherty, T.J. (1976). *Cancer Res.*, **36** : 2326-2329.
- [215] Wieman, T.J. and Fingar, V.H. (1992). Photodynamic Therapy. *Lasers in General Surgery*, **72** : 609-622.
- [216] Riley, J.F. (1948). Retardation of growth of a transplantable carcinoma in mice fed basic metachromatic dyes. *Cancer Res.*, **8**, 183-188
- [217] Barker, C.C., Bride, M.H., Hallas. G. and Stamp, A. (1961). *J. Chem. Soc.*, 1285.
- [218] Pooler, J.P. and Valenzo, D.P. (1979). Physicochemical determinants of the sensitizing effectiveness for photooxidation of nerve membranes by fluorescein derivatives. *Photochem. Photobiol.*, **30** : 491-498.
- [219] Goldacre, R.J. & Phillips, J.N. (1949). The ionization of basic triphenylmethane dyes. *J. Chem. Soc.*, 1724-1732.
- [220] Lin, C.W., Shulok, J.R., Kirley, S.D., Bachelder, C.M., Flotte, T.J., Sherwood, M.E, Cincotta, L. & Foley, J.W. (1993). Photodynamic destruction of lysosomes mediated by Nile Blue photosensitizers. *Photochem. Photobiol.*, **58** : 81-91
- [221] Cincotta, L. & Foley, J.W. (1988). Novel phenothiazinium photosensitizers for photodynamic therapy. *SPIE*, **997** : 145-153.
- [222] Gabbay, E.J., Grier, D., Fingerle, R.E., Reimer, R., Levy, R., Pearce, S.W. & Wilson, W.D. (1976). Interaction specificity of the anthracyclines with deoxyribonucleic acid. *Biochemistry*, **15** : 2062-2070.

- [223] Nishizuka, Y. (1984). Turnover of Inositol Phospholipids and Signal Transduction. *Science.*, **225** : 1365 - 1369.I
- [224] Zeisel, S.H. (1993). Choline phospholipids : signal transduction and carcinogenesis. *FASEB J.*, **7** : 551 - 557.
- [225] Molinari, A., Calcabrini, A., Crateri, P. & Arancia, G. (1990). Interaction of anthracycline antibiotics with cytoskeletal components of cultured carcinoma cells (CG5). *Exp. Mol. Pathol.*, **53** : 11 : 33.
- [226] Coley, H.M., Amos, W.B., Twentyman, P.R. & Workman, P. (1993). Examination by laser scanning confocal fluorescent imaging microscopy of the subcellular localisation of anthracyclines in parent and multidrug resistant cell lines. *Br. J. Cancer*, **67** : 1316 - 1323.
- [227] Broxterman, H.J., Schuurhuis, G.J., Lankelma, J., Baak., J.P.A. & Pineda, H.M. (1990). Towards functional screening for multidrug resistant cells in human malignancies. In : Mihich, E., (ed.), *Drug Resistance : Mechanism and Reversal.*, pp. 309-319, John Libbey, CIC, Roma.
- [228] Schuurhuis, G.J., Broxterman, H.J., Cervantes, A., van Heijningen, T.H.H.M., de Lange, J.H.M., Baak, J.P.A., Pinedo, H.M. & Lankelma, J. (1989). Quantitative determination of factors contributing to doxorubicin resistance in multidrug-resistant cells. *J. Natl. Cancer Inst.*, **81** : 1887 - 1893.
- [229] Meschini, S., Molinari, A., Calcabrini, A., Citro, G. & Arancia, G. (1994). Intracellular localisation of the antitumour drug adriamycin in living cultured cells : a confocal microscopy study. *Journal of Microscopy*, **176** : 204 - 210.

[230] Peterson, C. & Truet, A. (1978). Transport and storage of daunorubicin and doxorubicin in cultured fibroblasts. *Cancer Res.*, **38** : 4645 - 4649.

[231] Vale, R.D. (1987). Intracellular transport using microtubule-based motors. *Ann. Rev. Cell Biol.*, **3** : 347 - 378.

[232] Kornfield, S. (1987). Trafficking of lysosomal enzymes. *FASEB J*, **1** : 462 - 468.

[233] Fojo, A., Akiyama, S., Gottesman, M.M. & Pastan, I. (1985). Reduced drug accumulation in multiply drug-resistant human KB carcinoma cell lines. *Cancer Res.*, **45** : 3002 - 3007.

[234] Willingham, M.C., Cornwell, M.M., Cardarelli, C.O., Gottesman, M.M. & Pastan, I. (1986). Single cell analysis of daunomycin uptake and efflux in multidrug-resistant and -sensitive KB cells : effects of verapamil and other drugs. *Cancer Res.*, **46** : 5941 - 5946.

[235] Rutherford, A.V. & Willingham, M.C. (1993). Ultrastructural localisation of daunomycin in multidrug resistant cells with modulation of the multidrug transporter. *J. Histochem. Cytochem.*, **41** : 1573 - 1577.

[236] Ellis, C.N., Ellis, M.B. & Blakemore, W. (1987). Effect of adriamycin on heart mitochondrial DNA. *Biochem. J.*, **245** : 309 - 312.